NPL
National Physical Laboratory

NPL Report IR 72

Thermal neutron fluence and dose equivalent standards at NPL

David J. Thomas

May 2026

NPL Management Ltd

National Physical Laboratory

National Physical Laboratory (NPL)

Thermal neutron fluence and dose equivalent standards at NPL

David J. Thomas

We are the UK's National Metrology Institute (NMI), a world-leading centre of excellence that provides cutting-edge measurement science, engineering and technology that underpins prosperity and quality of life in the UK.

Abstract

A detailed description is given of the conventions used at NPL when deriving and quoting thermal neutron fluence standards. Values are given for the parameters involved in the analysis and their uncertainties. The way in which dose equivalent quantities are derived from these fluences is explained, and the fluence to dose equivalent conversion coefficients to be used are tabulated.

ISSN 1754-2952

https://doi.org/10.47120/npl.IR72

National Physical Laboratory
Hampton Road, Teddington, Middlesex, TW11 0LW

This work was funded by the UK Government's Department for Science, Innovation & Technology through the UK's National Measurement System programmes.

Contents

1 INTRODUCTION

Thermal neutron fluence standards have been available at NPL since the facility, commonly known as the thermal pile, was set up in the late 1960s by Ryves and Paul[1]. The thermal fluences are produced by moderating fast neutrons. These are produced by bombarding beryllium targets, located in a large graphite block[2], with beams of deuterons from a charged particle accelerator. Fluences are measured using the activation of thin gold foils, and are monitored by fission chambers within the graphite pile. The most commonly used foils have an area of 1 cm^2 and a thickness of about 0.005 cm (2 thou). A photograph of the pile, taken roughly along the accelerator beam line direction, is shown in Figure 1.

Figure 1. The NPL thermal pile.

Two locations are available for performing irradiations. One is within a vertical hole giving access to a cylindrical area near the centre of the pile. This hole was originally 9 cm in diameter, but was increased to 12 cm to allow the testing of reactor instruments. Near the bottom of the hole the fluence has a uniform spatial distribution at a particular height above the bottom, and fluence rates in the range from about 1×10^4 to 3×10^7 cm^{-2} s^{-1} are achievable. The hole diameter is, however, small and most objects, with the important exception of small amounts of materials for activation, or cylindrical/spherical instruments with diameters less than 12 cm, have to be irradiated in the field of the 'thermal column'.

The column is a larger diameter hole, also in the top of the pile, but in this case situated almost over one of the beryllium targets. A stainless steel column, cadmium-lined on its curved inner

surface, but not on its base, is placed in the hole. The column comes in sections and may be either 1 m or 1.5 m long. When it is 1.5 m long it can be evacuated to reduce air attenuation of the beam. The neutron beam emerging from the column is reasonably uniform over a horizontal circular area of about 30 cm diameter[3], although the intensity falls off as the height increases. Any device placed in the beam is irradiated with neutrons having a range of angles, the range getting smaller as the height in the column increases[3]. The maximum fluence rate achievable in the column is about 4 x 10^4 cm^{-2} s^{-1} at the 1 m height. In Figure 1 the column is set at the 1.5 m height and the connection to a roughing pump to allow evacuation is visible. The top of the access hole, which is at the centre of the pile, is behind the column in this figure.

In addition to thermal neutrons both the access hole and the column fluence contain a component of higher energy neutrons. For the column the spectrum of this component has been measured[4], and the fast fluence has been determined relative to the thermal component. Although the higher energy fluence is only about 24% of the thermal fluence, the dose equivalent due to this component is more than a factor of two greater than that due to the thermal neutrons.

An NPL report, DQL-RN 008[5], written in 2005, outlined the conventions used at NPL when deriving and quoting thermal neutron fluence and dose equivalent standards. Since then modifications have been made to the pile, and further information about the characteristics of the fields have been determined, in particular concerning the variation of the beam properties in the thermal column. These are addressed in the present report.

Standard fluences produced at NPL are derived using foil activation, and the measured data are analysed using the Westcott convention[6,7]. Equations for an analysis using this convention, and for deriving the various corrections that are needed, such as self-shielding, are distributed in a number of papers in the literature. This report attempts to bring together all the aspects of the analysis, and to present all the required equations. In some cases steps that are not present in the derivation of the equations in the published papers have been added here for completeness.

The Westcott convention allows a measure of the fluence to be given with small uncertainties. Although this convention is ideal for comparing thermal cross sections, and is used extensively in neutron activation measurements, a Westcott fluence is not the quantity required when using a thermal facility to calibrate devices used to measure neutron dose equivalent, for example area survey instruments or personal dosemeters, and the Westcott approach has to be extended to derive the ‘true’ fluence.

This report is essentially an update of DQL-RN 008 including considerable additional information and greater detail, of the various corrections in particular. It also investigates the uncertainties assigned to the parameters used in deriving the fluence and dose quantities.

2 THE MAXWELLIAN THERMAL NEUTRON DISTRIBUTION

For neutrons in thermal equilibrium with their surroundings in an ideal moderating material the energy spectrum is, to a good approximation, a Maxwellian distribution. This spectrum is presented in the literature in several different forms which should be clearly distinguished. In particular, the spectrum is sometimes presented in terms of the neutron density and sometimes in terms of the fluence. The neutron density distribution can be expressed as a function of the neutron velocity, v, or the energy, E, see equations (1) and (2) below[8,9]:

$$\frac{n(v)\mathrm{d}v}{n} = \frac{4}{\sqrt{\pi}}\left(\frac{m}{2kT}\right)^{3/2} v^2 \mathrm{e}^{(-mv^2/2kT)}\mathrm{d}v = \frac{4}{\sqrt{\pi}}\left(\frac{v}{v_T}\right)^2 \mathrm{e}^{-(v/v_T)^2}\left(\frac{\mathrm{d}v}{v_T}\right) \tag{1}$$

$$\frac{n(E)\mathrm{d}E}{n} = \frac{2}{\sqrt{\pi}}\left(\frac{E}{kT}\right)^{1/2} \mathrm{e}^{(-E/kT)}\left(\frac{\mathrm{d}E}{kT}\right) \tag{2}$$

where:

$n(v)$ is the neutron density (number per unit velocity) as a function of the velocity,

n is the total neutron density,

m is the neutron mass, 939.563 MeV/c^2.

k is Boltzmann's constant, (8.617 × 10^{-5}) eV K^{-1},

T is the moderator temperature in Kelvin,

$v_T = (2kT/m)^{1/2}$ is the neutron velocity for energy kT, and

$n(E)$ is the neutron density as a function of the energy E.

The neutron density distribution, $n(E)$, is shown as a function of E/kT in Figure 2.

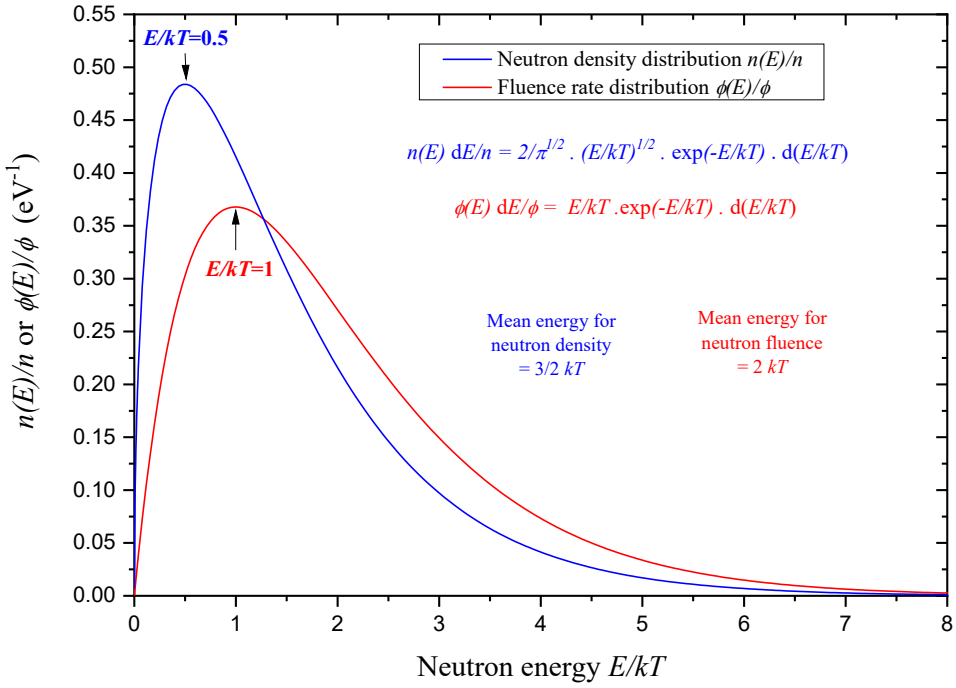

Figure 2. Maxwellian thermal neutron distributions for the neutron density and the fluence rate both as a function of the energy parameter kT.

If one considers the thermal neutron distribution of eq. (1) with dn neutrons cm^{-3} having a velocity between v and v+dv, i.e. dn = $n(v)$dv, then the fluence rate, $\mathrm{d}\phi$, of neutrons with velocity between v and v+dv is given by eq. (3):

$$\mathrm{d}\phi = \phi(v)\mathrm{d}v = n(v)v\mathrm{d}v \tag{3}$$

where $\phi(v)$ is the fluence rate as a function of velocity v.

This could be the fluence rate passing through a thin activation foil for instance. For a beam of thermal neutrons all travelling in one direction the relationship shown in eq. (3) is fairly obvious. If there are $n(v)$ neutrons per cm^3, all of velocity v, all travelling in the same direction, then $n(v)v$ neutrons per second will go through an area of one square cm perpendicular to the direction of motion, i.e. the number in a rectangular box of 1 cm × 1 cm × v cm. Although the derivation for an isotropic neutron field is not so obvious, the relationship given by eq.(3) is still true[9].

The total neutron density, n, is given by:

$$n = \int_0^\infty n(v)\mathrm{d}v \tag{4}$$

and the total fluence rate by:

$$\phi = \int_0^\infty \phi(v)\mathrm{d}v = \int_0^\infty n(v)\cdot v\,\mathrm{d}v = n\cdot\bar{v} \tag{5}$$

where $\bar{v}$ is the average velocity of the neutron density distribution, and for a Maxwellian is given by:

$$\bar{v} = \frac{\int_0^\infty n(v)\cdot v\,\mathrm{d}v}{\int_0^\infty n(v)\mathrm{d}v} = \frac{4}{\sqrt{\pi}}\int_0^\infty \mathrm{e}^{-(v/v_T)^2}\left(\frac{v}{v_T}\right)^3 \mathrm{d}v = \frac{2}{\sqrt{\pi}}v_T = 1.128v_T \tag{6}$$

Similarly the average energy of the neutron distribution, $\bar{E}$, is:

$$\bar{E} = \frac{\int_0^\infty n(E)\cdot E\,\mathrm{d}E}{\int_0^\infty n(E)\,\mathrm{d}E} = \int_0^\infty \frac{2}{\sqrt{\pi}}\mathrm{e}^{-E/kT}\left(\frac{E}{kT}\right)^{3/2}\mathrm{d}E = \frac{3}{2}kT \tag{7}$$

With the use of eqs (3), (5), and (6) expressions for the fluence rate distributions, i.e. the spectra can be derived from eqs (1) and (2), and these are:

$$\frac{\phi(v)\mathrm{d}v}{\phi} = \frac{n(v)v\mathrm{d}v}{\phi} = \frac{n}{\phi}\frac{4}{\sqrt{\pi}}\left(\frac{v}{v_T}\right)^2\mathrm{e}^{-(v/v_T)^2}v\frac{\mathrm{d}v}{v_T} = 2\left(\frac{v}{v_T}\right)^3\mathrm{e}^{-(v/v_T)^2}\frac{\mathrm{d}v}{v_T} \tag{8}$$

$$\frac{\phi(E)\mathrm{d}E}{\phi} = \frac{n(E)v\,\mathrm{d}E}{n\cdot\bar{v}} = \left(\frac{E}{kT}\right)\mathrm{e}^{(-E/kT)}\left(\frac{\mathrm{d}E}{kT}\right) \tag{9}$$

Note that $\phi(v)$ is the fluence rate per unit velocity interval, and $\phi(E)$ is the fluence rate per unit energy interval. The fluence rate distribution as a function of E/kT is included in Figure 2. It can be seen that the peak of the fluence rate distribution is at an energy kT, c.f. 0.5 kT for the density. When plotted on a linear energy scale the distributions are not symmetric, and the mean energies are 1.5 kT for the neutron density, and 2 kT for the fluence. If plotted on a logarithmic scale the distribution appears more symmetrical.

3 THE WESTCOTT CONVENTION

The formalism outlined above describes the thermal neutron spectrum in an ideal moderating material, however, in any real medium there are complications. Firstly, there will be slowing-down neutrons in the energy region above the Maxwellian distribution. These are normally assumed to have a $1/E$ energy dependence[8]. Secondly, the temperature parameterising the Maxwellian peak may not be that of the moderator material, but an effective or neutron temperature somewhat above the moderator temperature. Allowance must be made for these two facts and an approach to doing this was developed by Westcott and co-workers. Finally, it should be noted that, although the theory of neutron moderation predicts a Maxwellian peak and a $1/E$ component, it is to some extent a matter of faith that the actual spectrum in any particular, non-ideal, moderator assembly can be adequately described in terms of these two components, unless spectrum measurements can be performed.

The description below of Westcott fluences and their derivation is based primarily on the 1958 paper of Westcott, Walker, and Alexander[7], but it also includes elements from papers by Walker et al.,[10] Axton[11], Boot[12], Westcott[13], an IAEA report[9], and the book by Beckurts and Wirtz[8]. Newer references tend to be for neutron activation analysis, NAA, and follow closely the methodology of the earlier work when neutron spectrum information is limited.

The initial assumption is that the neutron density distribution per unit velocity interval, $n(v)$, is made up of two components and can be written as:

$$n(v) = n\,(1-f)\rho_m(v) + n\,f\,\rho_e(v) \tag{10}$$

where:

- n is the total neutron density including thermal and epithermal components,
- f is the fraction of the total neutron density in the epithermal, $1/E$, region,
- $\rho_m(v)$ is the Maxwellian neutron density distribution,
- $\rho_e(v)$ is the epithermal density distribution, i.e. for all neutrons not part of the Maxwellian distribution.

The individual density distributions are normalised to unity so that:

$$\int_0^\infty \rho_m(v)\,\mathrm{d}v = \int_0^\infty \rho_e(v)\,\mathrm{d}v = 1 \tag{11}$$

For a Maxwellian with an energy parameter kT and corresponding velocity, v_T, the distribution $\rho_m(v)$ is given, c.f. eq.(1) by,

$$\rho_m(v) = \frac{4}{\sqrt{\pi}}\frac{v^2}{v_T^3}\,\mathrm{e}^{-(v/v_T)^2} \tag{12}$$

The epithermal component is assumed to be proportional to $1/E$ per unit energy interval so that $\rho_e(v) \propto v^{-2}$ or $\rho_e(v) = a \cdot v^{-2}$ per unit velocity interval. Furthermore, this distribution is assumed to terminate at some lower energy; with the cut off being described by a delta function, Δ, at energy, μkT. The initial simplifying assumption is that $\Delta = 1$ *for* $E > \mu kT$, and $\Delta = 0$ *for* $E < \mu kT$. The velocity corresponding to this energy is $\sqrt{\mu}v_T$, so the normalisation of the epithermal distribution to unity gives:

$$\int_{\sqrt{\mu}v_T}^{\infty} a \cdot v^{-2} \mathrm{d}v = a \frac{1}{\sqrt{\mu}v_T} = 1 \tag{13}$$

so that:

$$\rho_e(v) = \sqrt{\mu}v_T \frac{\Delta}{v^2} \tag{14}$$

The neutron spectrum as a function of velocity can then be written as:

$$n(v) = n(1-f)\frac{4}{\sqrt{\pi}}\frac{v^2}{v_T^3}\mathrm{e}^{-(v/v_T)^2} + nf\sqrt{\mu}v_T\frac{\Delta}{v^2} \tag{15}$$

For a material irradiated in this field with an activation cross section for a particular reaction of $\sigma(v)$ the reaction rate per atom, D, (or the total reaction rate if the number of atoms is included in the equation) for a sample where self-shielding is negligible, is given by:

$$D = \int_0^{\infty} n(v)v \cdot \sigma(v)\,\mathrm{d}v = n(1-f)\int_0^{\infty}\frac{4}{\sqrt{\pi}}\frac{v^3}{v_T^3}\mathrm{e}^{-(v/v_T)^2}\sigma(v)\,\mathrm{d}v + nf\sqrt{\mu}v_T\int_0^{\infty}\frac{\Delta}{v}\sigma(v)\,\mathrm{d}v \tag{16}$$

The basis of the Westcott convention is the expression of the thermal neutron fluence rate as the quantity nv_0 where v_0 is a velocity of 2200 m.s^{-1} corresponding to an energy kT_0 where T_0 = 293.6 K (20.4°C), and the definition of an effective cross section $\hat{\sigma}$ so that:

$$D = nv_0\hat{\sigma} \tag{17}$$

To derive an expression for $\hat{\sigma}$ first consider a pure Maxwellian spectrum for a temperature T, i.e. one where $f = 0$ and designate the effective cross section for this spectrum as $\hat{\sigma}_m$, then:

$$\hat{\sigma}_m = \frac{1}{nv_0}n\int_0^{\infty}\frac{4}{\sqrt{\pi}}\frac{v^3}{v_T^3}\mathrm{e}^{-(v/v_T)^2}\sigma(v)\,\mathrm{d}v \tag{18}$$

The Westcott convention defines a function, g, which relates $\hat{\sigma}_m$ to the cross section σ_0 at kT_0 via $\hat{\sigma}_m = g\sigma_0$ then:

$$g = \hat{\sigma}_m / \sigma_0 = \frac{1}{v_0\sigma_0}\int_0^{\infty}\frac{4}{\sqrt{\pi}}\frac{v^3}{v_T^3}\mathrm{e}^{-(v/v_T)^2}\sigma(v)\,\mathrm{d}v \tag{19}$$

If $\sigma(v)$ can be written as $\sigma(v) = \sigma_0 v_0 / v$, i.e. the cross section of interest for the irradiated material has a pure 1/v dependence over the region of the Maxwellian, then $\sigma_0 v_0$ cancels out on the top and bottom on the right hand side, v^3 within the integral becomes v^2 and the value of the integral, and hence of g, is 1, c.f. eqs (11) and (12). (A number of materials have capture cross sections with a 1/v shape to a good approximation, particularly in the thermal region. A very simple explanation for this dependence is that the capture probability depends on the length of time for which the neutron is in the vicinity of the capturing nucleus.)

If this is not the case, values of g, which depend only on the Maxwellian part of the neutron spectrum and the cross section, can be calculated for reactions with known cross sections, as a function of the Maxwellian temperature T[10,14]. The quantity $nv_0g\sigma_0$ thus represents the activity produced by the Maxwellian part of the spectrum only, and the reason for g often being

close to 1 is that the intensity of the Maxwellian spectrum is very low in the higher energy epithermal region where the cross section may not have a 1/*v* shape.

For the gold foils used by NPL to measure thermal fluence *g* is very close to unity, the value at an effective temperature of 40 °C, similar to that in the column at the NPL thermal pile, is of the order of 1.0062, and this value changes only slowly with effective temperature. In the access hole *g* is of the order of 1.0052. The fact that *g* for gold is close to unity reflects the property that, except at large values of the temperature *T*, a Maxwellian spectrum does not extend into the region where the ^{197}Au cross section has resonance structure.

It is worth noting that σ_0 is not the fluence-averaged cross section for a 1/*v* detector in a pure Maxwellian field with a peak at velocity v_0, nor is it the neutron density averaged cross section in this field. Denoting the fluence averaged cross section by σ_ϕ and the neutron density averaged value by σ_n, then,

$$\sigma_\phi = \frac{\int_0^\infty n(v)\cdot v\cdot\sigma(v)\,\mathrm{d}v}{\int_0^\infty n(v)\cdot v\,\mathrm{d}v} \tag{20}$$

and

$$\sigma_n = \frac{\int_0^\infty n(v)\cdot\sigma(v)\,\mathrm{d}v}{\int_0^\infty n(v)\,\mathrm{d}v} \tag{21}$$

Using values for $n(v)$ from eq.(15) after setting *f* to zero, assuming $\sigma(v)=\sigma_0 v_0/v$, and setting $v_T = v_0$, the equations can be solved to give,

$$\sigma_\phi = \frac{\sqrt{\pi}}{2}\sigma_0 = 0.8862\sigma_0 \tag{22}$$

and

$$\sigma_n = \frac{2}{\sqrt{\pi}}\sigma_0 = 1.128\sigma_0 \tag{23}$$

For more realistic thermal calibration fields, when the fraction *f* is not zero, then:

$$\begin{aligned} D = nv_0\hat{\sigma} &= n(1-f)v_0\hat{\sigma}_m + nf\cdot v_T\sqrt{\mu}\int_0^\infty \frac{\Delta}{v}\sigma(v)\mathrm{d}v \\ &= nv_0\hat{\sigma}_m + nf\left[v_T\sqrt{\mu}\int_0^\infty \frac{\Delta}{v}\sigma(v)\,\mathrm{d}v - v_0\hat{\sigma}_m\right] \end{aligned} \tag{24}$$

The quantity $nv_0\hat{\sigma}_m$ is the activation that would occur if the neutrons were all in the Maxwellian distribution, so for a more realistic field $nfv_0\hat{\sigma}_m$ has to be subtracted in the term on the right.

Using the fact that $\rho_e(v)$ is normalised to unity, i.e. that:

$$v_T\sqrt{\mu}\int_0^\infty \frac{\Delta}{v^2}\,\mathrm{d}v = 1 \tag{25}$$

the value of $v_0\hat{\sigma}_m$ can be incorporated within the integral since it can be written as:

$$v_0\hat{\sigma}_m = v_0\hat{\sigma}_m v_T\sqrt{\mu}\int_0^\infty \frac{\Delta}{v^2}\,\mathrm{d}v \tag{26}$$

Inserting this expression into eq. (24) get:

$$D = nv_0\hat{\sigma} = nv_0\hat{\sigma}_m + nfv_T\sqrt{\mu}\left[\int_0^\infty\left(\frac{\Delta}{v}\sigma(v) - v_0\hat{\sigma}_m\frac{\Delta}{v^2}\right)\mathrm{d}v\right] \tag{27}$$

Writing $\hat{\sigma}_m$ as $g\sigma_0$, dividing by nv_0 and using the fact that dE/E = 2dv/v gives an expression for the effective cross section $\hat{\sigma}$:

$$\hat{\sigma} = g\sigma_0 + \frac{f\sqrt{\mu}}{2}\frac{v_T}{v_0}\left[\int_0^\infty\left(\sigma(v) - \frac{v_0\hat{\sigma}_m}{v}\right)\Delta\frac{\mathrm{d}E}{E}\right] = g\sigma_0 + \frac{f\sqrt{\mu}}{2}\frac{v_T}{v_0}\,\Sigma' \tag{28}$$

The integral, designated Σ', is a 'resonance integral' which, because of the Δ term, has an effective lower energy limit of μkT. It represents an integral over the cross section with the 1/v element subtracted. Over the relevant energy region the cross section is sometimes above, and in some cases below, a 1/v line. (See Figure 3 in the next section.) Note that Σ' differs slightly from the integrals sometimes defined in that the effective cross section $\hat{\sigma}_m = g\sigma_0$ is used rather than σ_0.

The quantities f and μ are independent of the cross section. They are characteristics of the field, and are usually combined together to form a parameter, r, sometimes called the spectral index, or the epithermal index, which is a measure of the magnitude of the 1/E epithermal component:

$$r = f(\pi\mu)^{1/2}/4 \tag{29}$$

Inserting the value for r into eq.(15), the neutron density distribution can then be expressed as:

$$n(v) = n\frac{4}{\sqrt{\pi}}\left[(1-f)\frac{v^2}{v_T^3}\,\mathrm{e}^{-(v/v_T)^2} + r\cdot v_T\frac{\Delta}{v^2}\right] \tag{30}$$

Similarly substituting r into eq.(28), the effective cross section can be written as:

$$\hat{\sigma} = g\sigma_0 + r\left(\frac{4T}{\pi T_0}\right)^{1/2}\left[\int_0^\infty\left(\sigma(v) - \left(\frac{E_0}{E}\right)^{1/2}\hat{\sigma}_m\right)\Delta\frac{\mathrm{d}E}{E}\right] = g\sigma_0 + r\left(\frac{4T}{\pi T_0}\right)^{1/2}\Sigma' \tag{31}$$

The integral Σ' depends only on the cross section and is, assuming a 1/E shape, independent of the intensity in the 1/E region. Defining the quantity s by:

$$s = \frac{1}{\sigma_0}\left(\frac{4T}{\pi T_0}\right)^{1/2}\left[\int_0^\infty\left(\sigma(v) - \left(\frac{E_0}{E}\right)^{1/2}\hat{\sigma}_m\right)\Delta\frac{\mathrm{d}E}{E}\right] = \frac{1}{\sigma_0}\left(\frac{4T}{\pi T_0}\right)^{1/2}\Sigma' \tag{32}$$

then the effective cross section in the Westcott convention can be written as:

$$\hat{\sigma} = \sigma_0(g + rs) \tag{33}$$

The expression for a reaction rate per atom is thus:

$$D = nv_0\hat{\sigma} = nv_0\sigma_0(g + rs) \tag{34}$$

The parameter s is a resonance integral divided by σ_0 and multiplied by a function of the temperature.

Values for g and s for a particular reaction, can be calculated; s from the cross section, and g from the cross section and a Maxwellian distribution, but the spectral index r is a feature of the spectrum and requires information about the full neutron distribution. Equation (34) links an activation or reaction rate to an effective cross section and the quantity nv_0. This is called a Westcott fluence where n is the total neutron density. Values of the Westcott fluence can also be derived for the Maxwellian distribution, the $1/E$ component, or any sub-section of the total field. As these Westcott fluences involve the velocity v_0 rather than an actual mean velocity, $\bar{v}$, they are not equal to the true fluences, the derivation of which requires information on the mean velocities of these distributions.

The interpretation of the quantities in eq.(34) is not immediately obvious. Because D is equal to $nv_0\sigma_0 g$ when there is no $1/E$ component, i.e. if $r = 0$, there is a tendency to think of $nv_0\sigma_0 g$ as the activity due to the Maxwellian component of the fluence, and $nv_0\sigma_0 rs$ as the activity due to the $1/E$ fluence. However, $nv_0\sigma_0 g$ is actually the activity that would be produced if all the neutrons were in a Maxwellian distribution, and $nv_0\sigma_0 rs$ contains a term $fnv_0\sigma_0 g$ which allows for the activity that is subtracted from $nv_0\sigma_0 g$ because a fraction f of the neutron field has a $1/E$ shape rather than a Maxwellian – see eq.(24). The use of the relationship shown in eq.(26) has allowed the term $fnv_0\sigma_0 g$ to be included in an integral over the energy range of the $1/E$ part of the spectrum, and to be a component in the quantity s which is a reduced resonance integral, i.e. one with the $1/v$ component of the cross section removed. This is possible because the activity induced by a particular fluence component in a material with a $1/v$ activation cross section does not depend on the energy of the fluence component.

If the cross section had a pure $1/v$ dependence over all energies, then g would be unity, and s would be zero, so D would be $nv_0\sigma_0$ regardless of the value of the spectral index r.

4 FLUENCE DERIVATION FROM ACTIVATION MEASUREMENTS

Unless reliable details of the neutron spectrum are available, from calculations for example, the derivation of Westcott fluences usually involves performing irradiations of activation samples both bare and under a cadmium cover. Cadmium has a very high cross section for absorbing thermal neutrons and a cadmium cover of suitable thickness, typically of the order of 1 mm, absorbs all thermal neutrons below a so-called cadmium cut-off energy at about 0.5 eV. These paired measurements provide information about the activation produced by the Maxwellian component and also that due to higher energy neutrons, and enables a value for r to be derived. There are, however, a number of issues involved in such measurements.

A $1/v$ detector would be the ideal measuring device as g would be unity and s zero and a measurement with such a detector would give the total neutron density or the fluence nv_0 in any spectrum. (To see this replace $\sigma(v)$ with $\sigma_0 v_0 / v$ in eq.(16).) Activation materials with this property over the full range of neutron energies do not exist. The reaction usually used to measure thermal neutron fluences is ^{197}Au(n,γ)^{198}Au. The cross section for this reaction satisfies the criterion of having a $1/v$ shape over the majority of the low-energy range up to the cadmium cut-off energy of about 0.5 eV, but not in the region above, where there is a very large resonance at 4.9 eV, and an unresolved resonance region at higher energies.

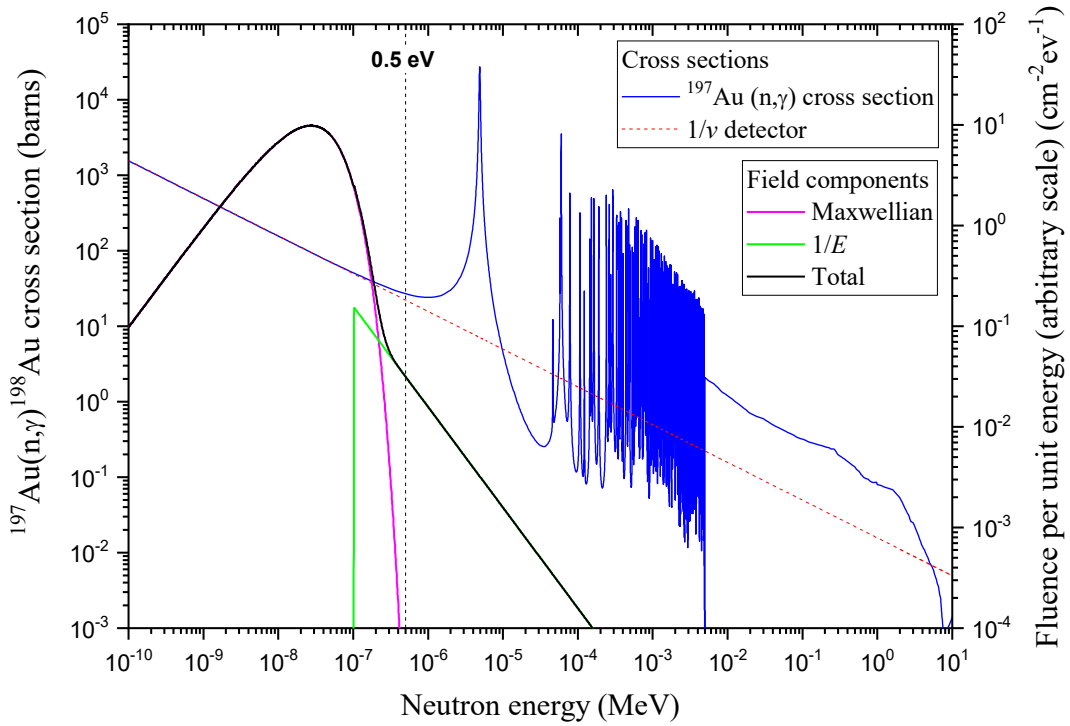

Figure 3. Cross sections for ^{197}Au(n,γ)^{198}Au with a representation of a thermal Maxwellian peak and a $1/E$ epi-thermal component. Note that the fluence is plotted (right hand scale) per unit energy. The spectrum is one calculated for the NPL thermal column. The response of a detector with a $1/v$ energy dependence has been included normalised to the ^{197}Au(n,γ) cross section at low energies.

A Fortran program, THERMALS, originally written simply to calculate a neutron spectrum consisting of a Maxwellian peak at a given temperature T and a $1/E$ component with an intensity that can be set, was modified during this work to calculate further quantities such as the activation of a foil, self-shielding corrections, etc. The program calculates the spectrum at a number of point energies (current maximum 50,000) distributed evenly on a linear or log scale between energy limits that can be set. Figure 3 shows a plot of a spectrum derived using THERMALS. Calculation of the activity, for example, requires the activation cross sections to

be available at the same energies as the spectrum. The approach used is to have them both as group averaged values. THERMALS includes interpolation procedures to allow for this, and the gold (n,γ) cross section in the same bin structure as the spectrum is shown in Figure 3.

The neutron spectrum is plotted as fluence per unit energy, with a Maxwellian peak and a $1/E$ component. The $1/E$ component is plotted with a sharp cut-off at an energy μkT of about 0.1 eV. It also has a cut-off at some point in the MeV region where the original neutrons are produced although this is off-scale in the figure. The plot highlights the importance of the resonance at 4.9 eV in terms of activation by neutrons above the cadmium cut-off. Neither the sharp beginning nor a sharp ending of the $1/E$ component is realistic although the value of the upper energy of the distribution is not important in view of the very small activation cross section in the MeV region compared to that in the lower energy region. The shape of the cut-off at the low energy end is discussed in section 7.2.3 and may depend on whether the neutron field is a beam or is isotropic.

A value for the activity of a bare gold foil, after subtraction of the activity of a cadmium covered foil, gives information about the thermal sub cadmium cut-off region, and the ratio of the bare to cadmium covered activities, a quantity called the cadmium ratio, enables information about the total spectrum to be derived. To obtain this information an expression for the activation produced in the foil irradiated under a cadmium cover, D_{Cd}, needs to be derived. Starting from eq.(16) and assuming that any contribution from the Maxwellian is negligible above a cadmium cut-off energy, E_{Cd}, this can be written as:

$$D_{Cd} = \int_{E_{Cd}}^{\infty} n(v) v \cdot \sigma(v)\, \mathrm{d}v = nf\sqrt{\mu} v_T \int_{v_{Cd}}^{\infty} \frac{\sigma(v)}{v}\, \mathrm{d}v = n\frac{4r}{\sqrt{\pi}} v_T \int_{v_{Cd}}^{\infty} \frac{\sigma(v)}{v}\, \mathrm{d}v \qquad (35)$$

Because $E_{Cd} >> \mu kT$ the Δ function of eq.(16) is 1 over the range of integration, so has been removed, $f\sqrt{\mu}$ has been replaced with $4r/\sqrt{\pi}$, and v_{Cd} is the velocity corresponding to E_{Cd}.

Before deriving an expression for D_{Cd} in a realistic situation an understanding of the twin foil technique is facilitated by first deriving the cadmium ratio, R, for a detector, often called an ideal detector, where self-shielding is negligible, and the cross section has an exact $1/v$ dependence and so can be written as $v_0\sigma_0 / v$. Assuming a sharp cadmium cut-off at energy E_{Cd}, substituting $v_0\sigma_0 / v$ for $\sigma(v)$, and denoting activities for this idealised detector with a dash, i.e. D'_{Cd}, get:

$$D'_{Cd} = n\frac{4r}{\sqrt{\pi}} v_T v_0 \sigma_0 \int_{v_{Cd}}^{\infty} \frac{1}{v^2}\, \mathrm{d}v = nv_0\sigma_0 \frac{4r}{\sqrt{\pi}} \frac{v_T}{v_{Cd}} = nv_0\sigma_0 \frac{4r}{\sqrt{\pi}} \sqrt{\frac{kT}{E_{Cd}}} \qquad (36)$$

As the activity, D' of a bare foil in this field for an idealised detector, where $g = 1$ and $s = 0$, is given by $nv_0\sigma_0$, the cadmium ratio, R, for this detector is:

$$R = \frac{D'}{D'_{Cd}} = \frac{nv_0\sigma_0}{nv_0\sigma_0 \left(\frac{4r}{\sqrt{\pi}} \sqrt{\frac{\mathrm{k}T}{E_{Cd}}} \right)} = \frac{1}{4r} \sqrt{\frac{\pi E_{Cd}}{kT}} \qquad (37)$$

This ratio R of activities for an ideal detector is a direct ratio of the total Westcott fluence to the epi-cadmium Westcott fluence (i.e. the fluence above the cadmium cut-off) and is used to provide this information when deriving the total Westcott fluence from that measured for the sub-cadmium region.

The expression for R in eq.(37) was derived on the basis of a delta function at E_{Cd}. This is an approximation to the shape of the true cadmium cut off function. This depends on the cadmium thickness and the angular properties of the neutron field. Computer calculations have been performed by Westcott et al.[7] using the energy dependence of the cadmium cross section. These provide a more accurate expression for R in terms of a parameter K, which allows for the characteristics of the cadmium cover and field direction, and the quantity $r(T/T_0)^{1/2}$ which tends to be used rather than r in situations where the neutron temperature is uncertain.

$$R = K / r(T/T_0)^{1/2} \tag{38}$$

According to eq.(37) K should be given roughly by:

$$K = \frac{1}{4}\left(\frac{\pi E_{Cd}}{kT}\right)^{1/2}\left(\frac{T}{T_0}\right)^{1/2} = \frac{1}{4}\left(\frac{\pi E_{Cd}}{kT_0}\right)^{1/2} \tag{39}$$

For $E_{Cd} = 0.50$ eV, $kT_0 =$ 0.0253 eV, the equation gives, K=1.97. For the calculations in reference (7), K varies from 1.82 for 0.5 mm of cadmium and beam geometry, to 2.62 for 2.5 mm of cadmium and isotropic incidence.

The expression for D'_{Cd} given in eq.(36) is for the activation of a material with a $1/v$ cross section in the epi-cadmium region. The derivation of the more general case for a cross section with structure in the epi-cadmium region starts from eq.(35) which can be rewritten as:

$$D_{Cd} = n\frac{4r}{\sqrt{\pi}}v_T\int_{v_{Cd}}^{\infty}\frac{\sigma(v)}{v}\,\mathrm{d}v = n\frac{4r}{\sqrt{\pi}}v_T\int_{v_{Cd}}^{\infty}\left(\frac{\sigma(v)}{v}-\frac{v_0\hat{\sigma}_m}{v^2}\right)\mathrm{d}v + n\frac{4r}{\sqrt{\pi}}v_T\int_{v_{Cd}}^{\infty}\frac{v_0\hat{\sigma}_m}{v^2}\,\mathrm{d}v \tag{40}$$

The first term involves an integral over the region above E_{Cd} where there are resonances, but with the activity due to a $1/v$ component in the cross section removed. The second term adds this back in. After further re-arrangement, and using the fact that $\mathrm{d}E/E = 2\mathrm{d}v/v$:

$$\begin{aligned} D_{Cd} &= nv_0\left[r\frac{4}{\sqrt{\pi}}\frac{v_T}{v_0}\frac{1}{2}\int_{E_{Cd}}^{\infty}\left(\sigma(E)-\left(\frac{E_0}{E}\right)^{1/2}\hat{\sigma}_m\right)\Delta\frac{\mathrm{d}E}{E} + \frac{4r}{\sqrt{\pi}}v_T\int_{v_{Cd}}^{\infty}\frac{g\sigma_0}{v^2}\,\mathrm{d}v\right] \\ &= nv_0\sigma_0\left[r\frac{1}{\sigma_0}\left(\frac{4T}{\pi T_0}\right)^{1/2}\int_{E_{Cd}}^{\infty}\left(\sigma(E)-\left(\frac{E_0}{E}\right)^{1/2}\hat{\sigma}_m\right)\Delta\frac{\mathrm{d}E}{E} + \frac{4r}{\sqrt{\pi}}v_T g\int_{v_{Cd}}^{\infty}\frac{1}{v^2}\,\mathrm{d}v\right] \end{aligned} \tag{41}$$

By comparing with eq.(32) it can be seen that the first term within the square brackets is equal to rs. The fact that the integral for s as shown in eq.(32) extends from the value defined by the function Δ rather than E_{Cd} which is the value appropriate for D_{Cd} is usually ignored [7]. If the cross section in the μkT to E_{Cd} region follows the $1/v$ law reasonably closely the two cross section terms in the integral are essentially the same in this interval and the contribution to the s factor is negligible so the value of s can be taken to be the same for the region above E_{Cd} as for the region above μkT. This conclusion is insensitive to the cut off function Δ. A correction can be applied [10], and this is addressed later in the report – see section 7.2.3 - together with other corrections to D_0 and D_{Cd} introduced by other effects such as self-shielding.

The second term in eq.(41) is the same as in eq.(36) except for the inclusion of the g factor. Thus using eq.(39) the expression for D_{Cd} can be written as:

$$D_{Cd} = nv_0\sigma_0\left(rs + g\frac{4r}{\sqrt{\pi}}\sqrt{\frac{kT}{E_{Cd}}}\right) = nv_0\sigma_0\left(rs + g\frac{r}{K}\left(\frac{T}{T_0}\right)^{1/2}\right) \tag{42}$$

The measured cadmium ratio R_{Cd} is then given by:

$$R_{Cd} = \frac{D_0}{D_{Cd}} = \frac{nv_0\sigma_0(g+rs)}{nv_0\sigma_0\left(rs + g\frac{r}{K}\left(\frac{T}{T_0}\right)^{1/2}\right)} = \frac{(g+rs)}{r\left(s + \frac{g}{K}\left(\frac{T}{T_0}\right)^{1/2}\right)} \tag{43}$$

With g, s, and K available from calculations, $r(T/T_0)^{1/2}$, which is a measure of the intensity of the $1/E$ component, can be calculated from a measured cadmium ratio R_{Cd} using eq.(43). (See later in this section for details.) The cadmium ratio for an ideal detector can then be derived from eq.(38). This allows the total fluence in the Westcott convention to be calculated – see below.

In practice, activity is not measured per atom, but per unit mass of the activated material requiring the introduction of the number of atoms per unit mass of any activated sample into the equations. Also, all the derivations to date have neglected self-shielding. This is an added complication for which allowance needs to be made.

Denoting the saturated activity per unit mass in the bare sample by D_0 and the corresponding value for the cadmium covered sample by $D_0(Cd)$ then the thermal (sub-cadmium cut-off) fluence in the Westcott convention $\phi_W(th)$ is given, c.f. eq.(34), by:

$$\phi_W(th) = n_{th}v_0 = \frac{1}{G_t}\cdot\frac{(D_0 - D_0(Cd)\cdot F_{Cd})}{N\sigma_0 g} \tag{44}$$

where the new quantities are:

n_{th}	the neutron density in the sub-cadmium-cut-off region,
G_t	the thermal neutron self-shielding factor, a number ≤ 1,
F_{Cd}	a correction factor for attenuation of epi-cadmium neutrons in cadmium,
N	the number of atoms per unit mass (usually mg).

An approximation in the above equation for $\phi_W(th)$, where (g+rs) has been reduced to just g, in the denominator, needs an explanation, c.f. eq.(34). There are two necessary conditions:

a) Since g is calculated by integrating a Maxwellian over the whole energy region, see eq.(19), the Maxwellian component above E_{Cd} needs to be negligible for the integral from zero to E_{Cd} to be the same as the integral over the full energy range. This is true except at high Maxwellian temperatures T.

b) The product rs is negligible for the region up to E_{Cd}. This is usually true, firstly, because the $1/E$ component below E_{Cd} is small, and secondly, because the gold cross section is quite closely $1/v$ between the lower limit of the $1/E$ spectrum at μkT and E_{Cd}. The integral in the expression for s is thus very small, c.f. eq. (32) with the upper limit of integration set to E_{Cd} and the two terms in the integral practically cancelling out.

The total Westcott fluence is obtained by multiplying $\phi_W(th)$ by the factor $R/(R\text{-}1)$ which represents the ratio of the total Westcott fluence to that below the cadmium cut-off energy. Thus:

$$\phi_W = nv_0 = \frac{1}{G_t}\cdot\frac{(D_0 - D_0(Cd)\cdot F_{Cd})}{N\sigma_0 g}\cdot\frac{R}{(R-1)} \tag{45}$$

The Maxwellian fluence $\phi_W(M)$ is then:

$$\phi_W(M) = n_M v_0 = nv_0(1-f) = nv_0\left[1-\frac{4r}{(\pi\mu)^{1/2}}\right] \tag{46}$$

where n_M is the total neutron number density for the Maxwellian peak.

The $1/E$ Westcott fluence $\phi_W(1/E)$ is given by:

$$\phi_W(1/E) = n_{1/E} v_0 = nv_0 - n_M v_0 \tag{47}$$

where $n_{1/E}$ is the total neutron density in the $1/E$ region.

It remains to derive values for r and R to complete the calculation of the four Westcott fluences defined above. For this eq.(43) for R_{Cd} requires further refinement to allow for self-shielding, and for the small effect of absorption of epi-cadmium neutrons in the cadmium.

The equation for the s factor contains the term $(T/T_0)^{1/2}$ and to remove this dependence on T a new factor s_0 is introduced defined by $s_0 = s(T_0/T)^{1/2}$. On introducing self-shielding factors G_t and G_r for the thermal and resonance regions respectively, and including a factor f_r for attenuation of resonance neutrons in the cadmium shield, eq.(43) can be written as:

$$\begin{aligned} R_{Cd} &= \frac{\left(G_t g + G_r r s_0\left(\frac{T}{T_0}\right)^{1/2}\right)}{\left(f_r G_r r s_0\left(\frac{T}{T_0}\right)^{1/2} + g\frac{r}{K}\left(\frac{T}{T_0}\right)^{1/2}\right)} = \frac{\left(G_t + G_r r\frac{s_0}{g}\left(\frac{T}{T_0}\right)^{1/2}\right)}{\left(f_r G_r r\frac{s_0}{g}\left(\frac{T}{T_0}\right)^{1/2} + \frac{r}{K}\left(\frac{T}{T_0}\right)^{1/2}\right)} \\ &= \frac{\left(\frac{G_t}{r(T/T_0)^{1/2}} + G_r\frac{s_0}{g}\right)}{\left(f_r G_r\frac{s_0}{g} + \frac{1}{K}\right)} \end{aligned} \tag{48}$$

There is no self-shielding term associated with the component $g\frac{r}{K}\left(\frac{T}{T_0}\right)^{1/2}$. This is because it corresponds to activation due to a $1/v$ cross section in the region above E_{Cd} where the value of the cross section and hence the self-shielding is small.

As discussed in the derivation of D_{Cd}, there is one other small correction that can be included in the general expression for R_{Cd}. The factor s_0 in the numerator is for the complete spectrum whereas in the denominator it is for the spectrum under cadmium i.e. for neutrons above E_{Cd}. Using the expression for s from eq.(32) then:

$$\begin{aligned} \frac{s_0}{g} &= \frac{s(T_0/T)^{1/2}}{g} = \frac{1}{g\sigma_0}\left(\frac{4}{\pi}\right)^{1/2}\int_0^\infty\left(\sigma(E) - \left(\frac{E_0}{E}\right)^{1/2} g\sigma_0\right)\Delta\frac{\mathrm{d}E}{E} \\ &= \frac{2}{\sqrt{\pi}}\frac{1}{g\sigma_0}\int_{\mu kT}^{E_{Cd}}\left(\sigma(E) - \left(\frac{E_0}{E}\right)^{1/2} g\sigma_0\right)\frac{\mathrm{d}E}{E} + \frac{2}{\sqrt{\pi}}\frac{1}{g\sigma_0}\int_{E_{Cd}}^\infty\left(\sigma(E) - \left(\frac{E_0}{E}\right)^{1/2} g\sigma_0\right)\frac{\mathrm{d}E}{E} \end{aligned} \tag{49}$$

Here the integration has been split into two regions, μkT to E_{Cd} and E_{Cd} to infinity, or more precisely the end of the spectrum. The second integral gives the appropriate s_0/g value for the cadmium covered measurement. The first term needs to be subtracted for any material with a cross section that diverges from a $1/v$ shape in the μkT to E_{Cd} region. This correction, denoted by W, is small for gold where the cross section shape in this region does not deviate significantly from a $1/v$ shape. The calculated value in reference (10) for W is 0.027, (c.f. a value of about 17 for s_0/g, so a very small correction) although W may be larger for other materials (see section 7.2.6 for further details).

The expression for the measured cadmium ratio R_{Cd} then becomes:

$$R_{Cd} = \frac{\left(\frac{G_t}{r(T/T_0)^{1/2}} + G_r\frac{s_0}{g}\right)}{\left(f_r G_r\left(\frac{s_0}{g} - W\right) + \frac{1}{K}\right)} \tag{50}$$

Equation (no. 4) in the paper of Walker, Westcott, and Alexander[10], from where the logic for obtaining the equation above was derived, differs slightly from eq.(50). A term $h(r\sqrt{T/T_0})^{-1}$ is included there for transmission of thermal neutrons through the cadmium cover. For a sufficiently thick cadmium layer this is unnecessary, although this raises the question of just how thick the cadmium needs to be.

Also, there is no correction for thermal self-shielding in reference (10), presumably because the gold layers used were very thin, roughly 1/100th of the thickness of the foils usually used at NPL which are typically around 98 mg/cm^2 (0.05 mm or 2 thou) thick. One other aspect that the introduction of the correction factor W highlights is that the G_r value in the numerator and denominator refer to slightly different energy regions. This is usually ignored, but is discussed in section 7.2.6.

Equation (50) is the one used to obtain the parameter r which is used in deriving the Maxwellian fluence from the total fluence – see eq.(46) – and in determining the cadmium ratio R for an ideal detector. The quantity that needs to be derived from eq.(46) in order to calculate R using eq.(34) and eventually nv_0 using eq.(41) is $r(T/T_0)^{1/2}$ and the equation for R is then:

$$R = K/r(T/T_0)^{1/2} = \frac{K\left(R_{Cd}\left(f_r G_r\left(\frac{s_0}{g} - W\right) + \frac{1}{K}\right) - G_r\frac{s_0}{g}\right)}{G_t} \tag{51}$$

When using the Westcott convention the quantities obtained from measurements with thin activation foils are the various Westcott fluence rates. These are a neutron density times v_0, where v_0 is 2200 m s^{-1}, which is the velocity at the peak of a Maxwellian thermal fluence distribution for a moderator at a temperature of 293.6 K (20.4 C). For such a distribution the peak energy, given by, kT, is 0.0253 eV.

This approach is simply a convention, and nv_0 is not equal to the true total fluence rate, this is given by $n\bar{v}$, i.e. for the true fluence rate one needs to know $\bar{v}$, and hence have information about the neutron spectrum. Because of the use of v_0 the high energy fluence is significantly underestimated.

Although the Westcott fluence differs from the true value the reason for quoting it is that the exact spectrum in most thermal neutron fields is not known. Using the Westcott convention means that this does not matter in many applications particularly those involving foil activation.

5 THE TRUE NEUTRON FLUENCE RATE VALUES

To derive the true fluence rate the ratio $\bar{v}/v_0$ of the average velocity $\bar{v}$ to v_0 needs to be known, and this depends on the effective temperature of the moderator. From the cadmium ratio obtained from gold foil activation measurements, an estimate of the intensity of the 1/*E* fluence relative to the Maxwellian fluence in the Westcott convention is available. From this an estimate of the effective temperature of the Maxwellian can be derived using an empirical relationship[8,15,16].

$$\frac{T - T_M}{T_M} = C \frac{n_{1/E} v_0}{n_M v_0} \tag{52}$$

where:

T	is the effective temperature of the Maxwellian,
T_M	is the physical temperature of the moderator,
C	is a constant.

Beckurts and Wirtz[8] derive the expression, and give a value of 1.65 for the constant *C*, but that is for a heavy gas moderator. Kűchle[16] quotes 4.8 ± 1.7 for a graphite moderator. Geiger and van der Zwan[15], using a technique based on the activation of ^{176}Lu foils, derived a value of 3.2 ± 0.4 for their graphite moderator which uses radioactive sources to produce the primary neutrons. Since 3.2 is near the mean, this value is assumed for the NPL thermal pile with an uncertainty* of 1.6 to cover the range of quoted values.

From extensive sets of measurements in the NPL thermal column $n_{1/E}/n_m$ varies with height going from roughly 0.030 at 1 m to roughly 0.020 at 2 m. This corresponds to $T - T_M$ varying from 28.1°C to 18.6°C and kT varying from 0.0278 eV to 0.0270 eV for T_M = 21.4°C (294.6 K), a typical pile temperature at NPL. A typical value of $T - T_M$ is thus about 23.4°C. In view of the spread of values for the constant *C,* an uncertainty of ±11°C is assigned to $T - T_M$ which mainly reflects the spread of values reported for the parameter *C*.

Down the access hole at the centre of the pile the spectrum is much better moderated. Again the ratio $n_{1/E}/n_m$ decreases with increasing height, but near the bottom of the column the value is about 0.008 giving a value for $T - T_M$ of 7.5°C when T_M = 21.4°C.

Knowing a value for the effective temperature an estimate of $\bar{v}/v_0$ can be made for both the thermal Maxwellian and the 1/*E* components, and finally an estimate for the true fluence can be derived. From eq.(6), if $\bar{v}_m$ is the mean velocity of the Maxwellian distribution, with corresponding temperature *T*, then:

$$\frac{\bar{v}_M}{v_0} = \left[\frac{4T}{\pi T_0} \right]^{1/2} \tag{53}$$

Where T_0 = 293.6 K, corresponds to energy $E_0 = kT_0$,

* Because this report includes estimates of uncertainties from the published scientific literature, where uncertainties are quoted at the 1σ level, i.e. k=1, all uncertainties quoted or derived in this report are quoted for consistency at k=1.

Even for a perfect room temperature moderator, which would give a Maxwellian with a temperature of 293.6 K, $\bar{v}/v_0 = 2/\sqrt{\pi} = 1.128$, which means that the true fluence rate is 12.8 % higher than $n_m v_0$; (see Section 2) and since few moderator assemblies are ideal, the actual value of this ratio is likely to be higher still.

To calculate the true $1/E$ fluence component the average velocity $\bar{v}_{1/E}$ for this region needs to be calculated from:

$$\bar{v}_{1/E} = \frac{\int_{v_L}^{v_H} n(v) \cdot v \, \mathrm{d}v}{\int_{v_L}^{v_H} n(v) \, \mathrm{d}v} \tag{54}$$

where:

v_L is the velocity of the low energy limit of the $1/E$ component, corresponding to an energy E_L

v_H is the velocity of the high energy limit of the $1/E$ component, corresponding to an energy E_H.

The energy E_L would normally be μkT, while the upper energy limit E_H would be E_{Cd} for the sub-cadmium fluence, or the highest energy in the spectrum if the total $1/E$ component is considered. Because the spectrum in this region is assumed to be a simple function of the energy E, it is convenient to convert the integrals in eq.(54) to ones over energy. The quantity $n(v)$ is the neutron density per unit volume so should be written as $\mathrm{d}n/\mathrm{d}v$, and this can be related to the fluence per unit velocity $\mathrm{d}\phi/\mathrm{d}v$, or the fluence per unit energy $\mathrm{d}\phi/\mathrm{d}E$ which can be written as Q/E, where Q represents the intensity of the $1/E$ spectrum. The quantities within the integrals of eq. (54) can then be written, using the fact that $E = 1/2mv^2$ as:

$$\begin{aligned} n(v) \cdot v \, \mathrm{d}v &= \frac{\mathrm{d}n}{\mathrm{d}v} \cdot v \, \mathrm{d}v = \frac{\mathrm{d}\phi}{\mathrm{d}v} \mathrm{d}v = \frac{\mathrm{d}\phi}{\mathrm{d}E} \frac{\mathrm{d}E}{\mathrm{d}v} \mathrm{d}v = Q \frac{\mathrm{d}E}{E} \\ n(v) \, \mathrm{d}v &= \frac{\mathrm{d}n}{\mathrm{d}v} \mathrm{d}v = \frac{\mathrm{d}\phi}{\mathrm{d}v} \cdot \frac{1}{v} \mathrm{d}v = \frac{\mathrm{d}\phi}{\mathrm{d}E} \frac{\mathrm{d}E}{\mathrm{d}v} \left(\frac{m}{2E} \right)^{1/2} \mathrm{d}v = Q \left(\frac{m}{2} \right)^{1/2} \frac{\mathrm{d}E}{E^{3/2}} \end{aligned} \tag{55}$$

With $v_0 = \left(2E_0/m\right)^{1/2}$ an equation for $\bar{v}_{1/E}/v_0$ can be derived, c.f. reference (12) as:

$$\frac{\bar{v}_{1/E}}{v_0} = \frac{\int_{E_L}^{E_H} Q \frac{\mathrm{d}E}{E}}{\left(\frac{2E_0}{m} \right)^{1/2} \int_{E_L}^{E_H} Q \left(\frac{m}{2} \right)^{1/2} \frac{\mathrm{d}E}{E^{3/2}}} = \frac{\ln(E_H/E_L)}{2E_0^{1/2} \left[E_L^{-1/2} - E_H^{-1/2} \right]} \tag{56}$$

Depending on the value of E_H, the average velocity $\bar{v}_{1/E}$, and thus the true fluence, is available for any part of the $1/E$ component. One important part is that between μkT and E_{Cd} and denoting this by $\phi(1/E<E_{Cd})$ it is given by:

$$\phi(1/E < E_{Cd}) = (n_{th} v_0 - n_m v_0) \cdot \frac{\bar{v}_{1/E}}{v_0} = (n_{th} v_0 - n_m v_0) \cdot \frac{\ln(E_{Cd}/\mu kT)}{2E_0^{1/2} \left[(\mu kT)^{-1/2} - E_{Cd}^{-1/2} \right]} \tag{57}$$

If the true Maxwellian fluence and the true sub cadmium cut-off fluences are denoted by $\phi(M)$ and $\phi(th)$ respectively then:

$$\phi(M) = n_m v_0 \cdot \frac{\bar{v}_M}{v_0} \tag{58}$$

$$\phi(th) = \phi(M) + \phi(1/E < E_{Cd}) \tag{59}$$

The quantity $\phi(th)$ is the one given as the thermal fluence when calibrating a device where an irradiation under cadmium can be performed to account for its response to epithermal neutrons.

6 CALCULATION OF WESTCOTT FLUENCES

Calculation of $\phi(th)$ was originally performed by hand, until that approach was replaced by the use of a Fortran program called WESTCOTT. This in turn has largely been replace by the use of spreadsheets, e.g. nvcalc. The WESTCOTT program does, however, print out a useful summary of the analysis and two examples have been included here, one for gold foil measurements at a height of 1.5 m in the thermal column, and one for a measurement near the bottom of the access hole. The symbols used are largely those of this report although it was not possible to produce $\bar{v}$ so this velocity is designated by v(bar) in the print-out.

These examples use the parameters in use at NPL up until production of this report and are for situations where the deuteron beam on the beryllium targets, and hence the neutron fluence rate, were near their maximum achievable values.

The two printouts highlight the differences in the fields in these locations in terms of the fluence rate and the epithermal component. For the column, the fluence rate was about 2.4×10^4 cm^{-2} s^{-1}, the cadmium ratio 7.6, the epicadmium fluence rate about 27% of the total, and the $1/E$ component in the region below the cadmium cut off energy about 3.4% of the total fluence rate in this region. The corresponding figures for the bottom of the access hole were: 1.1×10^7 cm^{-2} s^{-1}, 28.5, 10%, and 1.3%.

```
PROGRAM WESTCOTT  -  Version 1.6 compiled    July 2023
THERMAL AND EPITHERMAL FLUENCES CALCULATED FROM FOIL ACTIVATION

Run date: 10-08-2023                Run time: 16:56:08

Average at 1.5m posn in thermal column for demand 12 from Au foil calibration history

  D0(bare)      D0(Cd)     Eff Temp K     FC rate
 6.8870E+00  9.0460E-01  3.1880E+02  5.0000E+03

      FCd        At Wt        G(th)      W-cott g     Sigma(0)      Emax
 1.0100E+00  1.9697E+02  9.8430E-01  1.0046E+00  9.8690E+01  2.0000E+06

   G(res)        S(0)      Res Attn f        W       W-cott K        mu
 3.6700E-01  1.7300E+01  9.9000E-01  2.7000E-02  1.9939E+00  3.6810E+00


CALCULATED RATIOS AND FLUENCES  (kT = 0.0275 eV)

    R(Cd)    r(T/T0)^1/2        r         R(1/v)
 7.6133E+00  2.1845E-02  2.0964E-02  9.1276E+01

  n(th)v(0)      nv(0)      n(M)v(0)    n(1/E)v(0)     n(1/E)/n(M)
 2.0020E+04  2.0242E+04  1.9743E+04  4.9914E+02     2.5282E-02

  For the kT and mu values used:
  ECd =  5.1227E-01 eV    El =   1.0112E-01 eV
  Epithermal neutron density fraction f=[4*r/sqrt(Pi*mu)] =   2.4659E-02

  For the Maxwellian distn. v(bar)/v(0)  =   1.1758E+00
  thus v(bar) for the Maxwellian         =   2.5868E+05 cm/sec
  n(M)v(bar) i.e. the Maxwellian fluence =   2.3214E+04

  For total 1/E component v(bar)/v(0)    =   1.6797E+01
  thus v(bar) for total 1/E component    =   3.6954E+06 cm/sec
  n(1/E)V(bar) for total 1/E component   =   8.3843E+03
  n(1/E)v(bar) per unit lethargy         =   4.9895E+02

  For the total spectrum v(bar)/v(0)     =   1.5610E+00
  thus v(bar) for total spectrum         =   3.4342E+05 cm/sec
  total fluence n(m)v(bar)+n(1/E)v(bar)  =   3.1598E+04

  Total 1/E fluence is
  36.12 % of n(M)v(bar),34.90 % of n(th)v(bar), and 26.53 % of nv(bar)

  For 1/E fluence El to ECd v(bar)/v(0)  =   2.9186E+00
  thus v(bar) for this region            =   6.4210E+05 cm/sec
  n(1/E)v(bar) between El and E(Cd)      =   8.0956E+02
  this is  3.487 % of n(M)v(bar), 3.370 % of n(th)v(bar,) and 2.562 % of nv(bar)

  For total sub-Cd neutrons v(bar)/v(0)  =   1.2000E+00
  thus v(bar) for the sub-Cd neutrons    =   2.6399E+05 cm/sec
  n(th)v(bar) i.e. the sub-Cd fluence    =   2.4024E+04
  It is made up of 96.630 % from the Maxwellian and  3.370 % from the 1/E part
  It is 76.028 % of the total fluence nv(bar)

  Neutron densities
  Maxwellian neutron density n(M)        =   8.9741E-02
  Total sub-Cd neutron density n(th)     =   9.1002E-02
  Total 1/E neutron density n(1/E)       =   2.2688E-03
  Total neutron density n                =   9.2010E-02
  n(1/E) between El and E(Cd)            =   1.2608E-03
  this is  1.405 % of n(M) and  1.385 % of n(th)

  Fluences divided by the fission chamber count rate
  n(th)v(0)      nv(0)      n(M)v(0)   n(th)v(bar)  n(M)v(bar)
 4.0041E+00  4.0484E+00  3.9486E+00  4.8047E+00  4.6428E+00
```

```
PROGRAM WESTCOTT  -  Version 1.6 compiled  August 2023
THERMAL AND EPITHERMAL FLUENCES CALCULATED FROM FOIL ACTIVATION

Run date: 18-08-2023                Run time: 15:00:48

Data from access hole check at height 1 on 8 March 2021

  D0(bare)      D0(Cd)     Eff Temp K     FC rate
 2.7893E+03  9.7975E+01  3.0250E+02  1.0873E+04

      FCd        At Wt         G(th)       W-cott g     Sigma(0)      Emax
 1.0100E+00  1.9697E+02  9.3477E-01  1.0046E+00  9.8690E+01  2.0000E+06

   G(res)        S(0)      Res Attn f        W        W-cott K        mu
 2.6932E-01  1.7300E+01  9.9000E-01  2.7000E-02  2.2931E+00  3.6810E+00


CALCULATED RATIOS AND FLUENCES  (kT = 0.0261 eV)

    R(Cd)    r(T/T0)^1/2        r         R(1/v)
 2.8469E+01  6.7596E-03  6.6594E-03  3.3924E+02

  n(th)v(0)      nv(0)      n(M)v(0)    n(1/E)v(0)     n(1/E)/n(M)
 9.4946E+06  9.5227E+06  9.4481E+06  7.4593E+04     7.8950E-03

  For the kT and mu values used:
  ECd =  6.7754E-01 eV     El =   9.5952E-02 eV
  Epithermal neutron density fraction f=[4*r/sqrt(Pi*mu)] =   7.8332E-03

  For the Maxwellian distn. v(bar)/v(0)  =   1.1454E+00
  thus v(bar) for the Maxwellian         =   2.5198E+05 cm/sec
  n(M)v(bar) i.e. the Maxwellian fluence =   1.0821E+07

  For total 1/E component v(bar)/v(0)    =   1.6413E+01
  thus v(bar) for total 1/E component    =   3.6109E+06 cm/sec
  n(1/E)V(bar) for total 1/E component   =   1.2243E+06
  n(1/E)v(bar) per unit lethargy         =   7.2633E+04

  For the total spectrum v(bar)/v(0)     =   1.2650E+00
  thus v(bar) for total spectrum         =   2.7829E+05 cm/sec
  total fluence n(m)v(bar)+n(1/E)v(bar)  =   1.2046E+07

  Total 1/E fluence is
  11.31 % of n(M)v(bar),11.17 % of n(th)v(bar), and 10.16 % of nv(bar)

  For 1/E fluence El to ECd v(bar)/v(0)  =   3.0517E+00
  thus v(bar) for this region            =   6.7137E+05 cm/sec
  n(1/E)v(bar) between El and E(Cd)      =   1.4197E+05
  this is  1.312 % of n(M)v(bar), 1.295 % of n(th)v(bar,) and 1.179 % of nv(bar)

  For total sub-Cd neutrons v(bar)/v(0)  =   1.1547E+00
  thus v(bar) for the sub-Cd neutrons    =   2.5403E+05 cm/sec
  n(th)v(bar) i.e. the sub-Cd fluence    =   1.0963E+07
  it is made up of 98.705 % from the Maxwellian and  1.295 % from the 1/E part
  it is 91.015 % of the total fluence nv(bar)

  Neutron densities
  Maxwellian neutron density n(M)        =   4.2946E+01
  Total sub-Cd neutron density n(th)     =   4.3157E+01
  Total 1/E neutron density n(1/E)       =   3.3906E-01
  Total neutron density n                =   4.3285E+01
  n(1/E) between El and E(Cd)            =   2.1146E-01
  this is  0.492 % of n(M) and  0.490 % of n(th)

  Fluences divided by the fission chamber count rate
  n(th)v(0)      nv(0)      n(M)v(0)   n(th)v(bar)  n(M)v(bar)
 8.7320E+02  8.7578E+02  8.6892E+02  1.0083E+03  9.9522E+02
```

7 PARAMETER VALUES AND THEIR UNCERTAINTIES

The parameters discussed below are those used for calculation of the various fluence rate quantities from the bare and cadmium covered gold activities D_0 and $D_0(Cd)$ respectively. The uncertainties in the derivation of the saturated activities of the gold foils are not discussed, although typical uncertainties are used to identify the major components in the fluence uncertainties. The quantities used in the calculation of the thermal (sub-cadmium cut off) Westcott fluence via eq.(44) are first considered, followed by those involved in calculating the total Westcott fluence, and then the true thermal fluence.

7.1 Uncertainties in the Westcott fluence $n_{th}v_0$

7.1.1 The gold thermal neutron capture cross section at $v_0 = 2200$ m s^{-1}

The most recent evaluation of the ^{197}Au(n,γ) cross section at 0.0253 eV can be found in the journal Nuclear Data Sheets in the paper by Carlson et al.[17]. The value is 98.66 ± 0.14 (0.14%).

7.1.2 Number of atoms N per unit mass (mg)

This is Avogadro's constant (number of particles per mol) divided by the gram molecular weight, 197 for gold. With the activities quoted per mg, $N = 3.05692424\times10^{-6}$ mg^{-1}, with no uncertainty. The uncertainty arises in the foil masses which are used in deriving the activity per mg.

7.1.3 The Westcott g factor

Values for the Westcott g factor have been published in a number of papers and reports. The factor applies to the Maxwellian part of a thermal neutron spectrum and is dependent on the temperature of the distribution. Westcott in 1960 drew up a report tabulating g factors for several isotopes including gold. This report has been updated a number of times the most recent version being that of 1970[13]. Gryntakis and Kim in 1975[14] wrote a paper specifically about g-factors tabulating values as a function of temperature. A more recent technical report by Holden in1999[18], specifically on the temperature dependence, produced data for ^{197}Au(n,γ) calculated using cross sections from ENDF/B-VI. The most recent published data are by van Sluijs et al.[19] and were calculated using ENDF/B-VII data. More recent versions of the ENDF/B files are now available, and the calculations are not complex, so the Fortran program THERMALS was modified to perform them. This program was originally written to calculate neutron spectra with a Maxwellian at an arbitrary temperature T, and a $1/E$ component, and to use the spectral data to derive average values of quantities such as fluence to dose equivalent conversion coefficients. The values for g derived using THERMALS employed cross section data from ENDF/B-VIII, and the equation for g as a function of energy as given by Gryntakis and Kim which can be derived from eq(19). This is:

$$g = \frac{2}{\sqrt{\pi E_0}\sigma_0}\int_0^\infty \sigma(E)\frac{E}{E_T}\frac{1}{\sqrt{E_T}}\mathrm{e}^{(-E/E_T)}\mathrm{d}E \qquad (60)$$

This is simply eq.(19) written in terms of energy rather than velocity. A summary of all the data for effective temperatures from 0°C to 100°C are shown in Table 1.

There is some variation between the data sets. Holden's results tend to be high relative to the mean, and those of Gryntakis and Kim low. The THERMALS results are very similar to those of Westcott and are very close to the mean. The correction introduced by the g factor is small.

The use of results from THERMALS represents a good choice since the program can be used to perform calculations specifically for the temperatures in the two irradiation positions at NPL.

Table 1. Westcott g factors as a function of the temperature

Temp. °C	Westcott 1970	Gryntakis & Kim 1975	Holden 1999	van Sluijs 2015	THERMALS 2024	Mean	Standard deviation
0		1.0030	1.0056	1.0045	1.00428	1.0043	0.0011
20	1.0053	1.0038	1.0066	1.0055	1.00525	1.0053	0.0010
40	1.0064	1.0045	1.0076	1.0066	1.00623	1.0063	0.0011
60	1.0075	1.0053	1.0086	1.0076	1.00722	1.0072	0.0012
80	1.0086	1.0061	1.0096	1.0086	1.00820	1.0082	0.0013
100	1.0097	1.0068	1.0106	1.0097	1.00919	1.0092	0.0014

For a temperature of 45°C, representative of the thermal column, $g = 1.0065 \pm 0.0020$ (0.2%).

For a temperature of 29°C, representative of the access hole, $g = 1.0057 \pm 0.0020$ (0.2%).

The uncertainty is made up of nearly equal components due to the uncertainty in the g factor at a particular temperature and in the value of the temperature for the NPL irradiation positions.

7.1.4 *Self-shielding and flux depression corrections*

There are two effects that may require corrections to be made to the activity induced in a foil placed in a neutron field. Both are dependent on the sample thickness.

a) The fluence in the vicinity of the foil is reduced by the absorption occurring in the foil. This effect is termed flux depression, H, and it can result in the foil measuring a lower fluence than would be present if it were absent.

b) Self-shielding of the interior of the foil by the outer layers. Corrections for this are performed by applying the self-shielding correction factor G. This factor is defined as the ratio of the average fluence rate inside the sample to the fluence rate incident on the surface of the sample.

The product of these two, i.e. HG, is often termed flux perturbation. For beam geometry flux depression does not occur because the neutrons are incident as a stream of particles and there is no mechanism for returning the neutrons to the position of the foil. In a medium where the neutrons are incident isotropically, so that activation can occur when neutrons are scattered back into the foil after once traversing it, flux depression can occur, and will depend on the size of the foil, the more mass the more potential flux depression, and in the same way it will depend on the absorption cross section. Historically this effect has been ignored at NPL, even for irradiations in the access hole. The effect has been discussed by Hargrove and Geiger[20] for a system where foils were irradiated in a cavity inside a graphite moderator – a similar arrangement to the access hole in the NPL thermal pile. They make the point that flux depression is greatly reduced if the irradiations are in an air cavity as compared to being closely surrounded by graphite. For their foils (0.00254 cm thick and 1 cm in diameter) they estimate flux depression of -0.2%, but note that there is an edge effect (where neutrons are incident through the edge of the foil thus increasing the activation because of the long pathlength) of +0.15%. These two effects tend to cancel. The foils routinely used at NPL are approximately 2 thou thick, i.e. 0.00508 cm, but even though the two effects mentioned above depend on the thickness, they would again be expected to cancel to some extent even for a foil of twice the

thickness. Flux depression is therefore neglected, even for foils in the access hole, although this conclusion may need to be reviewed for irradiations with thicker foils or cases where the foils are not surrounded by air.

Two self-shielding factors are used in the Westcott convention. The thermal self-shielding correction, G_t, is for neutrons with energies below the cadmium cut-off energy, and occurs in eq.(44) for the Westcott sub-cadmium thermal fluence. The resonance self-shielding correction, G_r, is for neutrons with energies above the cadmium cut off. Both G_t and G_r occur in eq.(50) for the experimental cadmium ratio which is used in deriving the epithermal index r and the cadmium ratio R for an ideal $1/v$ detector. These in turn are used when deriving both the Maxwellian and the total fluences in the Westcott convention. The effects of uncertainties in both quantities cannot therefore be ignored although those in G_t will be the most significant. Different issues arise in determining G_t and G_r, and since G_r is not involved in the calculation of the Westcott sub-cadmium fluence its values and uncertainties are discussed separately in a later section.

As already noted, thermal self-shielding factors for foils depend on the thickness and on the directional properties of the neutron field, i.e. they are different for a beam and an isotropic field. A number of publications have investigated the values for G_t either experimentally or theoretically or both. IAEA Technical Report Series No. 107[9] gives useful explanatory information and also expressions for calculating these factors. Because the gold foils usually used at NPL all have very similar thicknesses, in the region of 96 mg cm^{-2}, single values have historically been used for G_t, although they are different for isotropic and beam geometry. These values are given in Table 2. Some of the background to the choice of these numbers can be found in NPL Report RS(EXT)104[21].

Table 2. G_t values used historically at NPL (since the 1960s) for foils with thicknesses ~ 96 mg/cm^2 (~ 0.00508 cm).

Geometry	G_t
Isotropic	0.9340
Beam	0.9843

To investigate the validity, or otherwise, of these values and to investigate the uncertainties, a review was undertaken of self-shielding factors reported in the literature. There is a large amount of resonance self-shielding data available for a variety of materials, although some is for irradiation of wires or spheres, but there is a real dearth of values for thermal self-shielding, particularly for beam irradiations. Determining appropriate values for the gold foils used at NPL in the two irradiation fields (thermal column and access hole) is made difficult by the fact that available data in the literature are for differing foil dimensions and neutron fields. Foil activation is a technique used both in neutron activation analysis (NAA), and reactor dosimetry and self-shielding calculations are covered in the literature for both technologies[22,23]. These calculated data vary, however, depending on the field considered, usually a pure Maxwellian, and whether or not they include scattering in the foil, and foil radius corrections.

7.1.4.1 Thermal self-shielding factors - beam geometry

The data for foils in a beam are very sparse. A paper in 1967 by Perlstein and Weinstock[24] provided extensive computational analysis of the problem, including the effects of scattering within the foil, and values were tabulated for G_t and G_r for both beam and isotropic geometries. However, the values are given for a Maxwellian at 293.6 K (20.4°C) corresponding to

kT = 25.3 meV, which does not correspond to the kT value of either the thermal column beam or the access hole.

A value is given for a 100 mg cm^{-2} foil in beam geometry in a 1979 paper by Boot[12], but this is referenced as a private communication from Axton at NPL, and the fact that it agrees exactly with the value of Perlstein and Weinstock suggests this was the source of the datum.

In view of just how sparse the data are for irradiations in a beam, calculational techniques for self-shielding were investigated. Ideally, neutron transport codes should be used to determine self-shielding factors including scattering, and cadmium cover effects for irradiations under cadmium. However, lengthy neutron transport calculations are not required for relatively thin samples, where the mean free paths for neutron scattering tend to be larger than the dimensions of the sample and approximate approaches have been developed. These involve equations that originally evolved from neutron diffusion theory in the 1950s, but significant deviations occur in the literature on the correct application of these equations. The basic equations can be found, for example, in the IAEA Technical Report Series No. 107[9].

For a foil in a beam with normally incident monoenergetic neutrons, a self-shielding factor, G, for the case where scattering is ignored, can be calculated knowing the foil thickness, from:

$$G = \frac{1 - \mathrm{e}^{-x}}{x} \tag{61}$$

For a foil in an isotropic field of monoenergetic neutrons the equation is:

$$G = \frac{1 - 2\mathrm{E}_3(x)}{2x} \tag{62}$$

The function $\mathrm{E_n}(x)$ is the exponential integral given by:

$$\mathrm{E_n}(x) = \int_1^\infty \mathrm{e}^{-xu} u^{-n} \mathrm{d}u \tag{63}$$

This expression cannot be solved analytically although approximations are available, e.g. in the IAEA Technical Report, or in an NBS Handbook[25].

The parameter x is the product of the thickness and a macroscopic cross section Σ, i.e. $x = t\Sigma = tN\sigma$ where t is the thickness, N the number of atoms in the material, and σ the cross section. If N is in atoms per mg, t needs to be in mg/cm^2.

The derivation of eq.(61) for self-shielding in a monoenergetic beam is relatively straightforward. If D_0 is the activation of a foil of thickness t in a fluence ϕ with no attenuation of the beam traversing it then,

$$D_0 = \int_0^t \phi\Sigma \, \mathrm{d}z = \phi\Sigma t = \phi x \tag{64}$$

(This is an unrealistic quantity because with no attenuation there would be no activation, however, it is a good approximation for a very thin foil.)

Attenuation of the beam in traversing a thickness z is given by $\mathrm{e}^{-\Sigma z}$ so the activity D_0' in a foil, after allowing for attenuation, is given by,

$$D_0' = \int_0^t \phi \, \mathrm{e}^{-\Sigma z} \Sigma \, \mathrm{d}z = \phi\Sigma \frac{(1 - \mathrm{e}^{-\Sigma t})}{\Sigma} = \phi(1 - \mathrm{e}^{-x}) \tag{65}$$

The self-shielding correction factor G is D_0' / D_0 giving the expression of eq.(61).

The expression for an isotropic field involves integration over the neutron incidence angles and is more complex.

Calculations using the equations above usually use the absorption cross section Σ_a, i.e. scattering is ignored. A correction allowing for scattering has been proposed by Lindstrom and Fleming[26] and this is supported in a paper by Blaauw[27]. The scatter corrected self-shielding factor G' is expressed as:

$$G' = \frac{G}{1-(\Sigma_s / \Sigma_a)(1-G)} \tag{66}$$

where Σ_s is the scatter cross section. The cross section to be used when calculating G should then be the total macroscopic cross section $\Sigma_t=\Sigma_a+\Sigma_s$. These expressions are used in neutron activation analysis and reactor dosimetry, although the values to be used for Σ are not always consistent in the literature. Reference (28) seems to give the most recent conclusion on this matter and there it is stated that the combination of Σ values given above is the correct one .

The equations for G or G' are for monoenergetic neutrons. For a Maxwellian neutron distribution the approach is usually to use an averaged cross section. Here again there is inconsistency in the literature for the values to be used, and how to calculate them. For a thermal Maxwellian the fluence averaged cross section $\bar{\Sigma}$ for a $1/v$ detector is:

$$\bar{\Sigma} = \frac{\sqrt{\pi}}{2}\sqrt{\frac{T_0}{T}}\Sigma_0 \tag{67}$$

where Σ_0 is the macroscopic cross section at $v_0 = 2200$ m/s. However the neutron density averaged value is:

$$\bar{\Sigma} = \frac{2}{\sqrt{\pi}}\sqrt{\frac{T_0}{T}}\Sigma_0 \tag{68}$$

Both values have been used when deriving self-shielding corrections as evidenced by the equations quoted in different papers. One paper[26] even states that eq.(67) should be used when the neutrons are in a beam, but that eq.(68) should be used for an isotropic field. The difference is not trivial $2/\sqrt{\pi}$ being 1.128 while $\sqrt{\pi}/2$ is 0.886. A definitive resolution of this issue was given by Blaauw in a paper specifically on this subject[27]. He concluded that the neutron density averaged value, eq.(68), is the one to use for all fields. This would seem to be logical, since one would expect the self-shielding to depend on the neutron density within the foil rather than the fluence passing through it. A more recent paper in Metrologia[29] supports this saying the averaging should be over the Maxwellian thermal neutron density although the expression given there is derived from an approximate form for eq.(61) so is not identical to eq.(68).

Using eq.(66) and a value for the macroscopic absorption cross section from eq.(68) values for the thermal self-shielding G_t can be calculated with $T=T_0$ for comparison with the calculations of Perlstein and Weinstock, and with T set to the actual values for the beam and isotropic fields at NPL to obtain an estimate of the effect of T being $>T_0$, although this does not allow for any effect of the $1/E$ component that extends below the cadmium cut off energy.

To allow for the fact that the thermal spectra at NPL do not correspond to the ideal Maxwellian at 25.3 meV assumed by Perlstein and Weinstock, and to investigate the effects of the presence of the small 1/E component below the cadmium cut-off, the Fortran program THERMALS was

extended to enable thermal self-shielding factors to be calculated. Cross section data were obtained from ENDF/B-VIII for both the ^{197}Au(n,γ) cross section and for scattering in gold. The number of point energies used was in the range 1000 to 50000. (Because the spectrum and gold cross section are smooth in this region a very large number of points is not required and the results did not change over the range of point energies tried.) The use of THERMALS allows calculations for different spectra and, with an option to set the gold scattering cross section to zero, providing an ability to perform calculations with and without correction for scattering in the foil. The basic equation for calculating average thermal or resonance self-shielding factors, G_i, where $i = t$ or r is,

$$G_i = \frac{\int_a^b \tau(E)\cdot\sigma(E)\cdot\phi(E)\cdot G(E)\,\mathrm{d}E}{\int_a^b \tau(E)\cdot\sigma(E)\cdot\phi(E)\,\mathrm{d}E} \tag{69}$$

where $\sigma(E), \phi(E),$ and $G(E)$ are the activation cross section, the fluence, and the self-shielding respectively at energy E. The quantity $\tau(E)$ is the cadmium attenuation factor, covered in section 7.2.2. The integration limits a and b are zero to E_{Cd} for thermal self-shielding, i.e. for i=t, and E_{Cd} to the maximum neutron energy for resonance self-shielding, i.e. for i=r. For the bare detector one can assign $\tau(E) = 1$ at all energies, and for the cadmium covered detector $\tau(E)$ can be included or excluded to estimate its effect on G_r, see section 7.2.4.

The results of the various calculations for a beam are compared to the results of Perlstein and Weinstock in Figure 4.

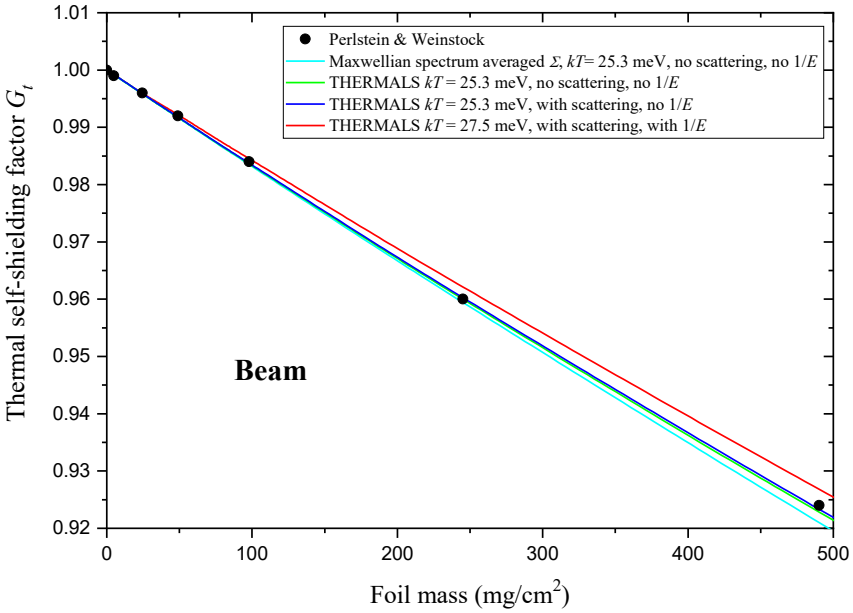

Figure 4. Comparison of self-shielding factors calculated with THERMALS for a gold foil in a beam with the values of Pearlstein and Weinstock. The Maxwellian spectrum averaged curve derived from eq.(61) used the spectrum averaging of eq.(68).

The immediate conclusion is that the calculations agree rather well. The use of eq.(61) with the neutron density averaged macroscopic cross section of eq.(68) give values for the correction factor that are only slightly lower than Perlstein and Weinstock for kT = 25.3 meV. (Using the fluence averaged macroscopic cross section, rather than the neutron density averaged one, the agreement is very much poorer.) Calculations with THERMALS, with or without the scatter correction of eq.(66), agree very well with the data of Perlstein and Weinstock, implying that

the scattering effect is negligible for the Maxwellian peak over this range of gold thicknesses. Including the scattering only increases the correction factor very marginally. Increasing the Maxwellian peak energy to 27.5 meV and including the small $1/E$ component increases the value of the correction factor, i.e. it decreases the self-shielding correction to be applied, as expected for a roughly $1/v$ detector with a higher mean energy Maxwellian peak and a $1/E$ component above the peak.

7.1.4.2 Thermal self-shielding factors - isotropic field

Values for thermal self-shielding in gold in an isotropic field are available in the literature. Sola[30] in a 1960 publication described measurements performed in a reactor, where the neutron field was isotropic, with gold foils of different thickness, and radii, and compared the results with the predictions of two theoretical equations for G_t one of which included a dependence on foil radius. He concluded that the results agreed with calculations to about 2%.

Data as a function of thickness were also published by Hasnain et al.[31]. The results are lower than most other published data and the experimental arrangement, where the foils were in water, was such that flux depression was probably occurring as well as self-shielding, so the results have not been included in the current analysis.

Crane and Doerner[32] published experimental data for different thickness and different diameter gold foils. Their data for edge effects indicate that they are negligible for foil thicknesses less than about 100 mg/cm^2 for 1 cm diameter foils.

In his 1963 paper Axton[11] gives values at two foil thicknesses, both thinner than the foils usually used at NPL nowadays, in the isotropic field at the UKAEA Harwell reactor Gleep.

In a paper describing the NPL thermal pile Ryves and Paul[1] quote a value for a gold foil irradiated in the access hole, but this foil was roughly half the thickness of the foils now used routinely at NPL.

The available data for isotropic irradiation of gold foils, together with THERMALS calculations for this quantity, are plotted in Figure 5. The THERMALS results are for a kT value of 25.3 MeV for comparison with the majority of the other data. .

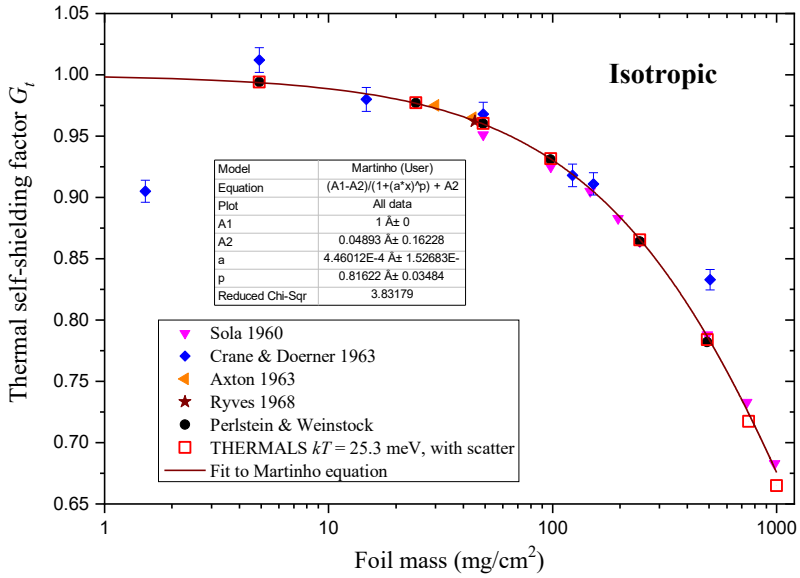

Figure 5. Thermal self-shielding factors for isotropic irradiation of gold foils.

The line labelled as 'Fit to Martinho equation' corresponds to a general equation applicable to any material[33, 34] and will be discussed in more detail in a later section on resonance self-shielding. The fact that the data, with the exception of some outliers in the results of Crane and Doerner, follow the type of curve expected for thermal shelf shielding in an isotropic field is reassuring, but the results are for different foil geometries in a range of different fields with varying characteristics in terms of Maxwellian temperature and $1/E$ component. Their applicability to irradiations at NPL is not obvious.

One consideration that was not taken into account for beam geometry, but may be relevant for isotropic irradiation, is the size and shape of the foil. The equations in 7.1.4.1 above for G were derived on the assumption of an infinite slab detector. For a foil with its surface placed perpendicular to a parallel beam the foil area should not matter, but for foils of finite radius in an isotropic field, neutrons can enter the foil at different angles and also from the side. A number of publications, e.g. the two IAEA reports (9,23), suggest that allowance for foil dimensions can be included in self-shielding calculations with the equations above by replacing the thickness, t, in the quantity $x = t\Sigma$ by a parameter, $2V/S$, which they call the mean chord. Here V is the foil volume, and S its surface area. The mean cord tends to the foil thickness when the thickness is much smaller than the other dimensions. The term 'mean chord' is perhaps a little confusing as the mean path length for radiation in a foil in an isotropic field is $4V/S$.

The data of Crane and Doerner are for a 0.5 cm radius foil; as were those of Axton. Ryves and Paul used 0.564 cm radius foils. Edge effects may be relevant in these cases. Sola published his results for disc foils of different thickness and diameters, and his data show self-shielding correction factors increasing very significantly with decreasing foil diameter for thicker foils, i.e. the self-shielding correction gets smaller. His data for foils of thickness 0.00508 cm (2 thou), notionally the same as that commonly used at NPL, are plotted in Figure 6. Results from TERMALS both with and without the $2V/S$ factor are included for comparison.

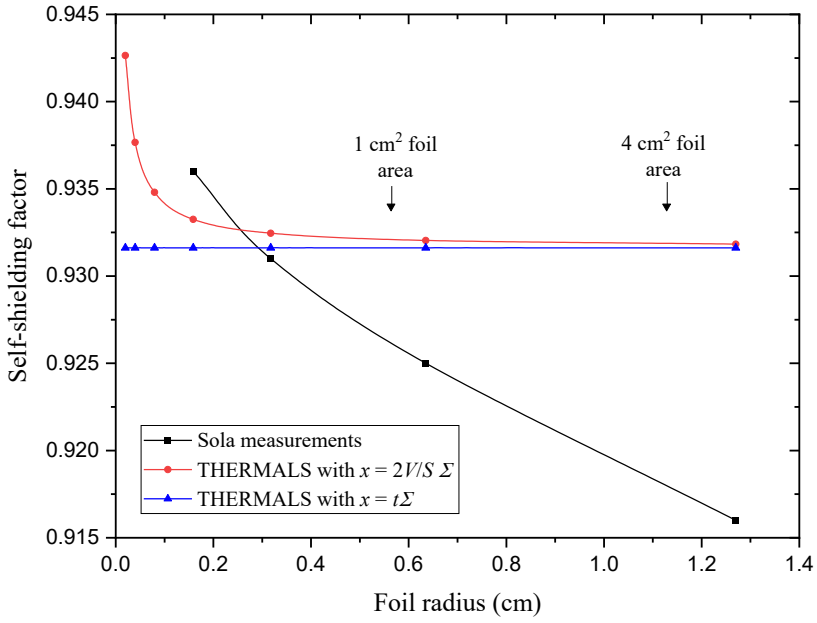

Figure 6. Variation of self-shielding factor with foil radius for 0.00508 cm thick foils (98.15 mg/cm^2 for a 1 cm^2 foil). The TERMALS calculations were for a pure Maxwellian at $kT = 25.3$ meV.

The figure shows that, for a fixed thickness, the self-shielding correction as calculated with THERMALS decreases as the foil radius decreases when $x = (2V/S)\Sigma$, but remains constant, as expected, for $x = t\Sigma$. Interestingly the self-shielding correction factor is larger with

$x = (2V / S)\Sigma$, i.e. the correction is smaller, presumably because path lengths tend to be shorter in smaller diameter foils. For the thickness considered, the differences in the values calculated with THERMALS are negligible for radii above about 0.2 cm. More generally, for thin foils such as those used at NPL, and typical foil radii, the effect of foil radius variations as calculated using $x = (2V / S)\Sigma$ is very small.

These calculated results do not, however, agree with the measurements of Sola where the self-shielding factor decrease significantly as the foil radius increases. There is no immediately obvious explanation for this. In his measurements Sola was not able to distinguish between self-shielding effects and those due to flux depression which would definitely occur in his reactor environment. As foil size increases flux depression increases and this may be influencing the measurement results. The differences between the THERMAL calculations and Sola's results amount to 0.6% for a 1 cm^2 foil and 1.5% for a 4 cm^2 foil, which highlight the problem of using data for irradiation facilities that differ from those at NPL.

The advantage of using THERMALS is that the effects of different Maxwellian temperatures, of scattering, and of foil dimensions can be taken into consideration. The data shown in Figure 7 are similar to those in Figure 5 in that they show the variation of the self-shielding correction with foil thickness, but in this case for isotropic incidence.

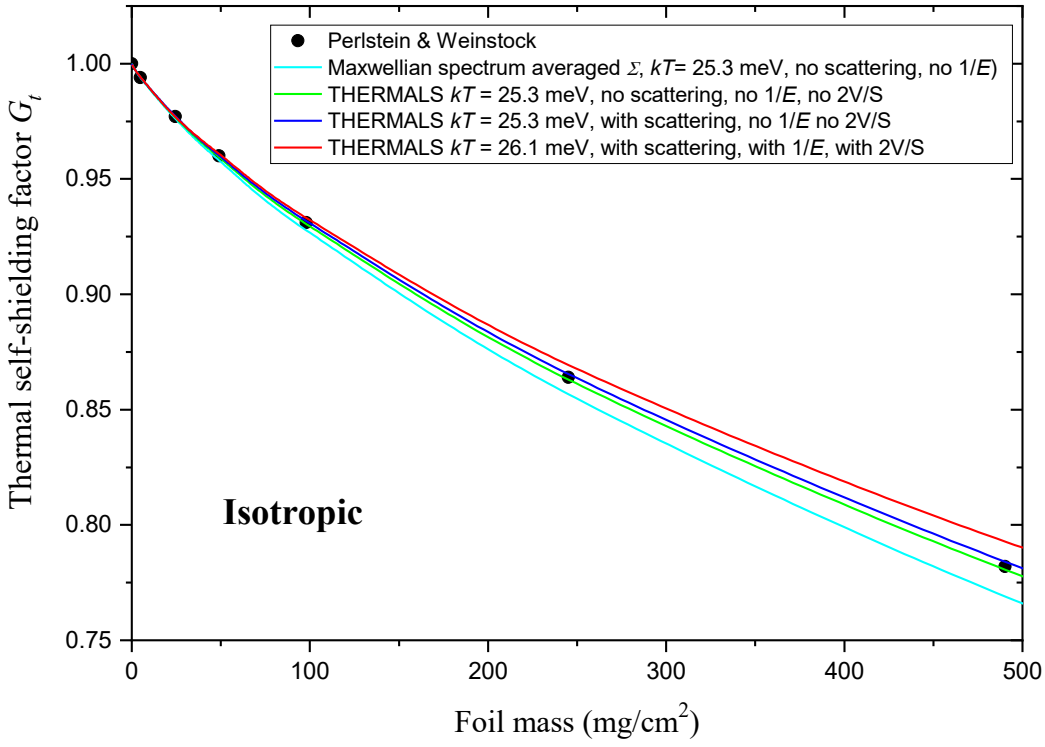

Figure 7. Comparison of self-shielding factors calculated at NPL for a gold foil in an isotropic field with the values of Pearlstein and Weinstock. The Maxwellian spectrum averaged curve used the spectrum averaging of eq.(68).

As was the case for beam geometry, the use of eq.(61) with the spectrum averaged macroscopic cross section of eq.(68) gives the lowest values for the self-shielding factor, while THERMALS gives excellent agreement with Perlstein and Weinstock for a pure Maxwellian at a kT value of 25.3 eV. Increasing the Maxwellian temperature, including the $1/E$ component, and using the scatter corrections and foil dimension corrections, increases the value of the self-shielding factor, i.e. it reduces the correction as expected.

7.1.4.3 Thermal self-shielding factors - recommended values

A number of factors need to be taken into consideration when deciding on the best thermal self-shielding correction factors to use. The detailed calculations of Perlstein and Weinstock allow for scattering within the foil, starting from first principles, but are restricted to a Maxwellian with $kT = 25.3$ meV, and include no allowance for foil dimensions or any 1/E component. The THERMALS program can allow for kT values different to 25.3 meV and for the small $1/E$ component between the Maxwellian distribution and the cadmium cut-off energy. It can also allow for scattering and foil dimensions using empirical correction formulae. The validity of these corrections is, however, questionable (see discussion of resonance self-shielding in later section). Fortunately, the differences are very small as evidenced in Figure 5 and Figure 7.

As a pragmatic approach average values of the Perlstein and Weinstock and the THERMALS results, with all corrections included, were taken for the beam fields at NPL. For the isotropic field the data from the fit to the Martinho formula were also included in the averaging. The results are shown in Table 3. What is clear from this analysis is that the self-shielding values used in the past, based on the work of Perlstein and Weinstock, were an acceptable estimate. The new values are marginally higher, which is reasonable in view of the fact that they were influenced by the THERMALS calculations which included the effect of the Maxwellian peak at NPL being at a higher energy than the one used in the Perlstein and Weinstock calculations.

The uncertainties shown are the standard deviation of the results rather than the standard error of the mean. This would normally be considered a rather pessimistic approach, but in view of the small self-shielding correction, it has been adopted here.

Table 3. Recommended thermal self-shielding factors. The foil thicknesses tabulated are those used by Perlstein and Weinstock.

Foil thickness (mg/cm^2)	Beam		Isotropic field	
	Value	Uncertainty	Value	Uncertainty
0.0	1.0000	0.00%	1.0000	0.00%
4.91	0.9991	0.02%	0.9940	0.03%
24.54	0.9961	0.01%	0.9769	0.01%
49.07	0.9921	0.02%	0.9602	0.07%
98.15	0.9843	0.04%	0.9318	0.12%
245.36	0.9612	0.17%	0.8664	0.31%
490.73	0.9256	0.25%	0.7871	0.68%

7.1.5 *Cadmium cover attenuation factor* F_{Cd}

The explanation given in the literature for including the attenuation factor F_{Cd}, in eq.(40), is that it corrects for attenuation of the epithermal fluence in the cadmium cover, i.e. it allows for the fact that the activation of the foil by epi-cadmium neutrons may not be the same for the bare and cadmium covered cases because the transmission factor through cadmium for neutrons in this region may not be quite unity. It is different for beam and isotropic irradiations, and its determination is complicated by uncertainty about the position and shape of the cadmium cut-off.

The value used at NPL for years has been 1.01 ± 0.01 for an isotropic field. This is based on data in the paper by Axton[11] in 1962, although there is no clear explanation of its derivation.

Hargrove and Geiger[20] in 1964 used a formula from a 1951 paper by Tittle[35] to calculate F_{Cd}, but say the derived value (1.048) is too high because the formula requires the absorption cross section, and they only had the total cross section. They therefore reverted to using their measured value of 1.01 ± 0.01, which agrees with that used by Axton.

Geiger and Van der Zwan[15] in 1965, and Ryves and Paul[1] in1968, quote values for isotropic fields of 0.99 for transmission through cadmium, and this gives an absorption correction F_{Cd} of 1.0/0.99 = 1.01.

In 1966 Powell and Beck[36] performed measurements with a range of gold foils and cadmium thicknesses in water in an isotropic field. Using fits of the data to an expression involving third-order exponential integrals of the foil and cadmium thicknesses in units of absorption mean free paths, they concluded that there was no evidence of variation in F_{Cd} with gold foil thickness and the average value for 1 mm thick cadmium was 1.045 ± 0.010.

In 1973 Mueck and Bench[37] published detailed calculations of a quantity they call the cadmium correction factor. It is denoted here by F_{MB}, to avoid confusion with other expressions for this factor. They tabulate values for different thickness foils and different cadmium cover thicknesses for both beam and isotropic fields. They define their cadmium correction factor by $F_{MB} = C_{ep}/C_{Cd}$, where C_{Cd} is the neutron activation, produced by the $1/E$ part of the spectrum, in a detector foil covered with a cadmium sheet, and C_{ep} is the activation, produced by the $1/E$ part of the spectrum, in the bare foil. Both quantities are derived from an integration only over the $1/E$ part of the spectrum. C_{Cd} is very similar to $D_0(Cd)$, but because the integration is over the $1/E$ part of the spectrum it does not include, and hence removes, any of the Maxwellian distribution that extends above μkT.

The low energy limit is the lower energy limit of the $1/E$ spectrum, although this is not defined as a sharp delta function, but as a more gradually rising curve, and the authors say the value of the correction factor is strongly dependant on the form of this function. The without-cadmium integral is a measure of the activation produced by all the $1/E$ neutrons; whereas the with-cadmium integral does not include the activation by those neutrons between the lower limit of the $1/E$ spectrum and the cadmium cut-off energy since these are absorbed in the cadmium. Using this expression for the cadmium correction factor in the quantity $D_0 - D_0(Cd)\cdot F_{MB}$ appears to give the activity produced just by the neutrons in the Maxwellian distribution since the $1/E$ neutrons between the lower energy limit of this component and E_{Cd} are removed in the process. This may be an interesting quantity, but it would not be the fluence seen by an instrument irradiated in the thermal field when a 'with and without cadmium cover' measurement is used. The results tabulated in the paper for F_{MB} for beam geometry range from 1.039 for a 9.66 mg/cm^2 (0.005 mm) gold foil under a 0.5 mm cadmium cover, to 1.225 for a 483 mg/cm^2 (0.25 mm) foil under 1.2 mm of cadmium. For a 96.6 mg/cm^2 foil under 1 mm of cadmium, similar to the values used at NPL, their value is 1.127 for a beam. For an isotropic field the value is even larger.

Although this paper does not calculate the quantity required for thermal neutron calibrations, it does give useful expressions for the absorption, $\xi(E)$, in a shielding material such as cadmium as a function of energy E, and hence the transmission factor, $\tau(E)$, since $\tau(E) = 1-\xi(E)$. If $\Sigma_{Cd}(E)$ is the macroscopic absorption cross section for cadmium at energy E, then:

For a beam
$$\tau(E) = e^{-\Sigma_{Cd}(E)\cdot d} \qquad (70)$$

For an isotropic field $$\tau(E) = 2\,\mathrm{E}_3(\Sigma_{Cd}(E)\cdot d) \quad (71)$$

where, d the thickness of the cadmium cover in appropriate units to match $\Sigma_{Cd}(E)$, and E_3 is the third order exponential integral – see eq.(63).

In two papers from the Jožef Stefan Institute[38,39] the equations used for thermal neutron activation analysis are presented and discussed, and these include the equation below for a cadmium transmission factor, called here F_{JS}, to differentiate it from other expressions,

$$F_{JS} = \frac{\int_0^\infty \sigma(E)\cdot\phi(E)\cdot\tau(E)\,\mathrm{d}E}{\int_{E_{Cd}}^\infty \sigma(E)\cdot\phi(E)\,\mathrm{d}E} \quad (72)$$

Here $\sigma(E)$ is the foil activation cross section at energy E, and $\phi(E)$ the fluence at energy E. Expressions for $\tau(E)$ can be taken from eq.(70) and eq.(71). Note that F_{JS} is called a transmission factor, and the quantities in the numerator and the denominator are reversed compared to the expression given by Mueck and Bench. Also, the integrations are over the whole spectrum, not just the $1/E$ component, and the lower energy limit for the integration for the bare foil in the denominator is E_{Cd}, rather than zero, so only the activation by neutrons above E_{Cd} is included. For the integration in the numerator, which is for the foil under cadmium, the lower limit for integration is 0, but the transmission factor $\tau(E)$ limits the integral to the region above a cadmium cut off whose shape is defined by $\tau(E)$. Possible implications of a non-delta shape for the cadmium cut-off are not discussed, and no actual values are reported. Also, eq.(72) makes no allowance for self-shielding or the thickness of the activation foil.

Recent papers about characterisation of thermal fields at reactors, presumably isotropic fields, give F_{Cd} values of 1.098[40] and 1.14[41], but with no explanation.

In view of the different values quoted, and the different expressions proposed for the quantity, the derivation of F_{Cd} values was investigated in more detail.

The program THERMALS calculates spectra with given ratios of Maxwellian to $1/E$ fluence components, and can thus, by including expressions for $\tau(E)$, be used to calculate values for the integrals in, for example, eq.(72).

Firstly, however, values for the natural cadmium cross section as a function of energy need to be derived. ENDF/B files provide data for individual isotopes of cadmium, and these are plotted in Figure 8 for the 6 isotopes with the highest abundance amounting to 97.9% of the total isotopic abundances. It is clear from this that it is the isotope ^{113}Cd that gives cadmium its property as an absorber of thermal neutrons. (The ^{113}Cd line is largely hidden by the total line.)

Figure 9 ,which is for the beam in the NPL thermal column, illustrates the fluence spectrum that induces the activity D_0 in the bare foil, the spectrum that induces the activity $D_0(Cd)$ in the under-cadmium foil, calculated by multiplying the fluence by the appropriate transmission factor, and the difference between the two which represents the neutron spectrum that produces the activity given by the quantity $D_0 - D_0(Cd)$. The data were calculated using THERMALS with 50,000 energy bins with equal widths on a log scale.

The fluence seen by the bare foil is largely hidden in the plot by the difference spectrum in the region of the Maxwellian peak, and by the under-cadmium spectrum, i.e. the fluence × the transmission factor, in the epithermal region. An interesting feature is the small contribution to the under-cadmium spectrum at the Maxwellian peak. Although the transmission there is very low, the large number of neutrons at the peak mean that a small number do get through.

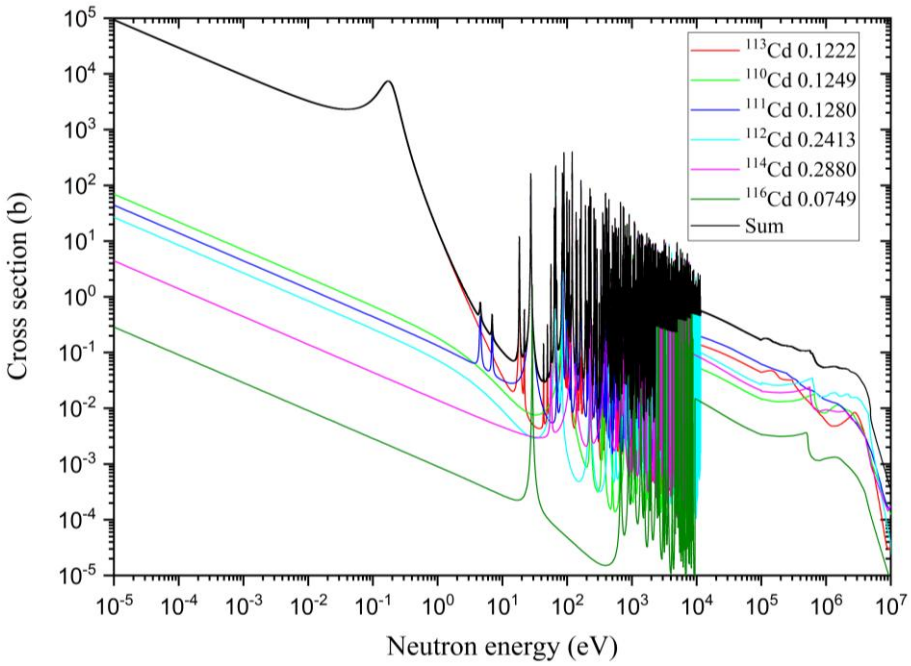

Figure 8. Cross sections for cadmium isotopes from ENDF/B-VIII, and for natural cadmium obtained by summing the components for the different isotopes using the program THERMALS. The quantity plotted for the individual isotopes is the cross section multiplied by the isotopic fraction, values for which are given in the legend.

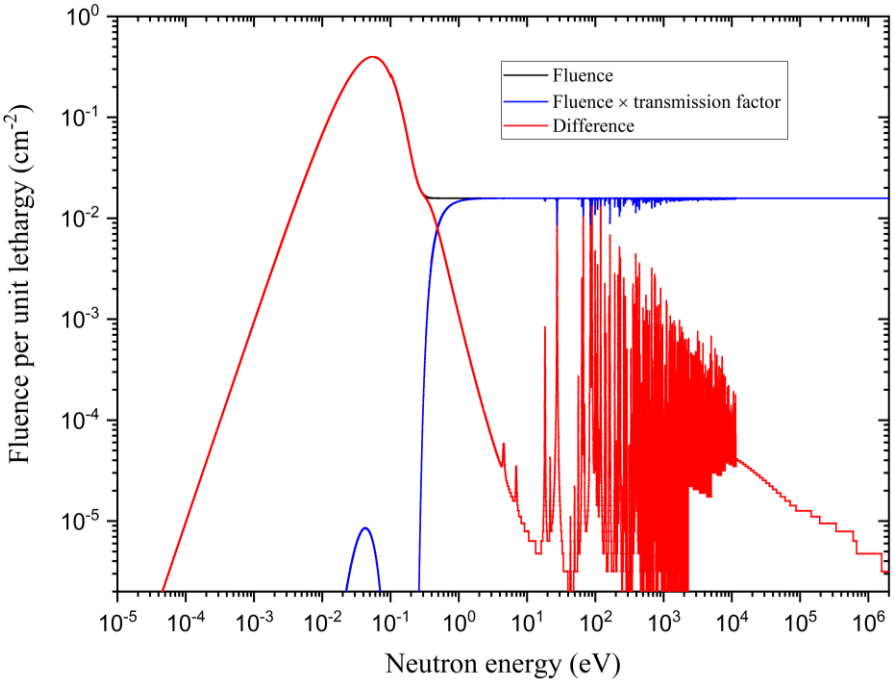

Figure 9. Fluence spectra seen by bare and under-cadmium foils and their difference which represents the neutron spectrum that induced the activity given by $D_0 - D_0(Cd)$. The spectrum is representative of that in the thermal column of the NPL pile.

The spectra in Figure 9 are an indication of how the fluence seen by a device under irradiation varies with energy, but the quantity measured by a gold foil is not the fluence, but the activity induced by the fluence. Figure 10 shows how the contributions to this activity are distributed with energy, as calculated with THERMALS using 50,000 equal width bins on a log scale.

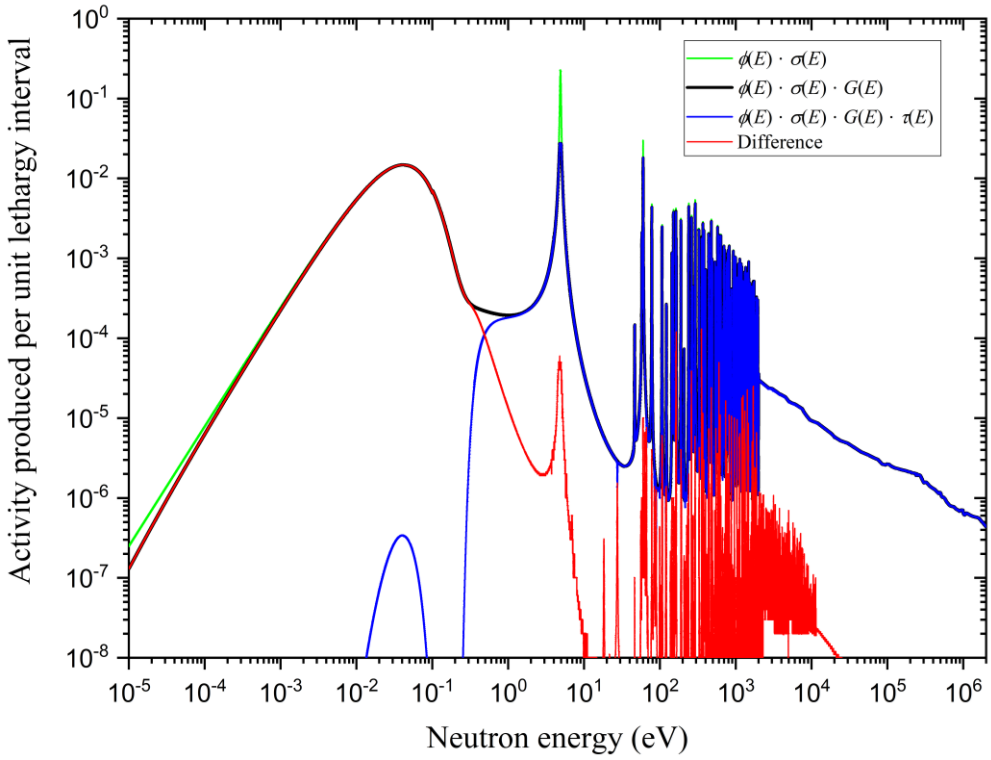

Figure 10. Contributions to activation of foils both bare and under a 1 mm cadmium cover. The spectrum is typical of that in the thermal column and the gold foil thickness was 98.15 mg/cm^2.

The curve labelled $\phi(E)\cdot\sigma(E)$ is a first order calculation of the activity. It is what would be obtained in an idealised thin foil where there was no self-absorption. The curve labelled $\phi(E)\cdot\sigma(E)\cdot G(E)$ includes the effect of the shelf-shielding factor *G(E)*. Since the field is a beam, the expression for *G(E)* was that of eq.(61). Eq.(66) which includes allowance for scattering was not used for reasons that are discussed in the section on resonance self-shielding. It is slightly lower than the $\phi(E)\cdot\sigma(E)$ curve at very low energies and at the 4.9 eV resonance because of the high gold capture cross section and thus self-shielding at these energies. The curve labelled $\phi(E)\cdot\sigma(E)\cdot G(E)\cdot\tau(E)$ where the cadmium transmission factor has also been included, shows where over the energy range the activity $D_0(Cd)$ of the foil under cadmium is produced. The difference curve shows where the activity for the quantity $D_0 - D_0(Cd)$ arises. The majority comes from the Maxwellian peak, although there is a component in the region above E_{Cd} where transmission through the cadmium is not 100%. The usual understanding of this component is that the cadmium cover attenuation factor, F_{Cd}, corrects for this.

With the data available from THERMALS for the various contributions to the gold activity as a function of energy, summations over regions can be performed to provide integrals of the activities produced by various energy intervals with and without cadmium cover.

This raises the question of exactly what quantity should be quoted as the 'thermal fluence', and how to deal with the shape of the cut-off at E_{Cd}. If the thermal fluence is to be defined as *all the neutrons below a cut-off at* E_{Cd} then the activity corresponding to this region is:

$$\int_0^\infty \phi(E)\cdot\sigma(E)\cdot G(E)\,\mathrm{d}E - \int_{E_{Cd}}^\infty \phi(E)\cdot\sigma(E)\cdot G(E)\,\mathrm{d}E \;=$$
$$\int_0^\infty \phi(E)\cdot\sigma(E)\cdot G(E)\,\mathrm{d}E - F_{Cd}\cdot\int_0^\infty \phi(E)\cdot\sigma(E)\cdot G(E)\cdot\tau(E)\,\mathrm{d}E \qquad (73)$$

Here the number of atoms involved has not been included as they are the same for both integrals. With this assumption:

$$F_{Cd} = \frac{\int_{E_{Cd}}^{\infty} \phi(E)\cdot\sigma(E)\cdot G(E)\,\mathrm{d}E}{\int_{0}^{\infty} \phi(E)\cdot\sigma(E)\cdot G(E)\cdot\tau(E)\,\mathrm{d}E} \tag{74}$$

which is essentially the inverse of eq.(72) with the addition of self-shielding.

The result of calculating F_{Cd} with THERMALS depends on a number of factors, in particular on the Maxwellian temperature, and hence kT, on the magnitude of the $1/E$ component, and most of all on E_{Cd}. Calculations were performed for the spectra of the NPL thermal pile access hole and the beam of the thermal column using values for these parameters from the WESTCOTT program outputs shown in section 5. The values for E_{Cd} are those derived from eq.(39) using K values published Westcott[7]. Results for three gold foil thicknesses and five cadmium cover thicknesses are shown in Figure 11 as a function of cadmium thickness (top) and of four gold foil thickness (bottom), for both a beam and an isotropic field. The figure highlights the fact that F_{Cd} depends not only on the cadmium thickness, but also on the gold thickness via self-shielding effects. The values are listed in Table 4.

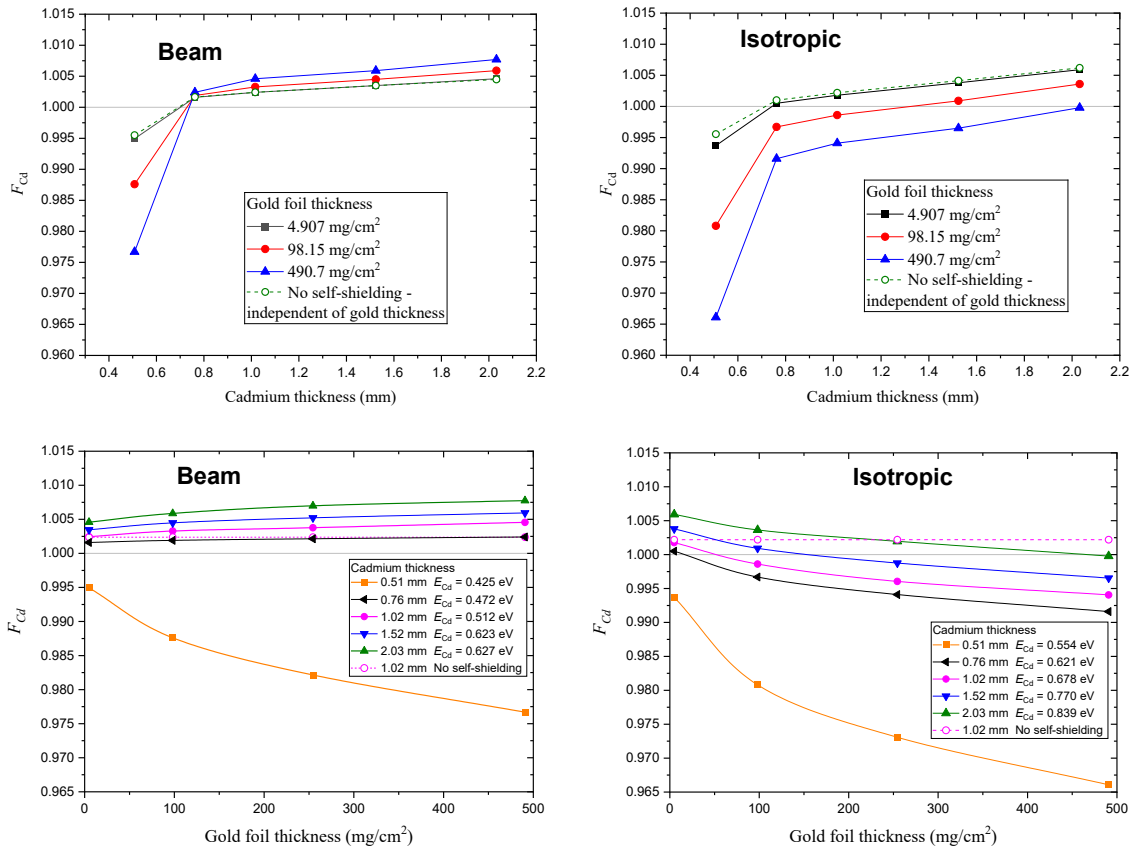

Figure 11. Cadmium correction factors F_{Cd} calculated with program THERMALS for the two fields, beam and isotropic, at the NPL thermal pile. All curves are for calculations with self-shielding included, except for those labelled 'No self-shielding'.

An understanding of the shape of the curves of F_{Cd} values as a function of cadmium and gold foil thickness is made easier by reference to eq.(74) and Figure 12 which shows the activation contributions over the energy region around E_{Cd} on a larger scale than Figure 10.

Table 4 Cadmium absorption factors F_{Cd} calculated with program THERMALS using E_{Cd} values from a Westcott analysis

Gold thickness (mg/cm^2)	Beam					Isotropic				
	0.51 mm Cd	0.76 mm Cd	1.02 mm Cd	1.52 mm Cd	2.03 mm Cd	0.51 mm Cd	0.76 mm Cd	1.02 mm Cd	1.52 mm Cd	2.03 mm Cd
	E_{Cd} 0.425 eV	E_{Cd} 0.472 eV	E_{Cd} 0.512 eV	E_{Cd} 0.578 eV	E_{Cd} 0.627 eV	E_{Cd} 0.554 eV	E_{Cd} 0.621 eV	E_{Cd} 0.678 eV	E_{Cd} 0.770 eV	E_{Cd} 0.839 eV
4.907	0.9949	1.0016	1.0024	1.0035	1.0046	0.9937	1.0005	1.0018	1.0038	1.0059
98.15	0.9876	1.0019	1.0033	1.0045	1.0059	0.9808	0.9967	0.9986	1.0009	1.0036
490.7	0.9767	1.0024	1.0046	1.0059	1.0077	0.9661	0.9916	0.9941	0.9965	0.9998

The reason for F_{Cd} being close to unity is explained by the fact that the area between the $\phi(E)\cdot\sigma(E)\cdot G(E)$ curve and the curve for $\phi(E)\cdot\sigma(E)\cdot G(E)\cdot\tau(E)$ in the region above E_{Cd} is largely compensated for by the area between the curve for $\phi(E)\cdot\sigma(E)\cdot G(E)\cdot\tau(E)$ and zero in the region below E_{Cd}.

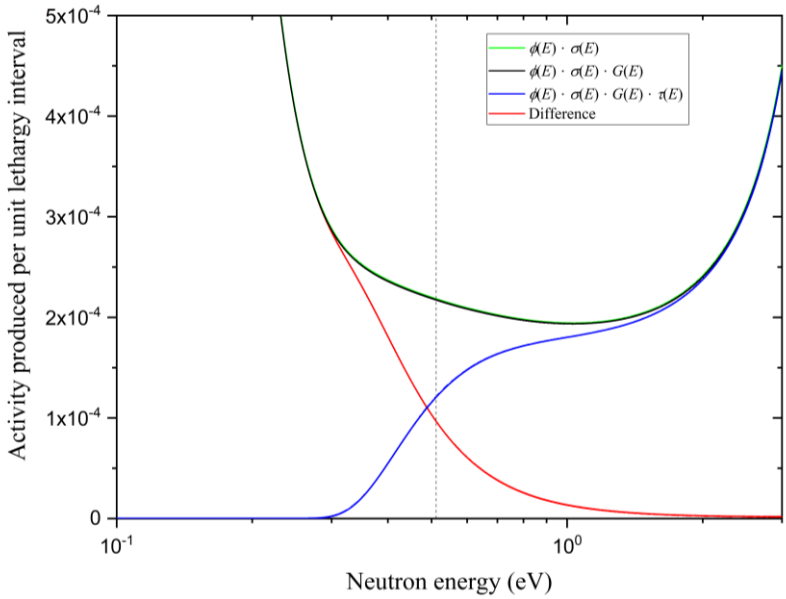

Figure 12. Contributions to the activation in the region around E_{Cd} for the spectrum in the NPL thermal column for a gold foil thickness of 98.15 mg/cm^2 and a cadmium thickness of 1 mm.

As the cadmium thickness increases E_{Cd} derived from eq.(39) using K values from Westcott's Table 1 gets larger and the integral in the numerator in eq.(74) gets smaller. However, so also does the integral in the denominator, because $\tau(E)$ increases. The resultant variation of F_{Cd} with cadmium cover thickness is difficult to predict. The actual variation is shown in the top two plots of Figure 11. The low values of F_{Cd} for a cadmium thickness of 0.5 mm strongly suggests there are issues with the use of such thin covers. If self-shielding is not included in the calculation, F_{Cd} follows the curve for a 4.907 mg/cm^2 foil as illustrated by the lines for no self-shielding in these two plots. This is to be expected as the thinner the gold foil the less self-shielding influences the activation.

The variation with gold foil thickness is a result of self-shielding. Excluding this effect from the calculations gives an F_{Cd} value that is constant as a function of gold foil thickness as illustrated in the lower plots. But self-shielding does occur, and allowance needs to be made for it.

Although the rationale for including the cadmium absorption factor F_{Cd} when calculating $D_0 - F_{Cd}D_0(Cd)$ initially appears straightforward, being simply a correction for less than 100% transmission of neutrons through the cadmium at energies above E_{Cd}, in practice it proves to be more complicated. The literature includes a range of different values for F_{Cd}, different equations for calculating this correction factor, and different interpretations of its function. Fortunately, except for cadmium cover thicknesses of less than 1.0 mm the values of F_{Cd} calculated with THERMALS can be expressed as 1.00 ± 0.01 for both a beam and an isotropic field for the range of gold and cadmium thicknesses considered. The plots of Figure 11 would indicate that there are problems with cadmium covers of 0.5 mm or thinner.

From historical data for irradiations in the thermal column beam and in the access hole the effect of an uncertainty of 0.01 in F_{Cd} is 0.12% for the beam and 0.03% for the access hole and so is almost negligible.

7.1.6 *The Westcott K factor, E_{Cd}, and F_{Cd}*

From the above section it is clear that E_{Cd}, F_{Cd}, and the Westcott K factor are intimately linked, but the precise nature of this link is not necessarily clear. Papers describing thermal fluence determination via bare and under cadmium activation measurements usually do little more than state that there is an energy E_{Cd} above which the cadmium is essentially transparent to neutrons, and this occurs at about 0.5 eV for cadmium thicknesses in the range 0.5 to 2.0 mm. The cadmium cut-off energy is obviously not a true delta function and the consequences of this and the choice of a value for E_{Cd} tend not to be discussed.

Westcott K factors, which link R and r, are tabulated in the 1958 paper by Westcott, Walker, and Alexander[7], and are widely used and quoted in subsequent publications; but calculations of this parameter seem never to have been repeated, certainly not with updated results published. The description of the calculations is in a section in the paper where the simple case of an ideal 1/v detector is considered. The importance of the cadmium ratio, R, calculated for such a detector is that it is a direct measure of the ratio of the total Westcott fluence to the epi-cadmium Westcott fluence, and is used when deriving the total fluence from that for the sub-cadmium region. If E_{Cd} is assumed to be a delta function, R for an ideal 1/v detector is given, c.f. eq.(37), by,

$$R = \frac{1}{4r}\left(\frac{\pi E_{Cd}}{kT}\right)^{1/2} \tag{75}$$

However, the authors acknowledge that a delta function is unrealistic, and say, “A better approximation is obtained for a stated thickness of cadmium by using the actual variation of the cadmium cross section with energy.” They perform calculations of R for, “normal incidence on, and isotopic (cos θ law) incidence on, one side of the Cd foil.” The results are used to derive the parameter K. For a pure 1/v detector. K is linked to R by,

$$K = R \cdot r(T / T_0)^{1/2} \tag{76}$$

This is eq.(38) in the earlier derivation of the equations for Westcott fluences in this report. Together the two equations above give a value for E_{Cd}.

$$E_{Cd} = \frac{16K^2 \cdot kT_0}{\pi} \tag{77}$$

The 1958 paper states that while the equations apply, “only when a 1/v law detector is used, the analysis may be extended to cover most other possible detectors.”

To address the uncertainty in the values of K, calculations of R were performed with the THERMALS program. The quantity calculated, see eq.(78), was R for an ideal $1/v$ detector for different cadmium thickness. K can then be calculated from eq.(76) and E_{Cd} from eq.(77).

$$R = \frac{\int_0^\infty \sigma(E)\cdot\phi(E)\,\mathrm{d}E}{\int_0^\infty \sigma(E)\cdot\phi(E)\cdot\tau(E)\,\mathrm{d}E} \tag{78}$$

Nothing is said in the 1958 Westcott paper about the magnitude of the $1/E$ component used in their calculations, implying that K is independent of the value. The THERMALS calculations were performed both for the spectrum of the NPL thermal column (beam geometry) and the access hole (isotopic incidence) using $r(T/T_0)^{1/2}$ values obtained from the WESTCOTT outputs shown in section 6. The results are shown in the upper part of Figure 13.Calculations were also performed for spectra with roughly half the values for $r(T/T_0)^{1/2}$ to check for any dependence on this parameter. See lower half of Figure 13. In the Westcott paper the temperature is not mentioned, so the calculations were performed for $T = T_0$, and since very thin foils were assumed the self-shielding option in THERMALS was not applied.

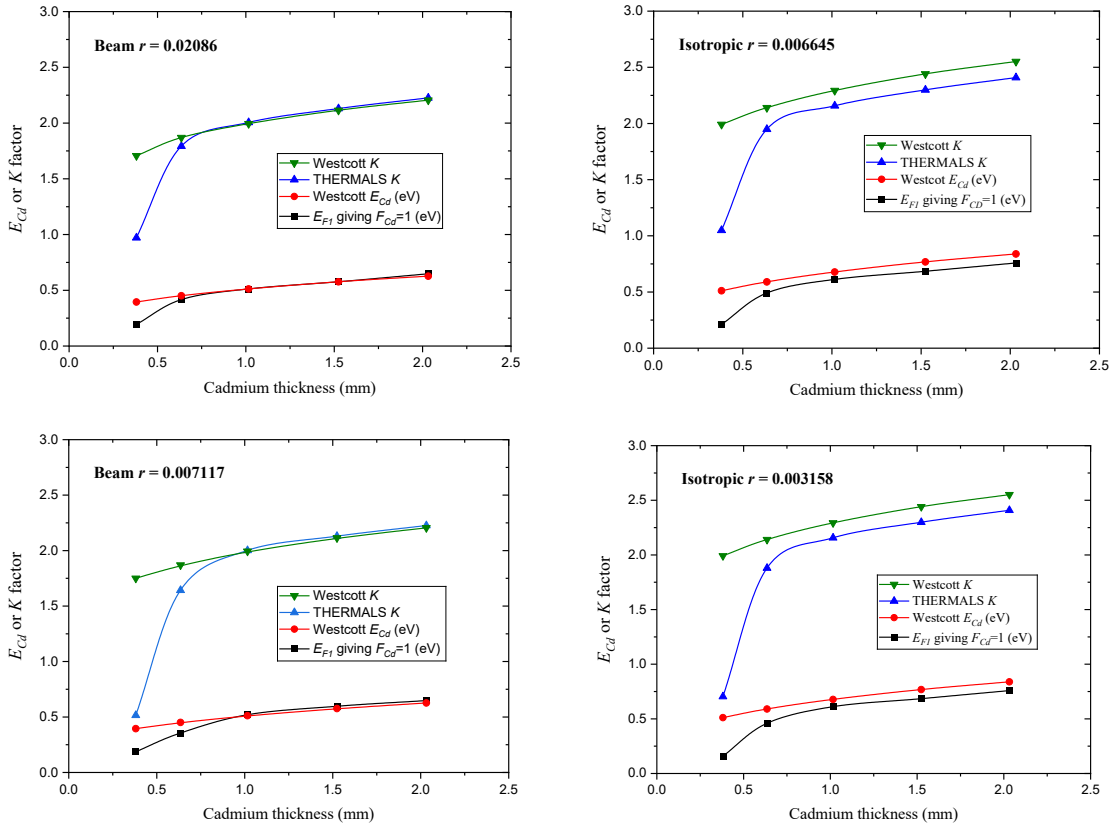

Figure 13. Comparison of Westcott K factor calculated using THERMALS with values from the Westcott et al. 1959 paper, and a comparison of E_{Cd} derived using the Westcott formalism and the value E_{F1} which makes the cadmium correction factor F_{Cd} unity.

As THERMALS can use cross section and spectrum data to calculate integrals, with or without cadmium attenuation, over any energy interval, it was also used to derive a value for a cadmium cut-off energy, designated here as E_{F1}, where the integral from E_{F1} to infinity of the activation in the bare foil equals the activation under cadmium integrated from zero to infinity, i.e. the cadmium cut-off value that makes the correction factor F_{Cd} equal to one – see eq.(74). This

would appear a sensible definition of a cadmium cut-off value. Values for E_{F1} were derived by performing the integral for the nominator in eq.(74) for several values of the lower limit of integration at around 0.5 eV and interpolating to find a value that made F_{Cd} exactly 1.0.

For beam geometry and cadmium thicknesses above 1 mm THERMALS reproduces the Westcott K values almost exactly. This agreement appears not to depend significantly on the $1/E$ intensity, i.e. on the value of r. Also, the Westcott E_{Cd} seems to coincide with E_{F1}.

For isotropic incidence for cadmium thicknesses above 1 mm there is a constant offset for both the K and the cadmium cut-off energy values. The Westcott calculations of K were for neutrons incident only on one side of the foil, but this should not be a reason for any difference.

The most noticeable feature in Figure 13 is, however, the differences for small cadmium thicknesses. For these thicknesses, values of K calculated by THERMALS are much lower than those of Westcott.

To investigate this the activation as a function of neutron energy for a $1/v$ detector under a very thin 0.038 mm (1.5 thou) cadmium cover, as calculated with the THERMALS code, was plotted and the results are shown in Figure 14. This should be compared with Figure 10 the corresponding figure for a real gold foil detector covered with a 1 mm cadmium cover.

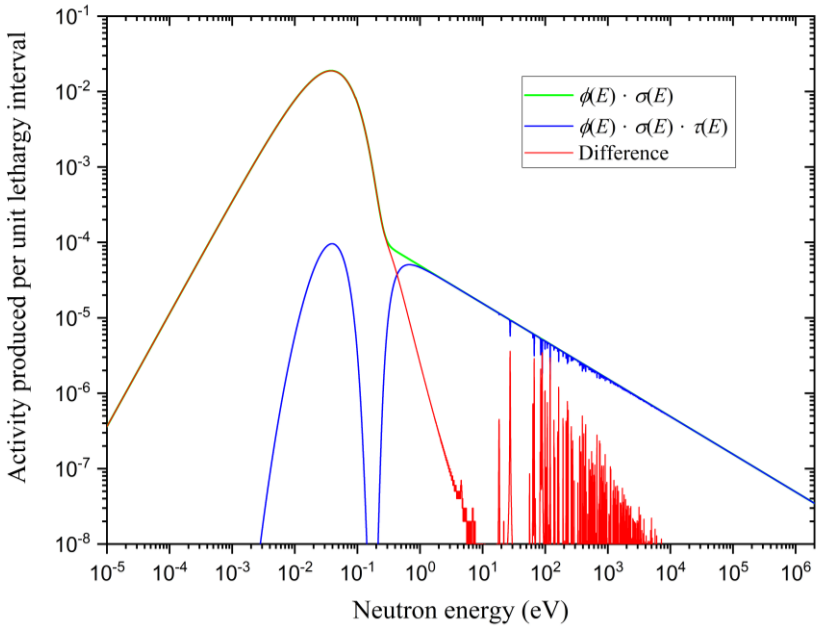

Figure 14. Contributions to the response of a $1/v$ activation detector bare and under a 0.38 mm (15 thou) cadmium cover.

What is apparent when comparing the two figures is that a large number of neutrons with energies below 0.5 eV pass through a cadmium thickness of 0.38 mm compared to the case for 1.0 mm. Despite the very low transmission at low energies the very large number of neutrons at the peak of the Maxwellian, and the higher cross section than at higher energies, result in a non-negligible number of thermal neutrons getting through and causing activation. This means that the integral of the fluence × cross section × transmission factor ($\phi(E)\cdot\sigma(E)\cdot\tau(E)$) from zero to the maximum neutron energy is too large and the cadmium cut-off has to come lower in energy to make F_{Cd} equal to one. The simple conclusion from this section, reenforced by Figure 11 in section 7.1.5, is that cadmium thicknesses of less than about 0.75 mm are too thin for reliable measurements of the thermal fluence using the bare and cadmium covered activation approach. It appears that transmission of thermal neutrons through the cadmium cover has not been included in the Westcott calculations of K.

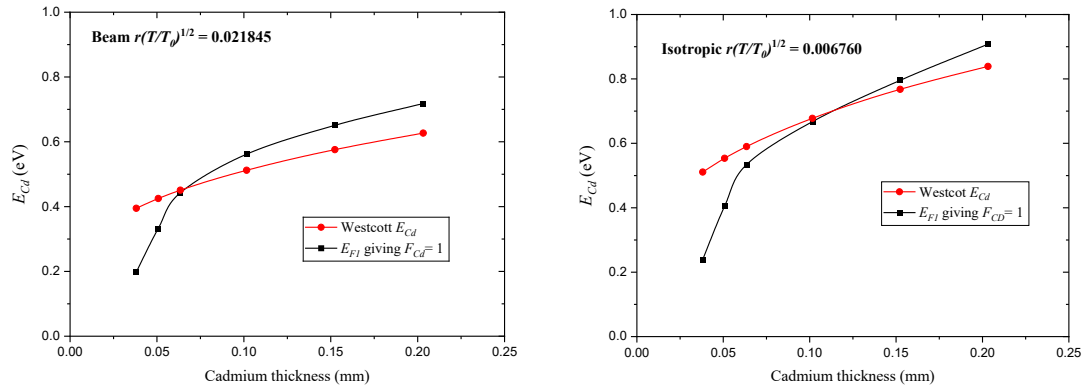

Figure 15. THERMALS calculation of E_{F1} the cadmium cut-off energy value that make F_{Cd} one. Calculations are for 98.15 mg/cm^2 gold foils in the spectrum of the NPL column (beam) or in the spectrum near the bottom of the access hole (isotropic). The values derived from the conventional Westcott approach are also plotted.

As these calculations can be performed with THERMALS, not just for a 1/v detector, but for any activation foil where the cross section is known, they were performed for gold foils and the spectra in the column and access hole at NPL and the values E_{F1} for the cadmium cut-off energy that result in F_{Cd} being one are compared in Figure 15 with the Westcott E_{Cd} values.

For a beam the values of E_{F1} are greater than the E_{Cd} values derived from the Westcott approach for cadmium thicknesses above about 0.64 mm, so F_{Cd} in the Westcott approach needs to be greater than one, if the thermal fluence is to be defined as that in the energy range from zero to E_{Cd}. Similarly for the isotropic case.

It is clear that F_{Cd} depends not only on the degree of absorption of epi-cadmium neutrons in the cadmium cover, but on the value assigned to the cadmium cut-off energy. Changing the value designated as the cadmium cut-off energy changes F_{Cd}.

For an activation foil or a detector where the cross section or the response decreases rapidly in the region above the Maxwellian the exact position of E_{Cd} is not important and the analysis according to the Westcott convention is completely adequate, but for any device where the response in the cadmium cut-off region is significant relative to the thermal response, greater care needs to be taken in considering the implications when measuring activation or a response with the bare and under cadmium experimental approach.

7.1.7 *Summary of the uncertainties in* $n_{th}v_0$

From a review of eq.(44) for $n_{th}v_0$ it is clear that the presence of the term $D_0 - D_0(Cd)\cdot F_{Cd}$ means that the uncertainty in the Westcott sub-cadmium fluence cannot be derived by simply adding all the percentage uncertainties in quadrature. However, if the uncertainty in $D_0 - D_0(Cd)\cdot F_{Cd}$ is derived and the term is treated as a single quantity, the procedure of adding percentage uncertainties in quadrature can be used.

With this approach the quantities with which to multiply $D_0 - D_0(Cd)\cdot F_{Cd}$ are: 3346.8 ± 8.3 (0.25%) for the beam of the NPL thermal column and 3537 ± 10 (0.28%) for the isotropic field in the access hole. These were calculated with the GUM workbench[42] using the values and uncertainties for G_t, σ_0 and g proposed in this report, The largest contribution to the uncertainty in both fields comes from that in the Westcott g factor.

7.2 Uncertainties in the Westcott fluence nv_0

To derive the total fluence in the Westcott convention using eq.(45) the cadmium ratio R for an ideal detector needs to be calculated from eq.(51). This includes various parameters.

7.2.1 *The Westcott parameter* K

The K parameter was discussed in section 7.1.6. The results of the calculations with THERMALS and a comparison with the Westcott data[7] are shown in Table 5. The cadmium thicknesses chosen were those for which K values were tabulated by Westcott.

The THERMALS results are an average of calculations performed for the $1/E$ components in the beam or in the access hole and a calculation with half of these $1/E$ components. Differences were insignificant indicating that K is independent of the intensity of the $1/E$ component.

The differences between the THERMALS and the Westcott K values for cadmium thicknesses less than about 0.75 mm are a result of the inadequate attenuation of Maxwellian peak neutrons in the cadmium as reported in section 7.1.6. Above this thickness there is reasonable agreement. Recommended values for K are the average of the Westcott and THERMALS values. Uncertainties, based on half the differences, with some allowance for the fact the agreement may simply be opportune, are: for beam geometry 0.5%, and for isotropic fields 3%.

Table 5. Westcott K factors

Cd thickness (inches)	0.0015	0.0025	0.004	0.006	0.008
Cd thickness (cm)	0.0381	0.0635	0.1016	0.1524	0.2032
			Beam geometry		
THERMALS K	0.7430	1.7175	2.0034	2.1295	2.2254
Westcott K	1.7506	1.8701	1.9939	2.1141	2.2054
Average	1.2468	1.7938	1.9986	2.1218	2.2154
Difference	-57.6%	-8.2%	0.47%	0.73%	0.91%
Average difference cadmium thickness 0.1 to 0.2 cm =				0.70%	
			Isotopic field		
THERMALS K	0.8766	1.9139	2.1572	2.2991	2.4087
Westcott K	1.9913	2.1399	2.2931	2.4409	2.5515
Average	1.4339	2.0269	2.2251	2.3700	2.4801
Difference	-56.0%	-10.6%	-5.9%	-5.8%	-5.6%
Average difference cadmium thickness 0.1 to 0.2 cm =				-5.8%	

7.2.2 *Attenuation of resonance neutrons in the cadmium shield* f_r

This parameter is essentially the inverse of F_{Cd}. The value should thus be 0.99 ± 0.01, however, see also section 7.2.6.

7.2.3 *Westcott factors* s, s_0, *and the expression for* μkT

The Westcott factor, s, can be calculated using eq.(32). It is a measure of the integral of the cross section over the $1/E$ spectrum after a $1/v$ component has been subtracted from the cross section. There is surprisingly little in the literature about this parameter. In the seminal paper

on the Wescott convention[7] a value for gold of 17.28 is given for the quantity s_0, which is $s(T_0/T)^{1/2}$, (s_0 is expected not to vary with the effective temperature T). In a subsequent AECL report, which has been updated several times[13], Westcott gave values for s for a large number of activation materials for a range of Maxwellian temperatures.

One complication in calculating s is the uncertainty in the low energy cut-off of the $1/E$ spectrum. This is defined by the function $\Delta\mu kT$, where Δ defines the shape of the cut-off, and μ is a multiplier of kT defining the energy where this occurs. The integral of eq.(32) includes the Δ term. There are significant uncertainties in both the shape and the position of this feature. Both the value and the uncertainty in μ are difficult to tie down. The uncertainty in T is outlined at the beginning of section 5.

Assuming the slowing down spectrum can indeed be described as having a $1/E$ shape, it must end somewhere in the thermal region. If it were a unit step function it would introduce a discontinuity in the spectrum at μkT. Any attempt to measure this, for example with a mechanical chopper and time-of-flight in a thermal beam, would be difficult because the $1/E$ component quickly becomes much smaller than the Maxwellian component as the energy decreases in the thermal region. A measurement would thus have to look for a small feature on the upper energy slope of the Maxwellian peak.

The value used for μ at NPL for some years has been 3.681 which is that given, without explanation, in Axton's paper on the Harwell GLEEP reactor[11], and again in a paper he wrote on the calibration of the National Bureau of Standards thermal neutron flux[43] with the explanation that it was the value "for which s_0 was computed". It is unlikely that μ can be known to such high precision. There is evidence that μ is higher for water or heavy water moderated thermal fluences than for graphite ones. Beckurts and Wirtz give $\approx 3.6 \pm 0.4$ for heavy water, and 3.4 ± 0.3 for graphite, based on a time of flight measurement[44]. The IAEA Technical Report[9] gives a figure of $\mu = 5$ for a heavy water reactor, which agrees with the value quoted by Walker et al.[10]. A recent paper on cross section data derived from reaction rates in reactor spectra[45] uses a value of $\mu = 3.0$ when considering a graphite reactor while noting that values μ ranges from $\sim$ 2 for light water moderators to $\sim$ 5 for heavy water moderators. In general there seems to be more data for water moderation than graphite.

There is, however, another consideration, and that is the shape of the cut off. The assumption in the early versions of the Westcott fluence convention, and one still often used, is that the low energy limit of the $1/E$ distribution can be represented by a vertical straight-line cut-off. Such a step function (Δ=1 for $E \geq \mu kT$, Δ=0 for $E < \mu kT$) may be good enough for many purposes, but is very unlikely to be an accurate representation of the cut-off.

In his AECL report[13], Westcott proposes various other possible cut-off functions Δ_1 to Δ_4.

$$\Delta_1 = \frac{1}{1+\left(\frac{3.5kT}{E}\right)^7} \tag{79}$$

$$\Delta_2 = \frac{1}{1+\left(\frac{4.95kT}{E}\right)^7} \tag{80}$$

$$\Delta_4 = \frac{1}{1 - \dfrac{0.26}{1+(E/16.4kT)^5} + \left(\dfrac{4.95kT}{E}\right)^7} \tag{81}$$

A function Δ_3 is also given, but as that is associated with heavy-gas models it is thought less appropriate for a graphite moderated system. The functions Δ_1 and Δ_2 give monotonic cut-offs whereas Δ_4 gives a function with a bump above μkT, and replicates measurements and analyses of reactor spectra which appear to show this feature.

Functions Δ_2 and Δ_4 seems to have found favour in the literature with attempts to incorporate Δ_4 into a formalism with a $1/E^{\beta}$ shape for the epithermal component[46] and a modification to the form of Δ_4 to provide a better fit for a calculated spectrum[47], although this was for a water moderated reactor. Suggestions that the bump also exists for graphite moderation can be found in reference (45). Unfortunately, none of these references provide values of s for gold, although reference (47) does provide plots of the dependence of this quantity on T.

The shapes corresponding to the various delta functions are shown in Figure 16. It is to be expected that the Δ chosen will affect the value of s.

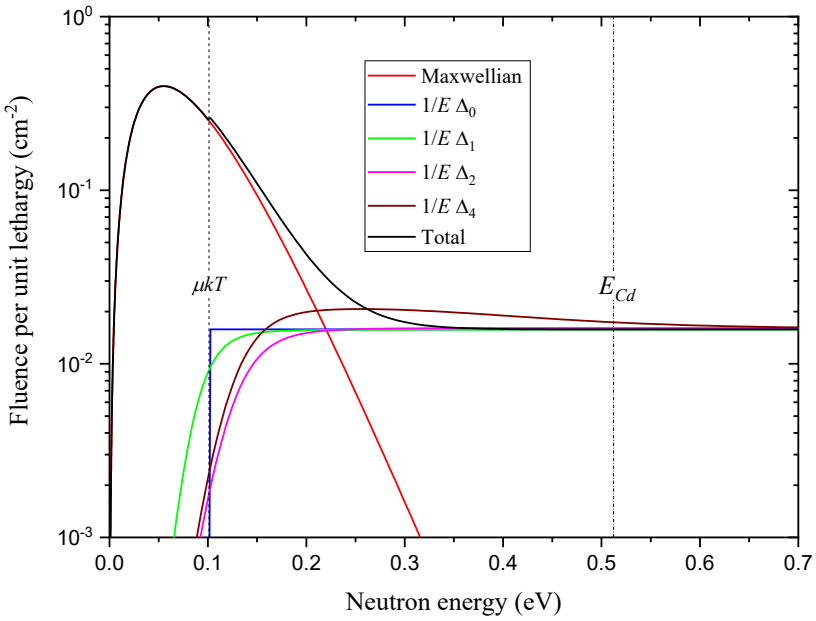

Figure 16. Different options for the cut-off of the $1/E$ component at the low energy end of its range. Δ_0 corresponds to a simple vertical straight line cut-off. The line for the total fluence corresponds to this cut off function. The data are representative of the temperature of the spectrum at a height of 1.5 m in the NPL thermal column.

In the AECL-1101 Westcott lists μ values that give neutron densities in the epithermal region that are the same when using Δ_0 as when using the delta functions 1, 2, or 4. (The delta functions do not depend on μ.) These are:

For Δ_1 $\mu = 3.442$

ForΔ_2 $\mu = 4.868$

ForΔ_4 $\mu = 3.681$

The value for Δ_4 would appear to be the source for the value of μ used at NPL for many years.

In the absence of definitive values in the literature for the factor s the program THERMALS was adapted to calculate values using gold cross sections from ENDF/B-VIII. Data at a mesh of 50,000 points distributed evenly on a log scale between 10^{-5} eV and 2.0 MeV were calculated and used to perform the integration of eq.(32) and derive values for s.

The integrand in eq.(32) involves the difference between the actual gold cross section and a hypothetical cross section with a $1/v$ shape normalised to the gold cross section at T_0. From Figure 3 it can be seen that the integrand is positive and large at the 4.9 eV resonance, however, it is negative in some energy regions. Because the integral for calculating s depends only on the cross section and the shape of the $1/E$ part of the spectrum it is independent of the foil thickness. The contributions to the integral as a function of neutron energy are shown in Figure 17.

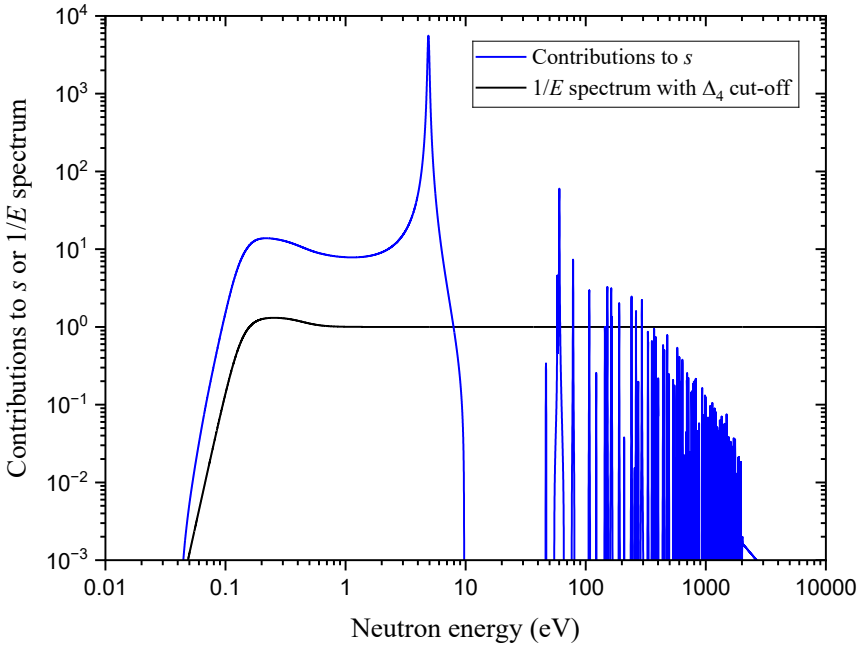

Figure 17. The integrand (the term within the integral sign in eq.(32)) for calculating the Westcott factor s plotted with the $1/E$ spectrum for Δ_4 cut-off function, normalised to one above the cut-off.

The results from the TERMALS calculations are listed in Table 6 where they are compared with data from Westcott's AECL report. Only values for Δ_4 are tabulated in that report. The calculation is straightforward, but the improved data now available for the gold cross section probably explains the small differences.

The THERMALS results for the various Δ functions are all very similar, and in the absence of any reason to prefer one over the others an average was taken and compared to the values in the AECL report. The differences are small of the order of 0.6%. The uncertainty was taken as half the difference between the two sets of results and is about 0.3%.

Also tabulated in Table 6 is the value for s_0 which is the quantity used in the equation for the cadmium ratio R_{Cd}. It does not vary with the Maxwellian temperature, and the uncertainty is taken to be the same as for s.

Typical values for the NPL facility are:

For a temperature of 45.65°C in the column s = 17.983, s_0 = 17.259.

For a temperature of 29.35°C in the access hole s = 17.517, s_0 = 17.260.

Table 6. Westcott *s* factors calculated with THERMALS for various Δ values and comparison with Westcott values for Δ_4 from AECL-1101[13]. The factors depend only on the cross section and so are the same for beam and isotropic irradiation.

T (°C)	AECL-1101	From program THERMALS				Average THERMALS Δ_0 to Δ_4	*s* from average of Westcott & THERMALS	s_0 from average of Westcott & THERMALS	Unc.
	s for Δ_4	*s* for Δ_0	*s* for Δ_1	*s* for Δ_2	*s* for Δ_4				
20	17.30	17.194	17.194	17.190	17.201	17.195	17.247	17.260	0.053
40	17.88	17.769	17.769	17.764	17.776	17.770	17.825	17.259	0.055
60	18.44	18.326	18.326	18.330	18.334	18.329	18.385	17.258	0.056
80	18.98	18.866	18.870	18.870	18.874	18.870	18.925	17.255	0.055
100	19.51	19.390	19.395	19.395	19.400	19.395	19.453	17.255	0.058

7.2.4 *Resonance self-shielding factors* G_r

The resonance self-shielding factor G_r does not appear directly in the equation for deriving the Westcott thermal fluence, $n_{th}v_0$, (eq.(44)), but does occur in eq.(45) for deriving the cadmium ratio, *R*, for an ideal detector, and hence directly in the equations for deriving nv_0. Its influence on the final uncertainty is less than the influence of the uncertainty in G_t.

Several sets of data are available in the literature for gold foils, for the case of isotropic irradiation at least. Perlstein and Weinstock published tables of G_r, for either a beam or an isotropic field. In both cases they tabulated results for a bare foil in a 1/*E* field, and for a foil under cadmium. These are slightly different, the 'with cadmium' datum being 6.5% smaller for 98 mg/cm^2 foils, and the difference increases as the foil thickness increases. In principle both values occur in eq.(50) for the quantity R_{Cd}. G_r in the numerator is for irradiation of the bare foil, whereas G_r in the denominator is for the foil under cadmium. However, only one value is conventionally used in a Westcott analysis. Considering the uncertainty in R_{Cd}, a 10% increase in G_r in the numerator for the NPL fields changes R_{Cd} by 1.2% for the beam and 0.3% for the access hole, whereas a 10% increase in G_r in the denominator changes R_{Cd} by -8.5% for the beam and -8.4% for the access hole. Since R_{Cd} is much more sensitive to the correctness of G_r in the denominator the best choice of G_r to minimise the effect of the approximation of using a single value, is that for irradiation under cadmium, if the data are available.

All the data found in the literature are plotted in Figure 18. The datum from Boot[12] for a beam probably drives from Perlstein and Weinstock. Axton[11] published G_r values for four different foil thicknesses, and as they are for a reactor field, they are assumed to be for isotropic incidence. Brose[48] in 1964 published both experimental and calculated resonance self-shieling factors for gold. This publication may be difficult to acquire, but the data are presented in a later paper by Shcherbakov and Harada[49].

In 1989 Lopes and Avila[50] published calculated resonance self-shielding factors, including data for gold, over the range of interest using an approach which allowed for multiple-scattering in the foil. The paper by Shcherbakov and Harada in 2002 contains calculated resonance self-shielding data at the same energies as the calculated values of Brose, and these data cover a wide range of foil thicknesses (2×10^{-6} to 8×10^{-2} cm, equivalent to 0.039 to 1544 mg cm^{-2}).

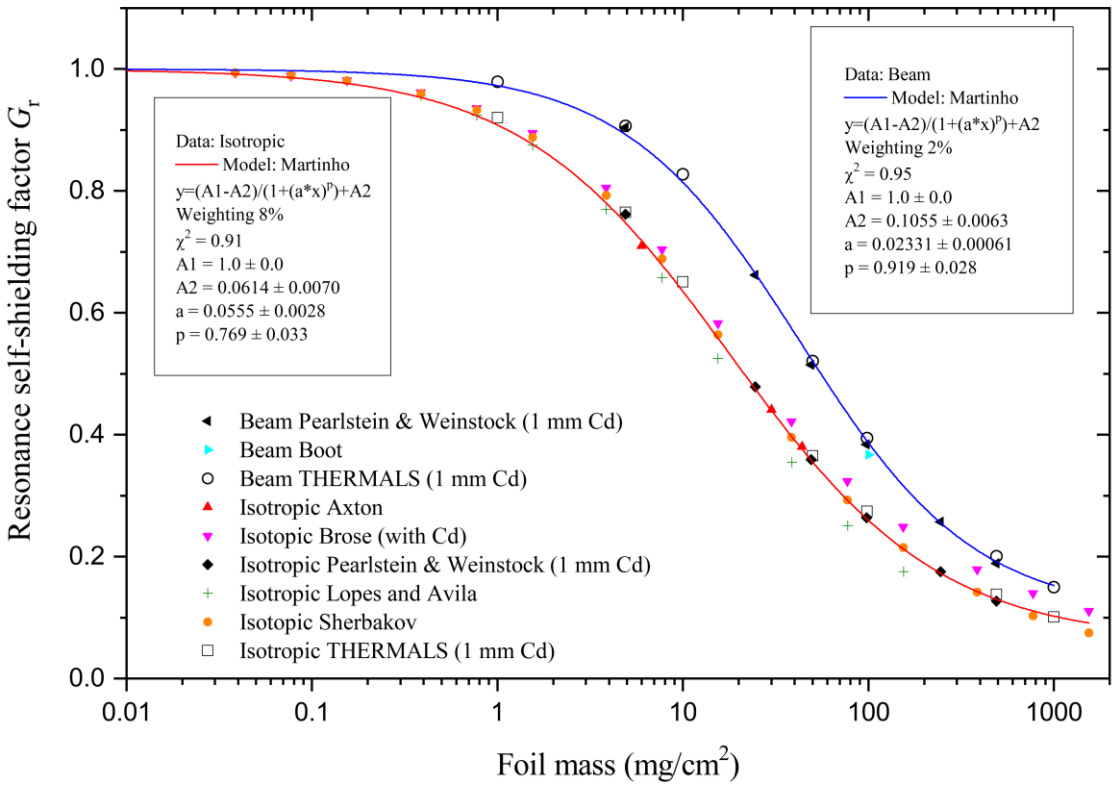

Figure 18. Resonance self-shielding data for gold

As was the case for thermal self-shielding, the program THERMALS was used to calculate resonance self-shielding factors either with or without cadmium cover and for either a beam or an isotropic field using eq.(69). No Doppler broadening of the cross sections at the resonances was introduced, the assumption being that the evaluated ENDF cross sections are already Doppler broadened at 300 K. The calculations are not expected to depend on the shape of the low energy end of the $1/E$ component so the vertical cut-off option, Δ_0, was used. The 'with cadmium' data are shown in Figure 18. At a foil thickness of 98 mg/cm2 the 'with cadmium' value is 2.1% smaller than the without cadmium value.

In a number of papers Martinho and co-workers[33,34] investigated functions for fitting thermal and resonance self-shielding for both beam and isotropic fields. They derived a general expression which seems to fit both resonance and thermal factors reasonably well for all geometries and all materials if the appropriate parameters are chosen. The function is:

$$G = \frac{(A_1 - A_2)}{[1 + (z / z_0)^p]} + A_2 \qquad (82)$$

where A_1, A_2, z_0, and p are parameters, to be adjusted to the optimum values, and z is the product of the foil macroscopic cross section, the thickness in cm, and the ratio of the absorption and total cross sections. The data were plotted using the Origin package and a fit performed using the package's Levenberg-Marquardt algorithm. As the fitting was only an attempt to obtain a parametric form for the data, the term z/z_0 was simplified to a, and was treated as a parameter to be fitted. To ensure that G was 1 at zero thickness A_1 was set to 1.0.

Very few of the data sets have associated uncertainties so for the fitting all data points were assumed to have a fixed percentage uncertainty, and this was varied to obtain a χ^2 per degree of freedom of about one. For the isotropic data this was 8%, and for the beam data 2%. There

are essentially only two sets of data for the beam case, and they agree well so the small percentage uncertainty required to give a χ^2 of about one is not surprising.

The average differences between the fitted curve and the individual data points are of the order of 1%, or less for the lower mass part of the range although they increase as the thickness increases. For the isotropic case, the data of Lopes and Avila are consistently below the curve and those of Brose above the curve at the higher masses. The remainder of the points are very close to the curve except at the highest foil mass where the curve differs from the values of Serbakov and of Brose by about 21%.

Values for the parameters obtained by fitting all the available gold data to the equation of Martinho et al. are shown in the figure and are listed in Table 7 together with the G_r values calculated from them. The uncertainties are those derived from the uncertainties in the Martinho parameters.

Table 7. Parameters for fits of resonance self-shielding factors, G_r, in gold foils

Geometry	Parameters for resonance self-shielding determination			Resonance self-shielding factor at 96 mg/cm^2	
	A2	a	p	New	Old
Isotropic	0.06143±0.0070	0.0555±0.0028	0.769±0.033	0.265±0.012(4.5%)	0.264
Beam	0.10550±0.0063	0.02331±0.00061	0.919±0.028	0.3944±0.0077(2.0%)	0.367

It is not clear where the value of 0.367, which has been used for G_r in the thermal column for some time, was obtained from. The value of Perlstein and Weinstock for a foil of thickness 98 mg/cm^2 is 0.384 which is closer to the most recent estimate than 0.367. The percentage uncertainty for a beam is less than for the isotropic case although there are fewer data. However the factor being closer to one means the correction is smaller and 2.0% is less than the difference between THERMALS and Perlstein and Weinstock for much of the thickness range so 2.0% can be taken as a reasonable estimate.

7.2.5 *Use of the expression for self-shielding at energies in the resonance region*

Equations (61) and (62) give expressions for calculating self-shielding corrections for a beam and for an isotropic field respectively. A correction for scattering in the foil is suggested in the paper Lindstrom and Fleming[26] and also by Blaauw[27], and this is shown in eq.(66). It involves an additional term which is the ratio Σ_s / Σ_a of the scatter to absorption macroscopic cross sections. The value of the parameter $x = t\Sigma$ used in equations (61) and (62) should then involve the total cross section $\Sigma_t = \Sigma_s + \Sigma_a$. For the thermal region below E_{Cd}, the scattering cross section is so much smaller than the absorption cross section that the additional scatter term in eq.(66) has essentially no effect. For higher energies, the resonance region in particular, this is not the case. For gold the effect of the scatter term is to produce large variations for the self-shieling at energies above about 10 eV as shown in Figure 19.

It is to be expected that the inclusion of scattering will change the foil activity. Scattering can increasing neutron path lengths in the foil, particularly for beam irradiation. This will increase the activity. Whether this should be reflected in an increased self-shielding factor, i.e. a reduced self-shielding correction is not clear. However, the large very narrow peaks in the self-shielding values shown in the figure are completely unrealistic. The reasons for their presence are not immediately obvious.

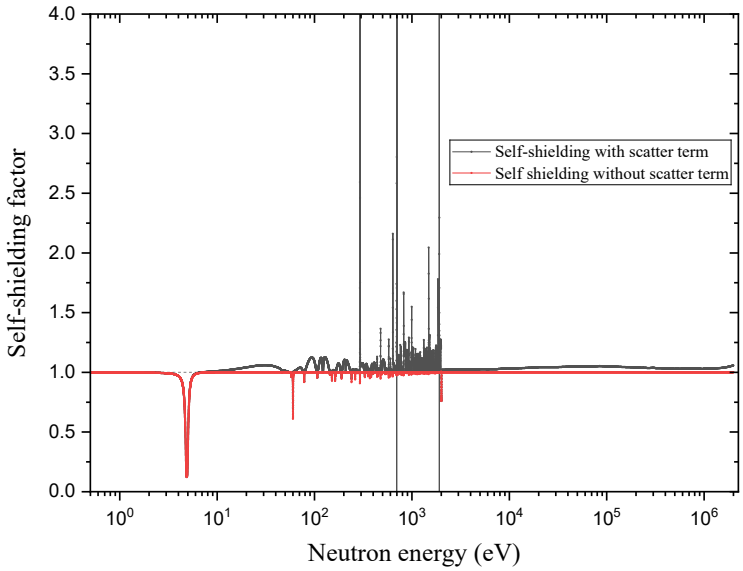

Figure 19. Self-shielding calculated with and without proposed scatter correction term. The data shown are for the energy region above E_{Cd} and a gold foil of thickness about 100 mg/cm^2, similar to those used at NPL. The neutrons were incident as a beam, and a 1 mm cadmium cover was included.

Figure 20 shows a small energy region where one of the peaks in the self-shielding values occurs. The cross sections Σ_s and Σ_a are plotted with the self-shielding factors. It is clear that the problem is not simply a case of the scatter cross section being larger than the absorption cross section. The effect depends critically on the relative values of Σ_s, and Σ_a and also on τ and hence the foil thickness.

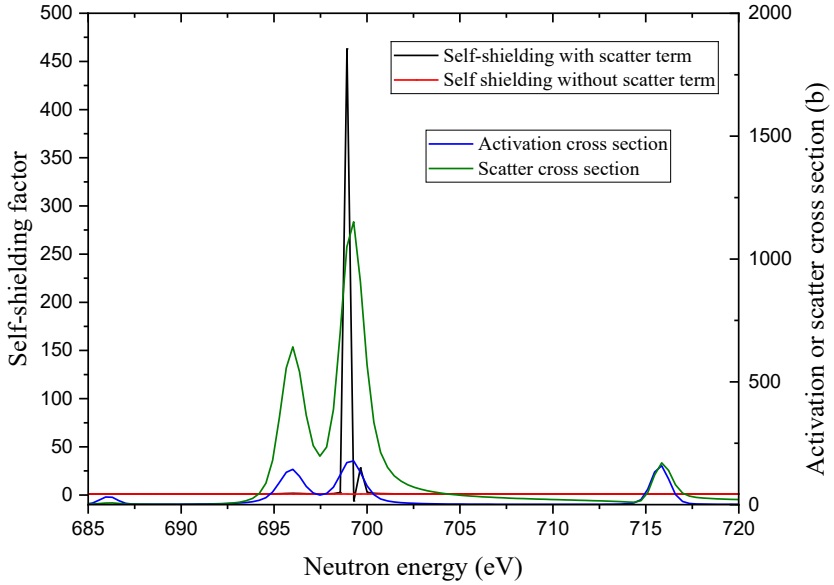

Figure 20. Plot of the self-shielding over a narrow energy region where there are resonances in both the scatter and absorption cross sections. The data are for the same input parameters as in Figure 19.

The scatter correction term was first introduced in a publication by Stewart and Zweifel[51] in 1959, but no derivation is given. The papers of Lindstrom and Fleming and of Blaauw discuss this correction pointing out discrepancies of interpretation in previous papers concerning which cross sections to use, but both are quite specific in saying that the Σ value to be used when calculating τ is the total value, i.e. the sum of the scatter and absorption cross sections. The data for with-scattering shown in Figure 19 and Figure 20 were calculated in this way.

If the scatter cross section Σ_s is removed from the calculation of τ, but retained in the ratio in eq.(66) many of the unrealistic positive spikes shown in Figure 19 are not present. This is illustrated in Figure 21 which shows data calculated in this way. This only highlights the fact that including scatter in the activation foil and using eq.(66) is likely to introduce problems for particular combinations of Σ_s, Σ_a; and τ.

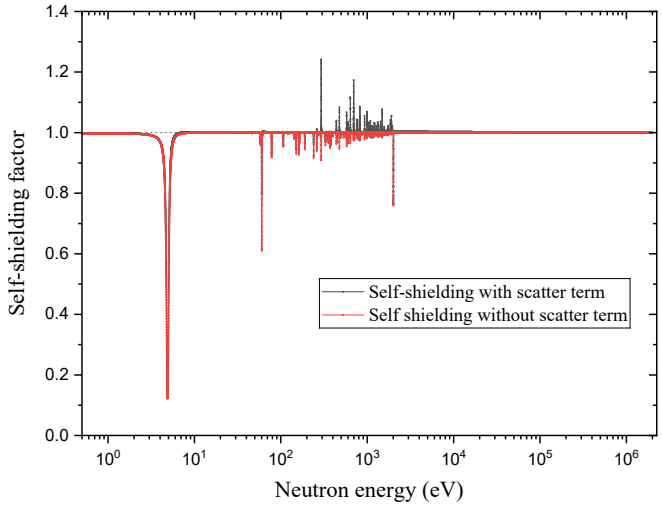

Figure 21. Equivalent picture to Figure 19, with the macroscopic cross section set to Σ_a rather than Σ_t.

Fortunately the effect on average self-shielding is relatively small because most of activation for energies above E_{Cd} is due to the region around the large first resonance at 4.9 eV where the fluence and the cross section are high, nevertheless because of the evident problem with including scattering in this way it was excluded from the THERMALS calculations of G_r although retained in the calculation of G_t .

7.2.6 The correction W and the term $f_r G_r (s_0/g - W)$

In the derivation of the expression in eq.(50) for R_{Cd} an explanation was given for the correction term W. It arises because the term s_0/g which occurs in the numerator involves an integral over the whole $1/E$ spectrum, whereas the corresponding term in the denominator, which is for the activation under cadmium cover, only involves an integration over the region above the cadmium cut off. The correction factor W, which is subtracted from s_0/g in the denominator, is the activation produced by neutrons in the region from μkT to E_{Cd}. It is given, c.f. eq.(49), by:

$$W = \frac{2}{\sqrt{\pi}} \frac{1}{g\sigma_0} \int_{\mu kT}^{E_{Cd}} \left(\sigma(E) - \left(\frac{E_0}{E} \right)^{1/2} g\sigma_0 \right) \frac{\mathrm{d}E}{E} \tag{83}$$

The correction is small for gold where the cross section in this region does not deviate much from a $1/v$ shape, however the available data for W are very sparse. Walker et al.[10] give a value of 0.027 for gold assuming that the cross section between μkT and E_{Cd} is all due to the first resonance (c.f. a value of about 17 for s_0/g). They also say W may be larger for other materials. De Corte et al.[52] in a paper which aimed to elucidate the Westcott convention as it is used in NAA, quotes a value of 0.055, while ASTM E262-17[53] gives 0.050. Both are for a quantity W' which is that of eq.(83), but without the $2/(\sqrt{\pi} \cdot g)$ term. This has a value of 1.12 for gold. Although the value of W has a near negligible effect on nv_0, the fact that available values are so varied prompted further investigation.

The term s_0 was discussed in section 7.2.3, and calculations for it were performed with the program THERMALS. These involved an integration over the range from μkT to the maximum energy of the spectrum, and the uncertainty introduced by uncertainty in the position and shape of the $1/E$ cut off at μkT is small as demonstrated in the THERMALS calculations for different cut off functions. A calculation of W involves an integral from μkT to E_{Cd} and, because it covers a much smaller range, is more sensitive to uncertainties at the two ends of the range. Also, because it depends on the value of E_{Cd}, it will vary with cadmium thickness, unlike s_0/g which does not depend on the cadmium thickness, and is the same for a beam and an isotropic field.

THERMALS was used to calculate W by performing the integral of eq.(83) taking an average of the values calculated with the four expressions for Δ described in section 7.2.3, and using E_{Cd} values derived for three different cadmium thicknesses. The values of E_{Cd} derived using eq.(39) increase as the cadmium thickness increases as the parameter K becomes larger. Increasing E_{Cd} increases the range of integration in eq.,(83) and hence the value of W.

Results for W as a function of temperature are shown in Figure 22 for three cadmium thicknesses. Values calculated with THERMALS for a beam at the temperature of the NPL thermal column are 0.038 for 0.508 mm of cadmium, 0.047 for 1.016 mm of cadmium, and 0.058 for 2.032 mm of cadmium. For a temperature typical of the NPL access hole, the figures for W in an isotropic field vary between 0.052 for a 0.508 mm cadmium cover, 0.065 for a 1.016 mm cover, to 0.079 for a 2.032 mm cover. The variation with the temperature of the Maxwellian peak is slight. The values are similar to those of De Corte et al., and in ASTM E262-17.

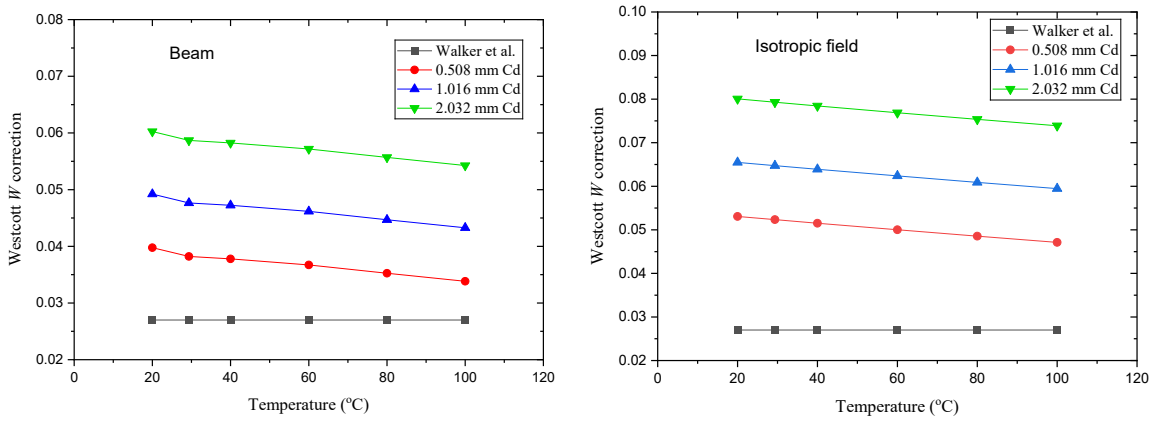

Figure 22. Values for Westcott convention correction factor W for a beam and an isotropic field for three cadmium thicknesses calculated using THERMALS assuming a fixed E_{Cd} value.

The use of eq.(83) with a fixed value for E_{Cd} makes no allowance for the shape of the cadmium cut-off. An alternative approach to deriving $f_r G_r \left(s_0/g - W\right)$ is to calculate it as a single entity. This can be illustrated by defining a quantity S_x based on eq.(49).

$$S_x = \frac{2}{\sqrt{\pi}} \frac{1}{g\sigma_0} \int_0^\infty \tau(E) \cdot G(E) \left(\sigma(E) - \left(\frac{E_0}{E} \right)^{1/2} g\sigma_0 \right) \Delta \frac{\mathrm{d}E}{E} \qquad (84)$$

Here $\tau(E)$ and $G(E)$ are the transmission through the cadmium cover and the self-shielding in the gold respectively at energy E. Depending on the settings for $\tau(E)$ and $G(E)$ various S_x quantities can be calculated the index x indicating choices for $\tau(E)$ and $G(E)$. For example:

S_0 If $\tau(E)$ and $G(E)$ are set to unity, i.e. no attenuation in the cadmium and no self-shielding, the integral gives s_0/g.

S_1 If $\tau(E)$ is set to give the cadmium attenuation factor as defined in eqs (70) and (71) for a beam and an isotropic field respectively, and $G(E)$ is set to the self-shielding factors as defined in eqs (61) and (62) for a beam and an isotopic field respectively, the integral will give $f_r G_r(s_0/g\text{-}W)$ directly. Inclusion of $\tau(E)$ gives both the cadmium attenuation effect f_r above E_{Cd}, and removes the contribution to the integral from neutrons below E_{Cd}. This approach has the advantage of using a realistic cut-off at E_{Cd}.

S_2 If $\tau(E)$ in the equation is replaced instead by the cadmium absorption $(1\text{-}\tau(E))$, and self-shielding factors $G(E)$ are included, the integral gives a measure of the neutrons that have been excluded in calculating $f_r G_r(s_0/g\text{-}W)$. Essentially another measure of W highlighting the fact that the cut-off at E_{Cd} is not sharp.

The contributions to these three integrals are illustrated in Figure 23. The differences between $f_r G_r(s_0/g\text{-}W)$ as derived from the integral S_1 and the use of parameters for f_r, G_r, s_0, g, and W derived in this report are shown in Table 8. The two approaches are not identical, when calculating W on its own from eq.(83) for instance, the upper limit is a sharp cut off at E_{Cd}, which it is not the case in the alternative approach, and the values of the parameters derived in this report include information from sources other than THERMALS. However, the differences are not large and the effect of any uncertainty in this quantity when calculating $R/(R\text{-}1)$ is very small.

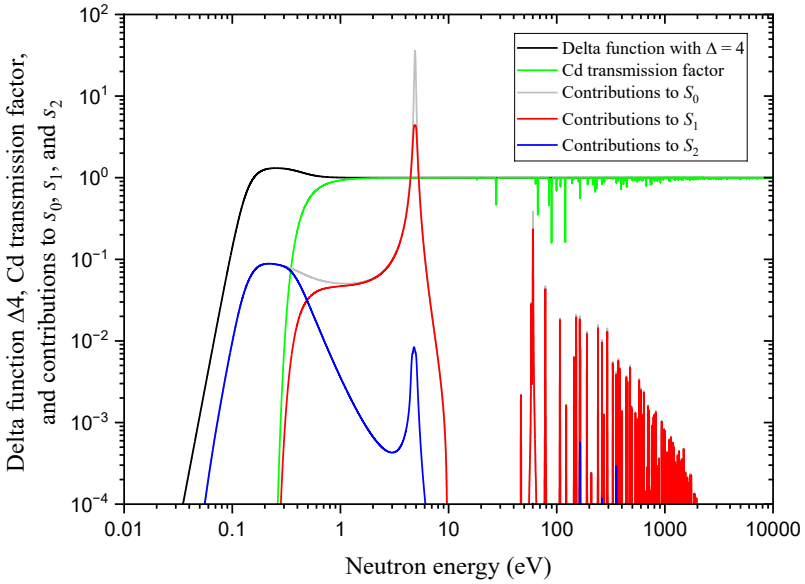

Figure 23. Illustration of the contributions to the term $f_r G_r(s_0/g\text{-}W)$. The data are for a 98 mg/cm^2 gold foil in a beam with a 1 mm cadmium cover. The form of the cut off at μkT was that for function Δ_4. All the quantities are dimensionless.

Table 8. Calculation of $f_r G_r(s_0/g\text{-}W)$ term for 98.15 mg/cm^2 foils covered in 1 mm of cadmium

Neutron field	$f_r G_r(s_0/g\text{-}W)$		Difference
	From the integral to calculate S_1	From the parameters derived in this report	
Beam	6.442	6.68 ± 0.15(2.3%)	3.5%
Isotropic	4.396	4.49 ± 0.21(4.7%)	2.1%

7.2.7 *Summary of the uncertainty in* $R/(R-1)$ *and hence* nv_0

The quantity $R/(R\text{-}1)$ that occurs in the equation to derive nv_0 from $n_{th}v_0$ is given by:

$$R/(R-1) = \frac{\left(R_{Cd}\left\{f_r G_r\left(\frac{s_0}{g}-W\right)+\frac{1}{K}\right\}-G_r\frac{s_0}{g}\right)}{\left[\left(R_{Cd}\left\{f_r G_r\left(\frac{s_0}{g}-W\right)+\frac{1}{K}\right\}-G_r\frac{s_0}{g}\right)-\frac{G_t}{K}\right]} \qquad (85)$$

Values were calculated using the data proposed for the various parameters in this report, and also with $f_r G_r(s_0/g\text{-}W)$ set to S_1. A value of 2.5% was assigned to the uncertainties in S_1 based on the data in Table 8. The data are shown in Table 9. For R_{Cd} the activity values shown in the WESTCOTT program outputs in section 6 were used with uncertainties of 1% which is typical for NPL foil data.

Table 9. Values for the ratio $R/(R\text{-}1)$ for NPL thermal fields

Neutron field	$R/(R\text{-}1)$		
	Using the integral to calculate S_1	Using the parameters derived in this report	Weighted mean
Beam	1.01080 ± 0.00032	1.01042 ± 0.00026	1.01057 ± 0.00019 (0.019%)
Isotropic	1.00314± 0.00019	1.00309± 0.00021	1.00312± 0.00014 (0.014%)

Two things are obvious from Table 9. Firstly the ratio $R/(R\text{-}1)$ required to convert $n_{th}v_0$ to nv_0 is very close to one, differing from unity by only 1.1% and 0.31% for a beam and an isotropic field respectively. Secondly, despite all the uncertainties in the parameters used to calculate the ratios the uncertainties are extremely small. This is largely because R is relatively large.

7.3 Uncertainties in the true thermal fluence $n_{th}\bar{v}$

The values of 0.0253 eV for the energy E_0, 2200 m s^{-1} for the velocity v_0 at E_0, and the temperature of 293.6 K for the temperature T_0 of a room temperature (20.4°C) Maxwellian are considered as constants with no uncertainty assumed.

Calculation of the true sub-cadmium fluence, $\phi(th)$, from the Westcott fluences is covered in section 5. It involves multiplying the Maxwellian fluence and the $1/E$ fluence in the region below E_{Cd} by the ratio of the velocities in these two regions to the velocity v_0, and then adding the two fluence components together – see eq.(59). The equations do not lend themselves to a simple derivation of the fluence uncertainties from the uncertainties in the various parameters in the equations. A review of the steps involved in calculating $\phi(th)$ does, however, allow the potentially important uncertainty components to be identified. They are:

a) Statistical variations in $\bar{v}_{<Cd}/v_0$ from repeat measurements of D_0 and $D_0(Cd)$.

b) The uncertainty in the energy range for the $1/E$ component below E_{Cd}.

c) The uncertainty in the effective temperature T.

Since a knowledge of the true fluence value is only of importance for the NPL thermal column beam where calibrations in terms of this quantity are performed, only this field is considered

here and contributions to the uncertainty were estimated for a typical height in the column (1.5 m) and typical pile temperature (21.4°C).

a) As part of the quality measures undertaken to ensure there is no variation in the thermal fluences delivered, repeat measurements are made with paired (bare and under cadmium) gold foils. From these historical data the variation in the measured $\bar{v}_{<Cd}/v_0$ is very small, with standard deviations significantly less than ± 0.1 %.

b) As outlined in this report, the appropriate energy range for the $1/E$ component below the cadmium cut-off is uncertain because of uncertainties in the lower energy limit at μkT and also because of uncertainty in the value of E_{Cd}. In section 7.2.3 various forms for the cut-off at μkT were outlined these being the four options Δ_0, Δ_1, Δ_2, and Δ_4. In routine derivations of the sub-cadmium fluence at NPL a vertical line cut-off at μkT is assumed, i.e. Δ_0, and E_{Cd} is derived from eq.(77). To investigate the implications of the use of the Δ_0 option THERMALS was used to calculate $\bar{v}_{<Cd}/v_0$ for the four options assuming a fixed value for E_{Cd}. If only the $1/E$ component below E_{Cd}, is considered a fairly wide range of values are obtained for the differences in the ratios from the mean, but when the Maxwellian fluence is added the variation in $\bar{v}_{<Cd}/v_0$ is very small, being less than ± 0.1%. The data are shown in Figure 24.

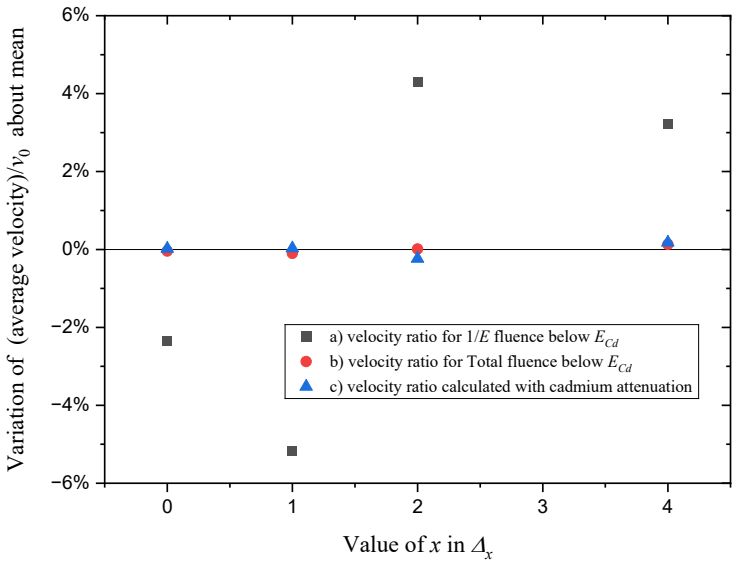

Figure 24. Variation about the mean for the average velocity divided by v_0 for different cut-off functions, Δ_0, Δ_1, Δ_2, and Δ_4, at the low energy end of the $1/E$ spectrum. Data are plotted for, a) just the $1/E$ part of the spectrum below a fixed E_{Cd}, b) the total spectrum below a fixed E_{Cd}, and c) the total spectrum as calculated using the cadmium transmission factor to derive the relevant spectrum. In all cases the data are plotted relative to the mean for that set.

This approach makes no allowance for the uncertainty in the energy of the cut-off at E_{Cd}. To allow for this $\bar{v}_{<Cd}/v_0$ was calculated using THERMALS after multiplying each bin in the spectrum by the appropriate cadmium transmission factor at that energy. This gives the relevant spectrum with a more gradual drop off at E_{Cd}. Calculations were performed for all four options for Δ. The results were on average about 0.2% larger than those calculated for a fixed E_{Cd}, and the variation with the value of Δ was about ± 0.2% - see points c) in Figure 24. From these calculations an uncertainty of ~0.3% can be assigned to the component from uncertainty in the exact energy range for the $1/E$ component.

The uncertainty in the value of $\bar{v}_M / v_0$ for the Maxwellian component can be calculated from eq.(53). Assuming an uncertainty of 11ºC in T – see section 5 - this gives an uncertainty of 1.7% in $\bar{v}_M / v_0$. This is not the total sub-cadmium fluence, but varying T in the input to THERMALS gave a variation of 1.7% in $\bar{v}_{<Cd} / v_0$, so this can be taken as a good estimate of the uncertainty in the sub-cadmium velocity ratio due to uncertainty in T. Because the other uncertainty components are small this dominates the total uncertainty – see Table 10.

Table 10. Contributions to the uncertainty in the average velocity for the sub-cadmium fluence, and hence in $\phi(th)$

Source of uncertainty	Contribution to uncertainty in $\bar{v}_{<Cd} / v_0$
Statistical variation of measured $\bar{v}_{<Cd} / v_0$	<0.1%
Energy range for 1/E fluence below E_{Cd}	0.3%
Effective temperature of the Maxwellian	1.7%
Total from addition in quadrature	1.7%

Actual values for $\bar{v}_{<Cd} / v_0$ in the thermal column depend on the value of kT and thus vary with height in the column and the actual temperature in the pile. Using data from repeat measurements with paired gold foils at various heights, and assuming different pile temperatures, $\bar{v}_{<Cd} / v_0$ can vary from a minimum of about 1.17 at 2.0 m with a pile temperature of 5°C below the typical NPL pile temperature of 21.4°C, to a maximum of about 1.22 at 1.0 m with a pile temperature of 5°C above 21.4°C.

8 DOSE EQUIVALENT STANDARDS

If the thermal column is used to calibrate devices in terms of dose equivalent quantities, not only is the 'true' fluence rate required, but also the fluence to dose equivalent conversion factor for the actual spectral distribution. Figure 25 shows a pure Maxwellian spectrum at $kT = 25.3$ meV, and also an estimate of the NPL thermal column sub-cadmium-cut-off spectrum, in both cases normalised to unit fluence. Note that when plotted as a fluence rate per unit logarithm of the energy, as in Figure 25, the peak of the spectrum occurs at $2kT$ rather than kT the peak energy in a linear plot.

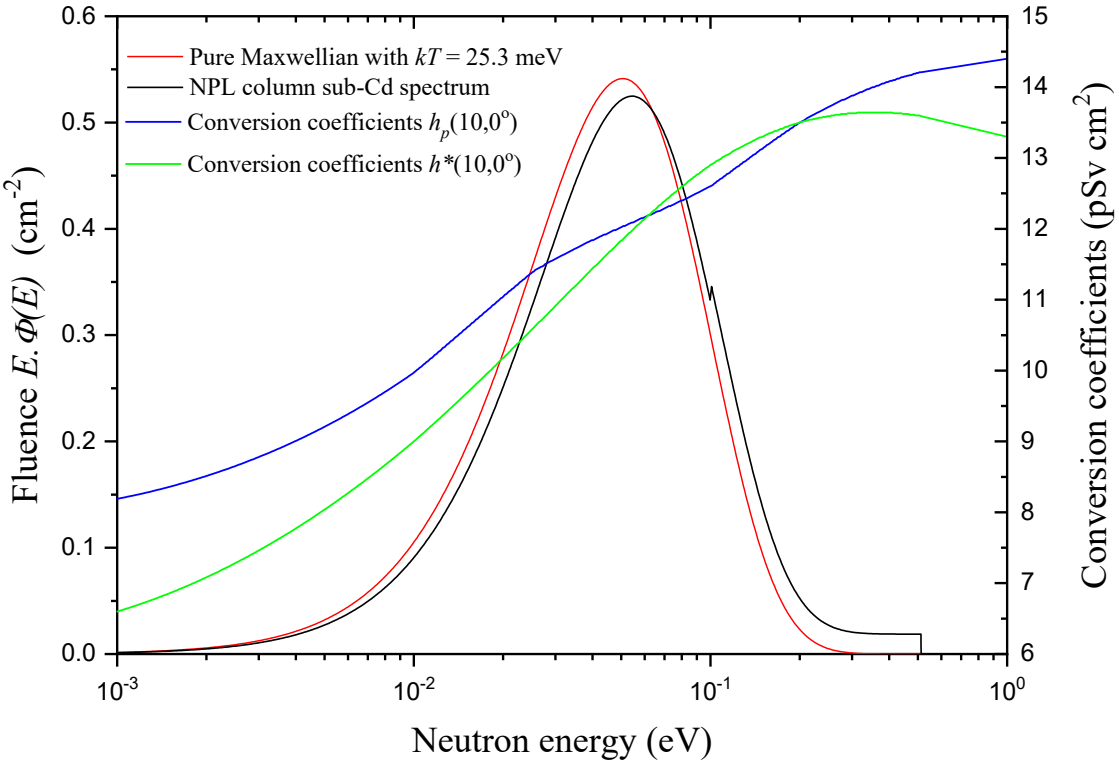

Figure 25. A pure Maxwellian distribution with $kT = 25.3$ meV, a typical NPL thermal column sub-cadmium-cut-off spectrum, and the fluence to ambient dose equivalent, $h^*(10)$, and to personal dose equivalent, $h_p(10,0°)$, conversion coefficients in this energy region.

Also shown in the figure are the fluence to ambient and personal dose equivalent conversion coefficients, $h^*(10)$ and $h_p(10, 0^o)$, from reference (54). These are assumed by convention to be exact, i.e. to have zero uncertainties. The uncertainties in these quantities when used for thermal pile calibrations arise solely from uncertainties in the spectrum.

The properties of the neutron field in the vertical thermal column change slightly with height. Table 11 shows values for the parameters describing the field. They were derived from repeat measurements with pairs of bare and cadmium covered gold foils at three heights in the column, 1.0 m, 1.5 m, and 2.0 m. From Westcott analyses of these data the average ratio $n_{1/E} / n_m$, of the $1/E$ number density below the cadmium cut-off, $n_{1/E}$, to the total Maxwellian number density, n_M, were calculated. From these values of $T - T_m$, the difference between the effective temperature of the Maxwellian distribution and the physical temperature of the graphite pile, were derived using eq.(52).

Table 11. Values for the parameters $n_{1/E} / n_M$, T-T_M, T, and kT for the three most commonly used heights in the NPL thermal column.

Height in column	$n_{1/E} / n_m$	T-T_M (°C)	T for T_M = 21.4°C	kT (eV)
1.0 m	0.02978 ± 0.00022	28.08 ± 0.19	323 ± 11	0.02780 ± 0.00095
1.5 m	0.02400 ± 0.00028	22.74 ± 0.25	317 ± 11	0.02734 ± 0.00095
2.0 m	0.01964 ± 0.00040	18.57 ± 0.22	313 ± 11	0.02698 ± 0.00095

The uncertainties shown in the second and third columns of the table are just those from the spread of the measured values. They highlight the variation from measurement to measurement, but are unrealistic for the true uncertainty in $T - T_M$ because the parameter C used in deriving this quantity from $n_{1/E} / n_M$ using eq. (52) has a 50% uncertainty. This is reflected in the uncertainty in T shown in the fourth column, c.f. section 5.

The fluence to dose equivalent conversion coefficients can be averaged over these spectra, and this was done with the program THERMALS. The values vary with kT, and thus with height, although the variations are only small over the range of kT values, roughly 0.0278 eV to 0.0270 eV between the 1.0 m and 2.0 m heights in the column. The variation in the coefficients over this range is slightly different for the different dose equivalent quantities, but is in the range for 0.4% to 0.7%. Changing kT by the uncertainty of 11 K in T changes the averaged conversion coefficients by less than 0.5%.

The variation of the conversion coefficients, h, with height, x, were not quite linear so were fitted to a polynomial $h = a + bx + cx^2$ and the data are shown in Table 12.

Table 12. Variation of spectrum averaged dose equivalent conversion coefficients, in pSv·cm^2, with height in the column[1].

Conversion coefficient	Height in column			Parameters for variations of conversion coefficients with height in the column		
	1.0 m	1.5 m	2.0 m	a	b	c
h*(10)	11.570	11.530	11.499	11.678	0.1275	0.0190
h_p(10,0°)	11.874	11.844	11.821	11.957	0.0980	0.0150
h_p(10,30°)	9.597	9.569	9.548	9.676	0.0932	0.0146
h_p(10,60°)	4.312	4.295	4.283	4.3573	0.05423	0.00855

Because T depends on the actual physical temperature, T_m, of the graphite pile the conversion coefficients also change slightly with temperature, increasing as the pile temperature increases. Coefficient values calculated using the TERMALS program for temperatures ranging from 5°C below to 5°C above a value of 21.4°C (taken as a typical NPL pile temperature) are shown in Table 13. The variation is linear over the small range of temperatures expected in the thermal pile, and the data were fitted to a straight line $h = a + bT$.

The variations for both height and temperature are illustrated in Figure 26 for h_p(10,0°) the conversion coefficient for personal dose equivalent for 0° incidence.

[1] All values in the tables in this report are for a deuteron bombarding energy of 3.0 MeV.

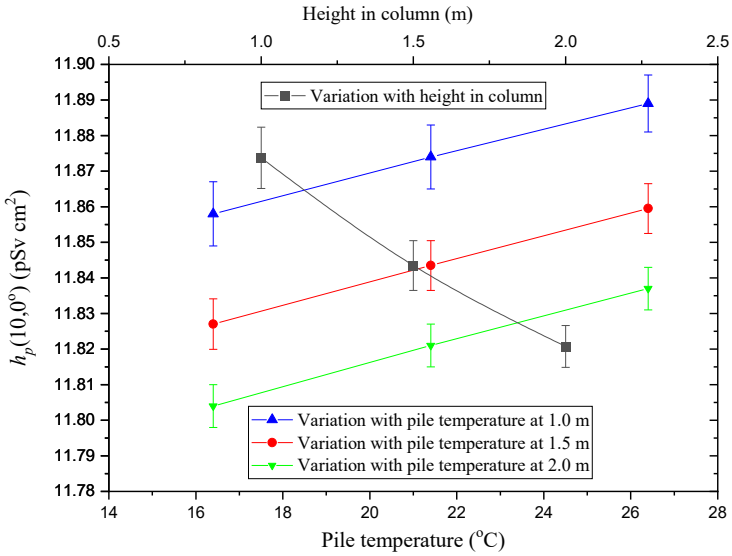

Figure 26. Variation of fluence to dose equivalent conversion coefficients $h_p(10,0°)$ with height in the thermal column and with the temperature of the pile. Note that the x-axis for the variation with height is on the top, and that for the variation with temperature is on the bottom.

Table 13. Variation of spectrum averaged conversion coefficients with temperature at the three standard heights in the NPL thermal column

Dose quantity	Spectrum averaged conversion coefficients			Linear fit parameters	
	(T-5)	T for T_M = 21.4°C	(T+5)		
	317.6 (K)	322.6 (K)	327.6 (K)	a	b
Height in the column = 1.0 m					
$h^*(10)$	11.546	11.570	11.593	10.069	0.004650
$h_p(10,0°)$	11.858	11.874	11.889	10.857	0.003150
$h_p(10,30°)$	9.583	9.597	9.612	8.651	0.002932
$h_p(10,60°)$	4.303	4.312	4.320	3.774	0.001665
Height in the column = 1.5 m					
$h^*(10)$	11.505	11.530	11.553	10.006	0.004800
$h_p(10,0°)$	11.827	11.844	11.860	10.812	0.003250
$h_p(10,30°)$	9.554	9.569	9.584	8.6185	0.002995
$h_p(10,60°)$	4.287	4.295	4.304	3.7557	0.001700
Height in the column = 2.0 m					
$h^*(10)$	11.474	11.499	11.524	9.9568	0.004928
$h_p(10,0°)$	11.804	11.821	11.837	10.7950	0.003275
$h_p(10,30°)$	9.533	9.548	9.563	8.5936	0.003048
$h_p(10,60°)$	4.274	4.283	4.292	3.7413	0.001730

Corrections for these variations are small, but are easily performed, and are included in the analysis routines used at NPL.

It is interesting to compare the values in the tables with those for monoenergetic neutrons at 0.0253 eV and the spectrum averaged value for a pure Maxwellian at $kT = 0.0253$ eV.

$h^*(10)$ at a point energy of 0.0253 eV = 10.6 pSv cm^2
Spectrum averaged $h^*(10)$ for a pure Maxwellian at $kT = 0.0253$ eV = 11.34 pSv cm^2,
Spectrum averaged $h^*(10)$ for 1.5 m in column at 21.4°C = 11.53 pSv cm^2.

$h_p(10,0^\circ)$ at a point energy of 0.0253 eV = 11.4 pSv cm^2,
Spectrum averaged $h_p(10,0^\circ)$ for a pure Maxwellian at $kT = 0.0253$ eV = 11.70 pSv cm^2,
Spectrum averaged $h_p(10,0^\circ)$ for 1.5 m in column at 21.4°C = 11.84 pSv cm^2.

From the above data, the uncertainty in the conversion coefficients introduced by the fact that the thermal spectrum is not simply a Maxwellian at 293.6 K is not large. Use of the value at 0.0253 eV would underestimate the coefficient. Changing the temperature by 11°C, the estimated uncertainty in T-T_M, changes the calculated spectrum averaged conversion coefficients by at most 0.5%. Changing the measured epithermal fraction in the sub-cadmium region from its typical value of about 3% to a value of 2% changes the coefficients by less than 0.2%. These are the parameters which have the biggest effect on the spectrum. From these arguments the uncertainty in the conversion coefficients is of the order of 0.5%. However, this assumes that the spectrum can be described adequately as a Maxwellian peak and $1/E$ component. Making allowance for the fact that this assumption may not be completely correct, an uncertainty estimate of 1% is assigned to the spectrum averaged conversion coefficients.

9 CONCLUSIONS

Thermal fluences are commonly measured, using the activation of gold foils, one bare and one under a cadmium cover, and are quoted using the Westcott convention with very low uncertainties, of the order of 0.5% for the sub-cadmium-cut-off fluence. Because of uncertainties in the spectra in thermal neutron irradiation facilities a Westcott analysis involves making assumptions and approximations which may not always be valid. This results in uncertainties in the quoted fluences which are hard to quantify. This report investigates and draws conclusions about the parameters used and the implications of some of the assumptions in a Westcott analysis and the effects on the quoted uncertainties. It attempts to draw together information on how the Westcott convention should be implemented from a number of papers that were published as the subject developed.

The Westcott fluences are not, however, the fluences required when calibrating neutron sensitive devices used in radiation protection. The 'true' sub-cadmium-cut-off fluence, which is quoted on NPL certificates along with the Westcott value, is derived by multiplying the Westcott fluence by a correction factor. For the NPL thermal column the value of this correction factor is about 1.2, the precise value depending on height in the column and the pile temperature, and has an uncertainty estimated as 1.7%.

In order to convert the true fluence to dose equivalent values spectrum averaged fluence to dose equivalent conversion coefficients need to be applied. The values to be used are given in section 8. The uncertainty in these spectrum averaged coefficients is estimated to be 1%, and is small because the coefficients do not change rapidly with neutron energy over the thermal region.

The largest uncertainty in deriving the true fluence form the Westcott fluence stems from the uncertainty in the effective temperature T for the Maxwellian spectrum. This has been determined from a relationship between the ratio $n_{1/E} / n_M$ of neutron densities and the temperature. This relationship involves a parameter C which is only known to about 50% - see section 5. Two other approaches are possible, a) calculation of the spectrum using neutron transport codes, b) measurement with an isotope with a low energy resonance.

a) The calculational approach requires a reliable model of the facility. By fitting the calculated spectrum to a Maxwellian, shape with the temperature a variable parameter, the temperature can in principle be derived[55]. The NPL thermal pile is, however, a complex structure and difficult to model accurately, and the 'start spectrum' for the calculations, that for neutrons from the two beryllium targets is not well known.

b) The activation of a material with a resonance in the low energy region close to the Maxwellian peak is sensitive to the effective temperature[9]. A good example of such a material is ^{176}Lu which has a resonance at 0.142 eV. Unfortunately, the cross section for ^{176}Lu(n,γ) and the decay scheme of ^{177}Lu are not sufficiently well known, and the approach has to be a relative measurement requiring a reference field of known temperature. Measurements can also be performed using a comparative approach involving ^{176}Lu and a $1/v$ detector and the k_0 neutron activation analysis approach[56]. The factor k_0 is a calculated value that allows activation in different materials to be compared, but still relies on good nuclear data.

A second determination of the temperature would provide more confidence in the true fluence values, and hopefully smaller uncertainties.

The applicability of the Westcott convention to the NPL thermal facility is an issue that has not tended to be questioned. Westcott[13] quotes a general "safe limit" of $T/T_M < 1.07$. For the access hole this is easily satisfied. For the column T/T_M varies from 1.10 at 1.0 m to 1.06 at

2.0 m. The conditions might thus be thought to be close to the limit, however, Westcott also writes, “for graphite moderation, T/T_M is enhanced by crystal forces and may rise to ~1.25 before the $g + rs$ system ceases to be a good approximation.”

The assumption has been made in this report that the intensity of the neutron fluence in the energy region between the Maxwellian thermal distribution and the energy region of the fast neutrons entering the moderator has a $1/E$ energy dependence. This dependence is caused by the nature of the slowing down process. In this region the macroscopic scattering cross section $\Sigma_s(E)$ varies very little with energy. The elastic scattering removes a constant fraction of the neutron energy per collision, independent of energy, resulting in larger energy losses per collision at higher energies than at lower energies. For a good moderator this results in a $1/E$ dependence of the fluence. However, this is not guaranteed and other options for example a $1/E^{1+\beta}$ dependence have investigated[57]. The precise shape of the spectrum in the epithermal region is an issue when investigating resonance integrals, but probably not for estimating sub-cadmium fluences.

Acknowledgements

Many of the results quoted in this report are based on data from paired gold foil measurements made over many years by NPL staff members, Peter Kolkowski, Catlin Matei, Paula Salvador Castiñeira, Alberto Boso, and most recently Kim Ward. The efforts of the NPL library staff who persevered in obtaining some of the very old publications referenced in this report is grateful acknowledged.

10 REFERENCES

1 T.B. Ryves and E.B. Paul, *The Construction and Calibration of a Standard Thermal Neutron Flux Facility at the National Physical Laboratory*, J. Nucl. Energ. **22** (1968) 759-775.

2 N.P. Hawkes, P. Kolkowski, N.J. Roberts, P. Salvador-Castiñeira, G.C. Taylor, and D.J. Thomas, *Additional Characterisation of the Thermal Neutron Pile at The National Physical Laboratory*, UK, Rad. Prot. Dosim. **180** (2018) 25–28.

3 David Thomas and Kim Ward, *Average distances and angles for radiation arriving at a measurement point from a circular source area*, NPL Report IR 68, (NPL, Teddington, December 2024). https://doi.org/10.47120/npl.IR68.

4 P. Kolkowski and D.J. Thomas, *Measurement of the fast neutron component in the beam of the NPL thermal neutron column using a Bonner sphere spectrometer*, NPL Report CIRM 28, (NPL, Teddington, May 1999).

5 David J. Thomas, and Peter Kolkowski, *Thermal fluence and dose equivalent standards at NPL*, NPL Report DQL-RN 008, (NPL, Teddington, March 2005).

6 C.H. Westcott, *The specification of neutron flux and nuclear cross-sections in reactor calculations*, J. Nucl. Eng. **2** (1955) 59-76.

7 C.H. Westcott, W.H. Walker, and T.K. Alexander, *Effective cross sections and cadmium ratios for the neutron spectra of thermal reactors*, Proceedings of the Second United Nations international conference on the peaceful uses of atomic energy, Vol. 16 Nuclear data and reactor theory, (UN, Geneva, 1958).

8 K.H. Beckurts and K. Wirtz, Neutron Physics, (Springer-Verlag, N.Y. 1964).

9 IAEA, Neutron Fluence Measurements, Technical Report Series No. **107**, (IAEA, Vienna, 1970).

10 W.H. Walker, C.H. Westcott, and T.K. Alexander, *Measurement of Radiative Capture Resonance Integrals in a Thermal Reactor Spectrum, and the Thermal Cross Section of Pu-240*, Can. J. of Phys. **38** (1960) 57-77.

11 E.J. Axton, *Absolute measurement of the neutron flux density in the A.E.R.E reactor GLEEP*, J. of Nucl. Energy Parts A/B **17** (1963) 125-135.

12 S.J. Boot, *Calibration of reference thermal and epithermal neutron flux densities from the GLEEP reactor at AERE Harwell*, Nucl. Instrum. Methods **164** (1979) 513-519.

13 C.H. Westcott, *Effective cross section values for well-moderated thermal reactor spectra*, Atomic Energy of Canada Limited Report AECL-1101.

14 E.M. Gryntakis and J.I. Kim, *Absorption, Activation and Fission g(Tn) – Functions for non 1/v Nuclides*, Radiochemica Acta **22** (1975) 128-147.

15. K.W. Geiger and L. van der Zwan, *Slowing Down Spectrum and Neutron Temperature in a Thermal Neutron Flux Density Standard*, Metrologia **2** (1966) 1-5.

16 M. Kűchle, *Neutron Temperature Measurements in graphite*, Nucl. Sci. & Eng. **2** (1957) 87-95.

17 A.D. Carlson et al., *Evaluation of the Neutron Data Standards*, Nuclear Data Sheets **148** (2018) 143–188. https://doi.org/10.1016/j.nds.2018.02.002.

18 Norman E. Holden, *Temperature dependence of the Westcott g-factor for neutron reactions in activation analysis*, Pure Appl. Chem., **71** (1999) 2309-2315.

19 R. van Sluijs, A. Stopic, and R. Jaćimović, *Evaluation of Westcott g(Tn)-factors used in k_0-NAA for ''non-1/v'' (n,γ) reactions*, J. Radioanal. & Nucl. Chem. **306** (2015) 579–587. https://doi.org/10.1007/s10967-015-4134-1.

20 C.K. Hargrove and K.W. Geiger, *A New Thermal Neutron Flux Density Standard*, Can. J. of Phys. **42** (1964) 1593-1604.

21 D.J. Thomas, and N. Soochak, *Determination of the ^{3}He number density for the proportional counter used in the NPL Bonner sphere system*, NPL Report RS(EXT)104, 1988.

22 F. Farina Arboccò, P. Vermaercke, L. Sneyers, and K. Strijckmans, *Experimental validation of some thermal neutron self-shielding calculation methods for cylindrical samples in INAA*, J. Radioanal. & Nucl. Chem. **291** (2012) 529–534. https://doi.org/10.1007/s10967-011-1211-y.

23 IAEA, International Reactor Dosimetry File 2002 (IRDF-2002), Technical Report Series No. **452**, (IAEA, Vienna, 2006).

24 S. Pearlstein and E.V. Weinstock, *Scattering and Self-Shielding Corrections in Cadmium-Filtered Gold, Indium, and 1/v Foil-Activation Measurements*, Nucl. Sci. & Eng. **29** (1967) 28-42.

25 National Bureau of Standards (now NIST), Applied Mathematics Series 55, Handbook of Mathematical Tables, 1964.

26 Richard M. Lindstrom and Ronald F. Fleming, *Neutron Self-Shielding Factors for Simple Geometries*, Revisited, Chem. Anal. (Warsaw), **53** (2008) 855-859.

27 Menno Blaauw, *The confusing issue of the neutron capture cross-section to use in thermal neutron self-shielding computations*, Nucl. Instrum. Methods Phys. Res. **A 356** (1995) 403-407.

28 M. Blaauw, *The Derivation and Proper Use of Stewart's Formula for Thermal Neutron Self-Shielding in Scattering Media*, Nucl. Sci. & Eng. 124 (1996) 431-435.

29 J.G. Williams and D.M. Gilliam, *Thermal neutron standards*, Metrologia **48** (2011) S254-S262, doi:10.1088/0026-1394/48/6/S03. http://stacks.iop.org/Met/48/S254.

30 Alain Sola, *Flux Perturbation by Detector Foils*, Nucleonics March 1960, 78-81, and 141.

31 S.A. Hasnain, T. Mustafa, and T.V. Blosser, *Thermal Neutron Density Perturbations by Foils in Water*, ORNL 3193, 1961.

32 J.L. Crane and R.C. Doerner, *Thermal Self-Shielding and Edge Effects in Absorbing Foils*, Nucl. Sci. & Eng. **16** (1963) 259-262.

33 E. Martinho, J. Salgado, and I.F. Gonçalves, *Universal curve of the thermal neutron self-shielding factor in foils, wires, spheres and cylinders*, J. Radioanal. & Nucl. Chem. **261** (2004) 637–643. https://doi.org/10.1023/B:JRNC.0000037107.17274.16.

34 E. Martinho, I.F. Gonçalves and J. Salgado, *Universal curve of the thermal neutron self-shielding factor in foils, wires, spheres and cylinders*, Applied Radiat. & Isotopes **58** (2003) 371-375. doi:10.1016/S0969-8043(02)00313-5.

35 C.W. Tittle, *Slow-Neutron Detection by Foils – II*, Nucleonics **9** (1951) 60-67.

36 J.E. Powell and C.L. Beck, *Cadmium Correction Factors for Iodine, Indium, and Gold Foils*, Nucl. Sci. & Eng. **25** (1966) 204-206.

37 K. Mueck and F. Bensch, *Cadmium correction factors of several thermal neutron foil detectors*, J. Nucl. Energy **27** (1973) 677-688.

38 Andrej Trkov, *Nuclear Reactions and Physical Models for Neutron Activation Analysis*, Lecture at the Workshop on Nuclear Data for Activation Analysis, International Centre for Theoretical Physics Miramare - Trieste, Italy, 7-18 March 2005.

39 Vladimir Radulović, Andrej Trkov, Radojko Jaćimović, and Robert Jeraj, *Measurement of the neutron activation constants Q_0 and k_0 for the $^{27}Al(n,\gamma)^{28}Al$ reaction at the JSI TRIGA Mark II reactor*, J. Radioanal. & Nucl. Chem. **298** (2013) 1791-1800. https://doi.org/10.1007/s10967-013-2596-6.

40 Alexandre Fonseca Póvoa da Silva, et al., *The Final Power Calibration of the IPEN/MB-01 Nuclear Reactor for Various Configurations Obtained from the Measurements of The Absolute Average Neutron Flux*, International Nuclear Atlantic Conference - INAC 2015 São Paulo, SP, Brazil, October 4-9, 2015.

41 Rose Mary G. do Prado Souza, Rogério R. Rodrigues and Luiz Claudio A. Souza, *Thermal Neutron Flux Measurements in the Rotary Specimen Rack of the IPR-R1 Triga Reactor*, 2017 International Nuclear Atlantic Conference - INAC 2017 Belo Horizonte, MG, Brazil, October 22-27, 2017.

42 GUM – Guide to the Expression of Uncertainty in Measurement. Workbench software versions available from: http://www.metrodata.de/edu_en.html or https://gum-workbench.software.informer.com/#google_vignette.

43 E.J. Axton, *An Absolute Calibration of the National Bureau of Standards Thermal Neutron Flux*, Journal of Research of the National Bureau of Standards- A. Physics and Chemistry Vol. **67A**, No.3, May- June 1963. https://nvlpubs.nist.gov/nistpubs/jres/67A/jresv67An3p215_A1b.pdf.

44 M.S. Coates, Brussels Euratom 1961, *Neutron Time-of-Flight Methods*, p. 233. Quoted in reference 8 on page 276.

45 Gašper Žerovnik et al., *Systematic effects on cross section data derived from reaction rates in reactor spectra and a re-analysis of ^{241}Am reactor activation measurements*, Nucl. Instrum. Methods Phys. Res. **A 877** (2018) 300–313. https://doi.org/10.1016/j.nima.2017.09.064.

46 H. Harada, N. Takayama, and M. Komeda, *A new convention for the epithermal neutron spectrum for improving accuracy of resonance integrals*, J. Phys. Commun. **4** (2020) 085004. https://doi.org/10.1088/2399-6528/aba735.

47 Hideo Harada, *Bias Effects on g- and s-Factors in Westcott Convention*, Appl. Sci. **11** 2021, 6558. https://doi.org/10.3390/app11146558.

48 M. Borse, *Fur messing und berechnung der resonanzabsorption von neutronen in goldfolien*, Nukleonik **6** (1964) 134.

49 O. Shcherbakov and H. Harada, *Resonance Self-Shielding Corrections for Activation Cross section Measurements*, J. Nucl. Sci. & Tech. **39** (2002) 548-553. https://doi.org/10.1080/18811248.2002.9715233.

50 M. Lopes and J.M Avila, *Multiple-scattering resonance self-shielding factors in foils*, Nucl. Instrum. Methods **A280** (1989) 304-309.

51 J. C. Stewart and P. F. Zweifel, Proc. 2nd Int. Conf. Peaceful Uses of Atomic Energy, New York, 1959, Vol. **16**, p. 650, United Nations (1959).

52 F. De Corte, F. Bellemans, P. De Neve, and A. Simonits, *The use of a Modified Westcott-Formalism in the k_0-Standardization of NAA: the State of Affairs*, J. Radioanal. & Nucl. Chem. **179**, (1994) 93-103.

53 ASTM E262 – 17, Standard Test Method for Determining Thermal Neutron Reaction Rates and Thermal Neutron Fluence Rates by Radioactivation Techniques, 2017.

54 Conversion coefficients for use in Radiological Protection Against External Radiation, results of a joint ICRP/ICRU task group, published by the International Commission on Radiological Protection as ICRP Publication 74, 1996, and by the International Commission on Radiation Units and Measurements as ICRU Report 57, 1998.

55 Tran Van Hung, *Determination of neutron temperature in irradiation channels of reactor*, J. Radioanal. & Nucl. Chem. **287** (2011) 103–106. https://doi.org/10.1007/s10967-010-0681-7.

56 Xiaosong Li, *In situ measurement of neutron temperature for the extended k_0 NAA at FRM II*, J. Radioanal. & Nucl. Chem. **326** (2020) 1391–1397. https://doi.org/10.1007/s10967-020-07386-0.

57 T.B. Ryves, *A New Thermal Neutron Flux Convention*, Metrologia **5** (1969) 119-124.

NPL
National Physical Laboratory

Thermal neutron fluence and dose equivalent standards at NPL

Providing the measurement capability
that underpins the UK's prosperity
and quality of life

To find out more about NPL:
npl.co.uk

To get in touch:
npl.co.uk/contact
020 8977 3222

Hampton Road
Teddington
Middlesex
TW11 0LW

Please consider the environment
before printing this document